JNC TN8400 2003-030

Principles of the Oxide Electrowinning Process

（Research Document）

December, 2003

Japan Nuclear Cycle Development Institute

Tokai works

Inquiries about copyright and reproduction should be addressed to:
Technical Cooperation Section,
Technology Management Division,
Japan Nuclear Cycle Development Institute
4-49 Muramatsu,Tokai-mura,Naka-gun,Ibaraki 319-1184,
Japan
Tel:029-282-1122
Fax:02-282-7980
Mail:jserv@jnc.go.jp

© Japan Nuclear Cycle Development Institute
2003

Ⓢ

JNC TN8400 2003-030
December, 2003

Principles of the Oxide Electrowinning Process
(Research Document)

Serguei VAVILOV*
Tsuguyuki KOBAYASHI*
Munetaka MYOCHIN*

Abstract

Principles and operation experience of the pyroelectrochemical technology being developed at Research Institute of Atomic Reactors (RIAR, RUSSIA) for spent MOX fuel of Fast Breeder Reactors processing were considered. The largest attention was paid to the thermodynamics and kinetics of the fundamental chemical reactions, and to the electrochemical properties of elements, which are nuclear materials, or minor actinides, and fission products, and components of cladding or other structural materials. Many data were checked by means of comparison and analysis, and some of them were corrected.

We hope that this report might be useful for those who participate in a development of "dry" technology for spent nuclear fuel cycle.

* Dry Process Technology Group, Advanced Fuel Cycle Technology Division,
Waste Management and Fuel Cycle Research Center

JNC TN8400 2003-030
2003年12月

酸化物電解プロセスの原理

(研究報告)

セルゲイ　バビロフ*、小林　嗣幸*、明珍　宗孝*

要旨

高速増殖炉用混合酸化物使用済み燃料の処理のためロシア原子炉科学研究所で開発された高温化学法の原理と設備の運転経験をまとめた。　特に、熱力学と基礎的化学反応の速度論や核物質、マイナーアクチニド、核分裂生成物および被覆管等の構造材中の元素の電気化学的特性について深く検討した。　多くのデータについて比較評価や修正を行い、妥当性を確認した。

今後、本報告が使用済燃料の乾式サイクルの技術開発に参加される人々に活用されることが望まれる。

* 環境保全・研究開発センター、先進リサイクル研究開発部、乾式プロセスグループ

Table of content

List of tables

List of figures

1. Introduction

RIAR started the development of a concept for the spent nuclear fuel cycle using “dry” high-temperature processes in 1964. The high-temperature “dry” processes have the following attractive advantages:

- Neither water nor organic reactants are used, therefore, there is no radiolysis of the solvent and, thus, fuel can be processed at high burnup and with small cooling period;

- Moderators do not exist, therefore, large masses of fissile materials can be reprocessed simultaneously in restricted volumes;

- Chemical reactions have high rates at high operating temperatures.

Due to these properties, dry processes can be the basis of high performance technology for spent nuclear fuel reprocessing.

At nearly the same time, the development of gas-fluoride and that of pyroelectrochemical processes of MOX fuel reprocessing were started. A specialized laboratory was organized to perform R&D of pyroelectrochemical technology of MOX fuel reprocessing.

The electrolysis in molten alkali metals chlorides was chosen to be the basis of future technology. This method is capable of creating polydisperse granular powder of UO_2 or UO_2-PuO_2 (MOX) with particles having nearly the theoretical density. The granules can easily form a fuel column by the vibropacking method even with remotely controlled equipment. So, a combination of the electrochemical processing of UO_2 or MOX spent fuel as well as vibro-packing of fuel elements in the fuel assembly fabrication looks promising.

At first, the investigations were successful in the field of the development of granulated MOX production technology. Production equipment has been developed and subjected to experimental and industrial testing including those under “hot” cell conditions with remote control.

Actually, the laboratory investigations on the development of reprocessing technology of irradiated MOX have been successfully completed. Possibility of practical implementation of this technology has been shown. Demonstration experiments have been conducted using real irradiated fuel of the BN-350 and BOR-60 reactors.

The objective of this report is the analysis of theoretical basis and the description of RIAR hands-on experience of the pyroelectrochemical process for spent UO_2 and MOX fuel cycle.

2. Some concepts and equations of high-temperature electrochemistry

2.1. Standard state

In standard state [1] the chemical compounds are formed from the pure initial substances on reaction

$$Me + n/2\ Cl_2 = MeCl_n. \quad (2.1)$$

The activities of initial reactants and final products are equal to 1

$$\alpha_{Me} = [Me] = 1;\ \alpha_{Cl2} = [Cl_2] = 1;\ \alpha_{Me}{}^{n+} = [MeCl_n] = [Me^{n+}] = 1, \quad (2.2)$$

where the activity equals to the concentration expressed in mole fraction.

Standard Gibbs' Energy (ΔG^0) is the change of Gibbs' energy at $MeCl_n$ compound formation from simple initial substances:

$$\Delta G^0 = \Delta H^0 - T\Delta S^0, \quad (2.3)$$

where ΔH^0 is the standard heat efficiency of $MeCl_n$ compound formation from simple initial substances; ΔS^0 is the standard change of entropy at $MeCl_n$ compound formation from simple initial substances; T is the absolute temperature.

Electrochemical processes of metal ($Me_{(s)}$) oxidation at the anode and its ions ($Me^{n+}{}_{(melt)}$) reduction in liquid $MeCl_n$ pure compound at the cathode may be presented as:

$$Me_{(s.)} - n\ e^- = Me^{n+}{}_{(melt)} \quad \text{(anode process)} \quad (2.4)$$

$$Me^{n+}{}_{(melt)} + n\ e^- = Me_{(s.)}. \quad \text{(cathode process)} \quad (2.5)$$

In standard state, the potential of metallic electrode in liquid pure $MeCl_n$ measured relative to chlorine reference electrode is the metal standard potential (E^0).

Practically however, it is difficult to measure the E^0 value. Usually, there are interactions between the metal electrode and the $MeCl_n$ melts.

There are relationships, which establish the connection between thermodynamic and electrochemical characteristics of elements:

$$\Delta G^0 = - nFE^0, \quad (2.6)$$

and

$$E^0 = - (\Delta H^0 - T\Delta S^0)/nF, \quad (2.7)$$

where F is the Faraday constant (F = 96487 coulomb per mole).

2.2. Diluted solutions

There is a following reaction of the $MeCl_n$ compound formation from the pure initial substances in a salt-solvent melt [1]

$$Me_{(s)} + n/2\ Cl_{2\ (gas)} = MeCl_{n\ (sol.)}. \quad (2.8)$$

Product of above reaction is a solution of liquid $MeCl_n$ in molten salt-solvent. In this case the activities of initial reactants equal of 1, that is to say,

$$\alpha_{Me} = [Me] = 1;\ \alpha_{Cl2} = [Cl_2] = 1. \quad (2.9)$$

The activity of $MeCl_n$ compound dissolved in the salt-solvent is less then 1, because of an interaction between dissolved compound and a salt-solvent. Activity of Me^{n+} ions $\alpha_{Me}{}^{n+}$ and mole fraction concentration of Me^{n+} ions in melt solution $[Me^{n+}]$ are connected as follows

$$\alpha_{Me}{}^{n+} = f^*{}_{Me}{}^{n+} \cdot [Me^{n+}], \tag{2.10}$$

where $f^*{}_{Me}{}^{n+}$ is the activity coefficient of Me^{n+} ions in the melt.

In number of experiments, it was shown (see Fig. 2.1 [1, P. 86]) that the value of the activity coefficient is constant when the Me^{n+} ions concentration in the melt is less than 0.05 – 0.08 in mole fraction.

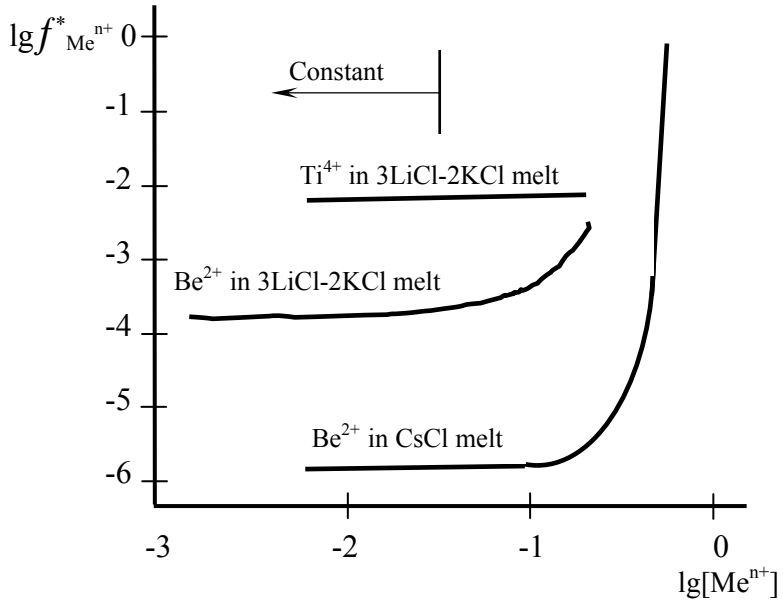

Fig. 2.1. Activity coefficient in chlorides melts. [1]

So, for diluted solutions, when the activity coefficient is constant ($f^*{}_{Me}{}^{n+}$ = const.), the equation for equilibrium electrode potential (E) takes the following form

$$E = E^0{}_{Me}{}^{n+}/_{Me} + \frac{RT}{nF} \ln f^*{}_{Me}{}^{n+} + \frac{RT}{nF} \ln [Me^{n+}] \tag{2.11}$$

or

$$E = E^*{}_{Me}{}^{n+}/_{Me} + \frac{RT}{nF} \ln [Me^{n+}], \tag{2.12}$$

where $E^*{}_{Me}{}^{n+}/_{Me}$ is the formal standard potential, which can be presented by following equation:

$$E^*Me^{n+}/_{Me} = E^0{}_{Me}{}^{n+}/_{Me} + \frac{RT}{nF} \ln f^*{}_{Me}{}^{n+} \tag{2.13}$$

In dilute solution, metals can react with the $MeCl_n$ with formation of other valency ions, for example on the reaction:

$$Me^{n+}{}_{(sol.)} + (n\text{-}m)/m\ Me_{(s.)} = n/m\ Me^{m+}{}_{(sol.)}. \tag{2.14}$$

Equilibrium constant of this reaction can be represented by equation:

$$K_{eq} = \frac{\alpha_{Me}^{n/m_{m+}}}{\alpha_{Me}^{n+}} = \frac{f^{*n/m}_{Me^{m+}}}{f^{*}_{Me^{n+}}} \frac{[Me^{m+}]^{n/m}}{[Me^{n+}]^{n/m}} = \frac{f^{*n/m}_{Me^{m+}}}{f^{*}_{Me^{n+}}} \frac{X^{n/m}}{1 - X} [Me]^{(n-m)/m}, \quad (2.15)$$

where α_{Me}^{m+}, α_{Me}^{n+} are the activities, and $f^{*}_{Me}{}^{m+}$, $f^{*}_{Me}{}^{n+}$ are the activity coefficients of Me^{m+} and Me^{n+} metal ion forms in the melt, respectively. The X is fraction of ions with lower valency from total content of dissolved metal in the melt.

By definition of diluted solutions, the activity coefficients are constant. It is allowed to introduce the formal equilibrium constant (K^{*}_{eq}) of above reaction

$$K^{*}_{eq} = \frac{f^{*}_{Me^{n+}}}{f^{*n/m}_{Me^{m+}}} K_{eq} \qquad K^{*}_{eq} = \frac{X^{n/m}}{1 - X} [Me]^{(n-m)/m}, \quad (2.16)$$

Formal standard Gibbs' Energy (ΔG^{*}) is the change of Gibbs' energy at the diluted solution formation of $MeCl_n$ compound in the melt from simple initial substances:

$$\Delta G^{*} = \Delta H^{*} - T\Delta S^{*}, \quad (2.17)$$

where ΔH^{*} is the formal standard heat efficiency of reaction at the diluted solution formation of $MeCl_n$ in melts from simple initial substances; ΔS^{*} is the formal standard change of entropy at the diluted solution formation of $MeCl_n$ in the melt from simple initial substances; T is the absolute temperature.

Next relationships establish the connection between thermodynamic and electrochemical characteristics of elements in dilute solutions:

$$\Delta G^{*} = \Delta H^{*} - T\Delta S^{*}, \quad (2.18)$$

$$\Delta G^{*} = - nFE^{*}, \; E^{*} = -\Delta G^{*}/nF, \quad (2.19)$$

$$\Delta G^{*} = - RT \ln K^{*}_{eq}, \; \ln K^{*}_{eq} = - \Delta G^{*}/RT, \quad (2.20)$$

$$E^{*} = (RT/nF) \ln K^{*}_{eq}, \quad (2.21)$$

Difference between ΔG^{*} and ΔG^{0} characterizes the interaction energy at between the solute compound and molten salt-solvent in the diluted solution

$$\Delta G_{mix} = \Delta G^{*} - \Delta G^{0}. \quad (2.22)$$

Formal parameters of E^{*} and K^{*}_{eq} are very useful parameters, because both of them can be found experimentally in many cases.

3. Properties of molten salt electrolytes

The technology of oxide fuel production and regeneration developed by RIAR is based on use of the molten salt electrolytes, mainly molten chlorides of alkali metals.

This choice is caused by:

⇒ Unique physical-chemical properties of molten salts:

* High radiation stability;
* Absence of moderators;

* High capability to form strong complex compounds;
* High reaction rate of chemical processes;

⇒ Availability of a great number of information related with:

* Fuel materials (U, Pu, Th);
* Minor actinides (Np, Am, Cm);
* Fission products of nuclear fuel (NM, REE etc.);
* Structural material elements (Fe, Ni, Co etc.).

Molten salts used commonly are:

- NaCl-KCl equimolar mixture (inexpensive; working temperature is more than 660°C). It was the first melt that was used as electrolyte for uranium dioxide deposition by electrolysis, and volume precipitation of plutonium dioxide;
- NaCl-2CsCl eutectic (expensive; the working temperature varies from 500 to 700°C). This electrolyte took the place of the NaCl-KCl equimolar mixture when it was found in RIAR that good crystalline form of uranium dioxide deposits can be obtained at temperature of 600 – 650°C. This molten salt became the basic electrolyte for MOX fuel production electrolysis;
- NaCl-KCl-CsCl eutectic (expensive; the working temperature varies from 500 to 700°C). This electrolyte has a characteristics similar to NaCl-2CsCl melt and it is less expensive than NaCl-2CsCl eutectic;
- 3LiCl-2KCl eutectic (inexpensive; it may be used in dry or inert atmosphere; the working temperature varies from 400 to 600°C) At RIAR this melt has been used in fundamental investigations.

Thermodynamic and electrochemical properties of elements in molten salts depend on complex formation properties of salt-electrolyte. In melts, the alkali metal cations are competing in complex formation with other element cations. Salt electrolyte complexion properties depend (for system with common anions) on cation specific charge "e/ r_{Me}^{+}", where e is the cation electric charge; r_{Me}^{+} is the cation radius. Because the e value equals to +1 for alkali metal cations, the element thermodynamic properties depend on value of $1/r_{Me}^{+}$ ratio.

Values of r_{R}^{+} for individual chloride melts are given in Table 3.1 [2].

Table 3.1. Cation radiuses of individual chloride melt [2. p.22]

R^+	Li^+	Na^+	K^+	Cs^+
r_{Me}^{+}, Å	0.68	0.98	1.33	1.65

The mixtures of individual chlorides are often used to lower the melting point. These electrolytes are characterized by value of cation effective radius ($r^{*}_{Me}{}^{+}$).

The value of cations effective radius is being usually calculated as follows:

$$r^*_{Me^+} = \sum_{i=1}^{n} N_i \cdot r_i \quad (3.1)$$

where N_i is mole fraction of i-cation; r_i is i-cation radius in salt mixture composed of n chlorides of different alkali metals.

For example, the effective radius of cations in NaCl-KCl equimolar mixture is

$$r^*_{Me} = (0.5 \cdot r_{Na^+} + 0.5 \cdot r_{K^+}) = 0.5 \cdot (0.98 + 1.33) = 1.155 Å. \quad (3.2)$$

Some characteristics of several chloride salt-solvents, including of $r^*_{Me^+}$ values, are presented in Table 3.2.

Table 3.2. Characteristics of chloride salt-solvents

Salt-solvent (mole fraction)	t_{melt}, °C	Melt density, g/cm^3 $d_t = a + b \cdot t$		Effective cation radius $r^*_{Me^+}$, Å (by Goldshmidt)	Mass of gram-mole, g
		a	$b \times 10^3$		
LiCl	610	1.895	0.446	0.68	42.5
KCl	770	1.977	0.583	1.33	74.6
CsCl	645	3.478	1.065	1.65	168.4
NaCl-KCl	662	1.976	0.568	1.15	66.5
3LiCl-2KCl	359	1.622	0.300	0.95	55.9
LiCl-CsCl(0.45)	318	2.860	0.869	1.17	99.2
NaCl-2CsCl	495	3.115	0.997	1.42	131.0

There was shown for many elements (for example, Fe, Zr, Ti, Be, Mo, U and others) (see Figure 3.1) that formal standard potential (in comparison with chlorine reference electrode) changes linearly with $1/r_{Me^+}$ or $1/r^*_{Me^+}$ in according with equations:

$$E^*_{Me^+/Me} = - K_1 + K_2/r_{Me^+}, V, \quad (3.3)$$

$$E^*_{Me^+/Me} = - K_1 + K_2/r^*_{Me^+}, V. \quad (3.4)$$

Influence of melt content on the behavior of elements in molten salts is very naturally connected with the ion radii. The relative dimentions of ion radii of alkali metal cations and halogen anions are illustrated in Figure 3.2.

It is seen that the radiuses are different, especially for cations. The bond strength between cation and anion is connected with their radius ratios. It maybe seen on melting points of individual halides of alkali metals (see Fig. 3.3.). Such character of these regularities maybe explained by the different ability of cations to polarize large size anions [3]. In the case of Li^+, the bond of cations Li^+ with anions is very strong that leads to decreasing the bond between molecules of lithium halides. In this connection, the melting points of lithium halides become lower. Cations Na^+ show also some ability to polarize Cl^- anions in chloride system.

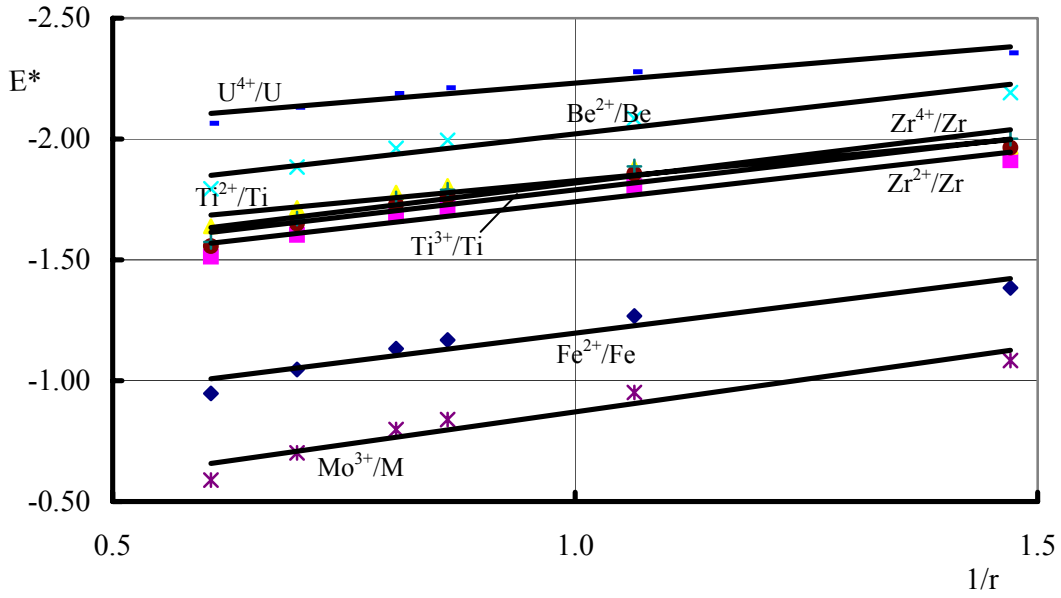

Figure 3.1. Dependence of formal standard potential on 1/r

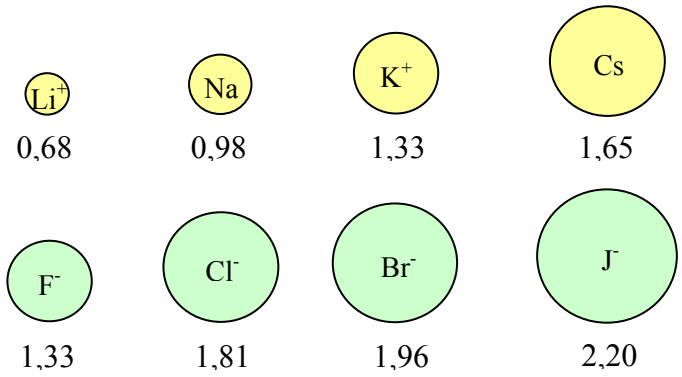

Figure 3.2. Correlation of ions radiuses of alkali metals cations and halogens anions

If the bond between cations and anions of salt-solvent will be strong, the bond between cations of other elements and anions of salt-solvent will be weaker. Consequently, the bonding strength of compound dissolved in the melt will be small, and, as a result, the formal standard potential of metals will change in positive direction See Figure 3.1).

During the selection of molten salts for working media in pyroelectrochemical technology, it is need to consider the following factors:

- Dissolution rate of initial fuel materials;
- Stability of plutonyl ions in the case of MOX deposition;
- Growth rate of plutonium dioxide crystals in the case of volume precipitation;
- Growth rate of uranium dioxide crystals during the electrolysis;
- Rate of corrosion processes in the melt.

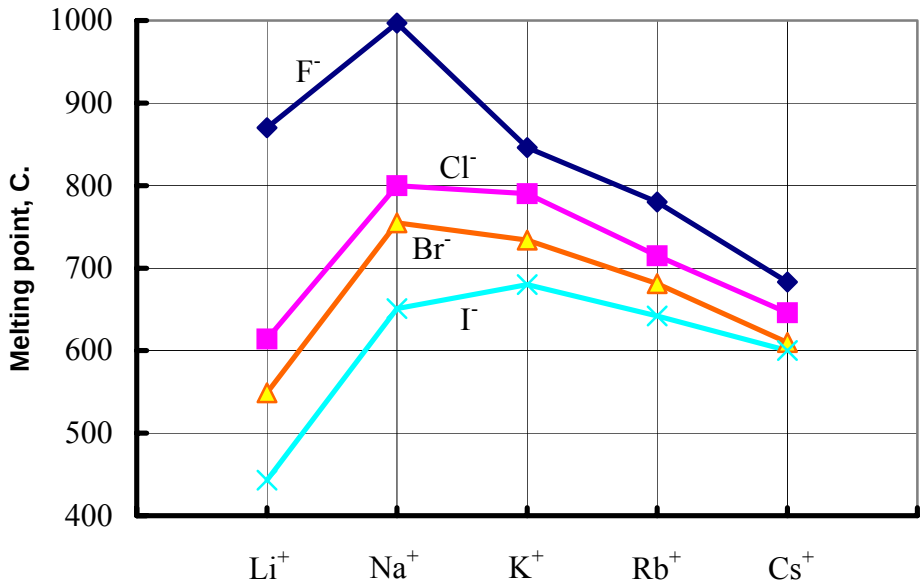

Figure 3.3. Melting points of individual halides of alkali metals [3].

Dissolution rate of initial fuel materials. Usually in the chloride melts the rate of initial fuel materials chlorination increases with process temperature. There are two reasons. At first, the chemical activity of reagents (oxides and chlorine gas) becomes higher with temperature. Secondly, the solubility of chlorine gas increases with temperature.

Besides, the solubility of chlorine gas in the chloride melts is different among the melts. Among LiCl, NaCl, KCl and CsCl, it becomes higher by ten times. The chlorination rate of initial fuel materials rises in this order.

Therefore, the melts with CsCl (NaCl-2CsCl, NaCl-KCl-CsCl) are better than that with LiCl (3LiCl-2KCl).

Stability of plutonyl ions in the case of MOX deposition. Stability of plutonyl ions increases from LiCl to CsCl. During MOX deposition electrolysis the concentration of plutonyl ions must be enough to keep the MOX composition. In this case, it is better to use the NaCl-2CsCl or NaCl-KCl-CsCl melts.

Growth rate of plutonium dioxide crystal in the case of the volume precipitation. During PuO_2 volume precipitation, the concentration of PuO_2Cl_2 must be enough to provide the plutonium dioxide particle size suitable for vibropac technology. In this case it is better to use the NaCl-KCl or NaCl-KCl-CsCl melts. The operation process temperature must be higher than 600°C.

If the PuO_2 precipitated must be a fine powder like for pallet application, it is better to use the 3LiCl-2KCl melt. The operation process temperature must be less then 500°C.

Growth rate of uranium dioxide crystals during the electrolysis. Uranium dioxide granular powder (or MOX granular powder) must be suitable for vibropac technology. To obtain such product, it is necessary to balance the rate of electrolysis process with the rate of uranium dioxide crystals growth. When the rate of electrolysis process exceeds the growth rate of uranium dioxide crystals too much, the cathode product will become very fine crystals. When the rate of electrolysis is much slower than the growth rate of uranium dioxide crystals, the cathode product will becomes larger, but the process will be lower productivity. The rate of uranium dioxide crystals growth increases with temperature.

Now there is additional restriction on electrolysis process rate. It connects with analytical possibility of process control. Because the duration of melt analysis needs 2 hour, the electrolysis rate must provide the process controllability. At RIAR, the following electrolysis conditions were chosen to provide high quality of uranium dioxide or MOX granular powder:

- the melt is NaCl-2CsCl;
- the temperature is 600 – 650^{o}C;
- process duration is 35 – 40 h.

Rate of corrosion processes in the melt. Corrosion of material in gas atmosphere depends on temperature only. Corrosion of graphite materials in the melt depends mainly on presence of uranium and plutonium oxychloride forms. It is known that plutonium oxychloride forms are the most corrosive. To decrease the corrosion activity of uranium and plutonium oxychloride forms, it is necessary to lower the process temperature. But this possibility is not larger than 50 or 70^{o}.

It is difficult to find a new molten salt for pyroelectrochemical reprocessing. Many kinds of molten salts were studied during the last 50 years. But only fluoride and chloride melts will find application in nuclear cycle technology:

- The fluoride melts for the liquid fuel of molten salt reactors,
- The chloride melts for the electrolyte in the spent fuel reprocessing technology (for metallic, oxide, and nitride systems).

In the MOX reprocessing, there is practically no possibility to use the mixture chloride-fluoride melts. It connects with plutonium behavior. The fluoride anions stabilize the three and tetravalent plutonium states, and there are no the oxygen contained forms of plutonium in these states.

Other melts are known, such as molibdates and tungstenates, which were being investigated for oxide fuel reprocessing. But now there are considerable difficulties to create the reprocessing process based on of these melts due to the following reasons:

- Very high temperature conditions (the more than 900^{o}C);

- Problem of final product cleaning from salt (for example, it is very difficult to remove the salt without water for molibdate system, whereas, vacuum distillation and water washing can be applied for this purpose in chloride system.);

- (It is the main.) Nobody successfully prepares a granular uranium dioxide or MOX powder that will be suitable for vibropac technology. Crystalline products were being prepared in above melts, but their particles dimension was not more 0.2 mm.

In conclusion, it is necessary to note that the melts of alkali metal chlorides are the only electrolytes for MOX fuel reprocessing.

The basic disadvantage of technology is that all technological stages are carried out consistently in one apparatus. Thereupon, productivity of technology cannot be very high, and it is difficult to find structural materials, which would be equally stable in reducing and oxidizing environments simultaneously.

4. Nuclear materials and actinides chemistry

Now in the literature there is a big volume of the information, concerning chemical and electrochemical behaviour of actinides in molten salt systems. Extensive investigations have been carried out in Russia, including within the RIAR program of the pyroelectrochemical method development for the oxide nuclear fuel reprocessing.

The basic partners of RIAR were:

- Institute of High-temperature electrochemistry (HTEI, Ekaterinburg);
- The Ural polytechnic institute (UPI, Ekaterinburg);
- Radium institute (RI, St. Petersburg);
- The State University in Nizniy. Novgorod (SUNN, N. Novgorod);
- Institute of general and inorganic chemistry in Kiev (GIChI, Kiev) etc.

These organizations and institutes had carried out the fundamental researches in areas:

- Theory of molten salts structure;
- Theory of complex formation in molten salts;
- Physic chemistry and electrochemistry, including the behavior of uranium and FP elements.

HTEI and UPI have possibility to study uranium. SUNN carried out investigations on pure materials in its laboratories. HTEI, UPI and SUNN have possibility to spend some experiments with actinides, using RIAR facilities. RI can work with uranium, plutonium and MA in a small amount.

Many kinds of investigation methods were used.

The information that helps understanding the main principles of the pyroelectrochemical technology will be described here.

4.1. Degrees of actinide oxidation in molten chlorides of alkali metals

The degree of actinide oxidation in molten chlorides is summarized in Table 4.1.1. One can see, uranium, neptunium and plutonium have the same degrees of oxidation. Each of them forms the chloride compounds in tri- and tetravalent states. In special conditions these elements form the oxygen-contained compounds in tri- and tetravalent states, for example, MeOCl or $MeOCl_2$, but such conditions are not typical for the technology. In penta- and hexavalent states, the uranium, neptunium and plutonium exist in the oxygen-contained compounds like MeO_2Cl and MeO_2Cl_2. There is no information for higher chloride forms of these elements without oxygen in chloride systems.

Table 4.1.1. The degree of actinide oxidation in molten chlorides of alkali metals

Element	Degree of oxidation				
	2	3	4	5	6
U	-	+	+	+(Ox)	+(Ox)
Np	-	+	+	+(Ox)	+(Ox)
Pu	-	+	+	+(Ox)	+(Ox)
Am	+(M)	+	-	-	-
Cm	-	+	-	-	-

where, + - basic state; (M) - in equilibrium with metal;
(Ox) - in the presence of oxygen

The stability of uranium, neptunium and plutonium in the chloride and oxygen-contained compounds of is very different. Due to above, the unique possibility exists for realization of conditions, which can be used for different practical purposes, for example, for:

- Elements separation;
- Metal mixture preparing;
- Dioxide mixture preparing;
- Decontamination from impurities and etc.

4.2. Uranium Chemistry

4.2.1. Reactions of formation and mutual transformation of uranium valent forms

Uranium exhibits the valency state of U(III), U(IV), U(V) and U(VI) in molten chlorides of alkali metals.

Trivalent uranium can be obtained in the melt by:

Dissolution of uranium trichloride

$$UCl_3 + Melt = UCl_{3(melt)}; \quad (4.2.1)$$

Anodic dissolution of uranium metal

$$U_{(solid)} - 3e^- + 3Cl^-(melt) = UCl_{3(melt)}; \quad (4.2.2)$$

Reduction of tetravalent uranium by, for example, uranium metal

$$3UCl_{4(melt)} + U_{(solid)} = 4UCl_{3(melt)}. \quad (4.2.3)$$

In chloride melts trivalent uranium presents in the form of $[UCl_6]^{3-}$ complex compound

$$U^{3+}_{(melt)} + 6Cl^-_{(melt)} = UCl_6^{3-}{}_{(melt)}. \quad (4.2.4)$$

Uranium trichloride pure compound can be obtained by reduction of the uranium tetrachloride by hydrogen

$$UCl_4 + H_2 = 2\ UCl_3 + 2\ HCl. \quad (4.2.5)$$

The vacuum distillation method at 900°C can be used for the uranium trichloride decontamination.

Tetravalent uranium can be obtained in the melt by:

Dissolution of uranium tetrachloride:

$$UCl_4 + Melt = UCl_{4(melt)}; \quad (4.2.6)$$

Oxidation of trivalent uranium by molecular chlorine

$$UCl_{3(melt)} + 1/2Cl_{2(gas)} = UCl_{4(melt)}; \quad (4.2.7)$$

Uranium dioxide chlorination in presence of reducing reagent

$$UO_{2(solid)} + Cl_{2(gas)} + C_{(solid)} = UCl_{4(melt)} + CO_{2(gas)}. \quad (4.2.8)$$

In chloride melts tetravalent uranium presents in the form of UCl_6^{2-} complex compound

$$U^{4+}_{(melt)} + 6Cl^-_{(melt)} = UCl_6^{2-}{}_{(melt)}. \quad (4.2.9)$$

Pure uranium tetrachloride compound can easy be obtained by the chlorination method of uranium dioxide with help of carbon tetrachloride

$$UO_2 + CCl_4 = UCl_4 + CO_2. \quad (4.2.10)$$

The uranium tetrachloride can be decontaminated by the vacuum distillation method at temperature about 650°C. (The boiling point of uranium tetrachloride is 791°C).

Pentavalent uranium forms the UO_2Cl oxygen-contained compound in the chloride melts. UO_2Cl can be obtained by reducing uranyl chloride in the melt

$$UO_2Cl_{2(melt)} \rightarrow UO_2Cl_{(melt)} + 1/2\ Cl_{2(gas)}. \quad (4.2.11)$$

Any chlorine gas absorber can be used as an uranylchloride reducer.

UO_2Cl can be obtained with help of reaction:

$$UO_2 + UO_2Cl_2 = 2\ UO_2Cl. \quad (4.2.12)$$

UO_2Cl exists in the chloride melts due to the formation of $UO_2Cl_4^{3-}$ complex compound

$$UO_2^+{}_{(melt)} + 4Cl^-_{(melt)} = UO_2Cl_4^{3+}{}_{(melt)}. \quad (4.2.13)$$

Uranium pentachloride does not exist in chloride melts. In pure state, it can be obtained with help of the uranium tetrachloride chlorination by chlorine gas

$$UCl_4 + 1/2Cl_2 = UCl_5. \quad (4.2.14)$$

UCl_5 impurity presents in UCl_4 obtained by uranium dioxide chlorination with the carbon tetrachloride.

Hexavalent uranium forms the uranylchloride compound in the chloride melts. Uranylchloride can be obtained with help of the uranium oxides chlorination by chlorine gas:

$$UO_{2(solid)} + Cl_{2(gas)} = UO_2Cl_{2(melt)}, \quad (4.2.15)$$

$$U_3O_{8(solid)} + Cl_{2(gas)} + C_{(solid)} = 3UO_2Cl_{2(melt)} + CO_{2(gas)}. \quad (4.2.16)$$

Using of the other chlorinating regents results in partly to reducing of uranylchloride up to uranium tetrachloride, for example,

$$U_3O_{8(solid)} + 2CCl_{4(gas)} \rightarrow 2UO_2Cl_{2(melt)} + UCl_{4(melt)} + CO_{2(gas)}. \quad (4.2.17)$$

The oxidation of tri- and tetravalent uranium with oxygen results mainly in formation of uranylchloride:

$$UCl_{3(melt)} + O_{2(gas)} = UO_2Cl_{2(melt)} + 1/2Cl_{2(gas)}, \quad (4.2.18)$$

$$UCl_{4(melt)} + O_{2(gas)} = UO_2Cl_{2(melt)} + Cl_{2(gas)}. \quad (4.2.19)$$

UO_2Cl_2 exists in the chloride melts due to the formation of $UO_2Cl_4^{2-}$ complex compound

$$UO_2^{2+}{}_{(melt)} + 4Cl^-_{(melt)} = UO_2Cl_4^{2-}{}_{(melt)}. \quad (4.2.20)$$

The oxygen-contained compounds of hexavalent uranium can be obtained by the anode dissolution of uranium dioxide

$$UO_{2(anode)} - 2e^- = UO_2^{2+}{}_{(melt)}. \quad (4.2.21)$$

The penta- and hexavalent uranium is always present in the equilibrium

$$UO_2Cl_{(melt)} + 1/2Cl_{2(gas)} \rightleftarrows UO_2Cl_{2(melt)}, \quad (4.2.22)$$

which is directed to the right in molten chlorides of alkali metals.

Uranylchloride can be reduced by uranium dioxide

$$UO_2^{2+}{}_{(melt)} + UO_{2(solid)} = UO_2^{+}{}_{(melt)}. \quad (4.2.23)$$

The UO_2^+ and UO_2^{2+} cations can participate in the cathode process. At the cathode they can be reduced to uranium dioxide

$$UO_2^{n+}{}_{(melt)} + n\ e^-_{(cathode)} = UO_{2(solid)}. \quad (n \text{ is } 1 \text{ or } 2). \quad (4.2.24)$$

At a temperature of 400^0C and higher, the uranium dioxide has a high electrical conductivity and behaves like a metallic electrode. (Specific resistance of $UO_{2.01}$ is 0.5 – 5 ohm·cm.) Thus, the uniform cathode deposits can be obtained.

The capability of UO_2^{n+} ions for cathode reduction up to the uranium dioxide due to its high electrical conductivity is a unique property that had been used at the development of the pyroelectrochemical technologies for the uranium and MOX fuel production and the spent MOX fuel reprocessing technology.

The reactions of uranylchloride with carbon, which used usually as a structural material,

$$UO_2Cl_{2(melt)} + C_{(solid)} + Cl_{2(gas)} = UCl_{4(melt)} + CO_{2(gas)} \quad (4.2.25)$$

and of tetravalent uranium with the plutonium oxychloride compounds, for example with PuO_2Cl_2,

$$UCl_{4(melt)} + PuO_2Cl_{2(melt)} = UO_2Cl_{2(melt)} + PuCl_{4(melt)} \quad (4.2.26)$$

are very important for the pyroelectrochemical technology.

The hexavalent uranium can form the compounds with the increased content of oxygen, such as $U_3O_8^{2+}$; $U_2O_7^{2-}$; UO_4^{2-}; UO_3Cl^-; $(UO_2\text{-}O\text{-}UO_2)^{2+}$; $(UO_2)_2O_2^{2+}$ and others. Their presence in salt electrolyte results to the formation of the dendritic uranium dioxide deposit having the low density and excess of oxygen.

4.2.2. Thermodynamic and electrochemical characteristics of uranium

(1) Literature data

Formal standard potential of metallic uranium for different molten salt electrolytes is shown in Table 4.2.1 [1]. The value of the formal standard potential of metal uranium in any melt of the alkali metal chlorides can be calculated by the equation presented in the bottom of the Table 4.2.1.

Table 4.2.1. Formal standard potentials of U metal
in melts of alkali metal chlorides [1]

Melt	$E^*_{U^{3+}/U}$, V	Temperature, °C
LiCl	$- 2.83 + 6.0\cdot10^{-4}\cdot T$	630 – 735
NaCl	$- 2.99 + 6.7\cdot10^{-4}\cdot T$	830 – 960
KCl	$- 3.12 + 7.1\cdot10^{-4}\cdot T$	830 – 960
CsCl	$- 3.18 + 7.4\cdot10^{-4}\cdot T$	700 – 820
3LiCl-2KCl	$- 2.84 + 5.4\cdot10^{-4}\cdot T$	400 – 610
NaCl-KCl	$- 3.01 + 6.6\cdot10^{-4}\cdot T$	

$$E^*_{U^{3+}/U} = - 3.50 + 0.52/r^*_{Me^+} + (8.58\text{-}1.99/r^*_{Me^+})\cdot10^{-4}\cdot T \pm 0.02, \text{ V}$$

Some thermodynamic parameters of tetravalent uranium in typical salt composition are presented in Table 4.2.2 [4]. Equation presented in this table can be used for calculation of $E^*_{U^{4+}/U^0}$ and $E^*_{U^{4+}/U^{3+}}$ parameters.

Electrochemical parameters of penta- and hexavalent uranium are presented in Table 4.2.3 [5,6]. The equation on the bottom of this table shows the relationship between the electrochemical parameters of penta- and hexavalent uranium.

Formal equilibrium constant of $UO_2^{2+} + UO_2 = 2UO_2^+$ reaction is given in Table 4.2.4 [5,6]. This reaction has a great importance in the cathode process of the uranium dioxide deposit formation.

Table 4.2.2. Thermodynamic parameters of tetravalent uranium [4]

Melt	$Log_{10}\gamma U^{4+}$ = $\alpha + \beta/T$		E^*U^{4+}/U = a + b*T, V		E^*U^{4+}/U^{3+} = A + B*T, V		T, K
	$-\alpha$	$-\beta\cdot10^3$	-a	$b\cdot10^4$	-A	$B\cdot10^4$	
LiCl	1.20	0.60	2.53	5.20	1.62	2.62	900-1215
NaCl	2.20	1.10	2.55	4.70	1.23	-1.46	1050-1220
KCl	0.90	3.90	2.69	5.30	1.40	-0.08	1050-1300
RbCl	0.15	5.25	2.76	5.70	1.58	0.81	980-1200
CsCl	0.05	5.90	2.79	5.70	1.62	0.70	1025-1190
3LiCl-2KCl	0.81	3.40	2.66	5.30	1.62	1.60	990-1200
NaCl-KCl	0.48*	4.65*	2.73*	5.50*	1.51*	0.54*	-

$E^*U^{4+}/U = - 3.06 + 0.44/r^*_{Me}{}^+ + (6.87\text{-}1.67/r^*_{Me}{}^+)\cdot10^{-4}\cdot T \pm 0.01$, V

$E^*U^{4+}/U^{3+} = - 1.74 + 0.20/r^*_{Me}{}^+ + (1.74\text{-}0.71/r^*_{Me}{}^+)\cdot10^{-4}\cdot T \pm 0.05$, V

Table 4.2.3. Electrochemical parameters of penta- and hexavalent uranium [5,6]

Melt	$E^*UO_2{}^+/UO_2$ = $\alpha + \beta\cdot T$		$E^*UO_2{}^{2+}/UO_2$ = a + b·T		$E^*UO_2{}^{2+}/UO_2{}^+$ = A + B·T		T, K
	$-\alpha$	$\beta\cdot10^4$	-a	$b\cdot10^4$	-A	$B\cdot10^4$	
KCl	0.712	4.60	1.008	4.66	1.295	4.73	1063-1223
RbCl	0.846	5.17	1.085	5.00	1.323	4.83	1023-1143
CsCl	0.970	5.85	1.172	5.38	1.374	4.90	973-1123
3LiCl-2KCl	0.683	5.73	0.783	4.29	0.886	2.88	673-1073
NaCl-KCl	0.537	3.67	0.920	4.63	1.303	5.59	973-1173

$E^*UO_2{}^{2+}/UO_2{}^+ = 2E^*UO_2{}^{2+}/UO_2 - E^*UO_2{}^+/UO_2$

$E^*U0^+{}_2/UO_2 = - 1.214 + 0.533/r^*_{Me}{}^+ + (4.95+0.50/r^*_{Me}{}^+)\cdot10^{-4}\cdot T$, V

$E^*U0^{2+}{}_2/UO_2 = - 1.646 + 0.828/r^*_{Me}{}^+ + (6.48\text{-}2.14/r^*_{Me}{}^+)\cdot10^{-4}\cdot T$, V

$E^*U0^{2+}{}_2/UO^+{}_2 = - 2.069 + 1.101/r^*_{Me}{}^+ + (7.93\text{-}4.69/r^*_{Me}{}^+)\cdot10^{-4}\cdot T$, V

Table 4.2.4. Conventional constant equilibrium of $UO_2{}^{2+} + UO_2 = UO_2{}^+$ reaction [5,6]

Melt	LgK^* = a – b/T		Interrelationship of the equilibrium constant and formal potentials:
	a	b	
KCl	0.05	2980	$lgK^* = lg([UO_2{}^+]^2/[UO_2{}^{2+}]) =$ $(2F/2.303R)\cdot(E^*UO_2{}^{2+}/UO_2{}^+ - E^*UO_2{}^+/UO_2)$
RbCl	-0.17	2400	
CsCl	-0.47	2980	
3LiCl-2KCl	-1.45	1010	
NaCl-KCl	0.966	3855	
NaCl-2CsCl	-0.08	2640	

(2) Evaluation of formal potentials of UO_2 ions in NaCl-2CsCl.

Formal potentials of UO_2 ions are the most fundamental parameters for the Oxide pyroprocess. In Japan, these values have been arbitrary quoted from various research papers or

RIAR's report without any critical point of view. Therefore, authors review these values from the original papers. In this report, we will describe how these potentials are evaluated by the measured by the electro-motive force method. As the result, new correlations are recommended for NaCl-2CsCl melt.

It will be useful to know how the formal potentials of UO_2 ions were measured. In this section, we are going to follow the measurement by the electro-motive force method in KCl melt reported by the Institute of High Temperature Electrochemistry in Russia (used to be the Ural Scientific Center of the Science Academy of the USSR) [5,6]. The measured values of the electro-motive force of the UO_2 electrode in three different temperatures were shown in Table 4.2.5.

Table 4.2.5. Measured electro-motive force at different temperature [6]

1063 K			1153 K			1223 K		
$[UO_2]$, mol%	$Log_{10}[UO_2]$	E, V	[UO2], mol%	$Log_{10}[UO_2]$	E, V	[UO2], mol%	$Log_{10}[UO_2]$	E, V
0.3508	-2.455	-0.801	0.4084	-2.389	-0.787	0.7961	-2.099	-0.731
0.8222	-2.085	-0.753	0.6564	-2.183	-0.762	0.8484	-2.071	-0.72
1.0490	-1.979	-0.74	0.8978	-2.047	-0.738	1.7320	-1.761	-0.688
1.7320	-1.761	-0.712	0.9867	-2.006	-0.728	1.6880	-1.773	-0.679
2.5460	-1.594	-0.691	1.1460	-1.941	-0.719	1.9700	-1.706	-0.664
2.9460	-1.531	-0.682	1.4300	-1.845	-0.711	2.0950	-1.679	-0.658
			2.0500	-1.688	-0.684	2.5670	-1.591	-0.646
			2.3550	-1.628	-0.675			
			2.9320	-1.533	-0.669			

The institute presented the following correlations (Fig. 4.2.1).

$$E = -(0.486 \pm 0.001) + (0.128 \pm 0.001)\log_{10}[UO_2] \pm 0.001 \quad (1063K) \qquad (4.2.27)$$

$$E = -(0.444 \pm 0.009) + (0.144 \pm 0.001)\lg[UO_2] \pm 0.003 \quad (1153K) \qquad (4.2.28)$$

$$E = -(0.396 \pm 0.014) + (0.159 \pm 0.025)\lg[UO_2] \pm 0.006 \quad (1223K) \qquad (4.2.29)$$

If the UO_2 ion exists only as UO_2^{2+}, the following Nernst equation holds.

$$E = E_f(2+/0) + \frac{2.303RT}{nF}\log_{10}\left[UO_2^{2+}\right] \qquad (4.2.30)$$

where $\boldsymbol{n}$ =2.

Fig. 4.2.1. Electromotive force vs total concentration of UO_2 ion

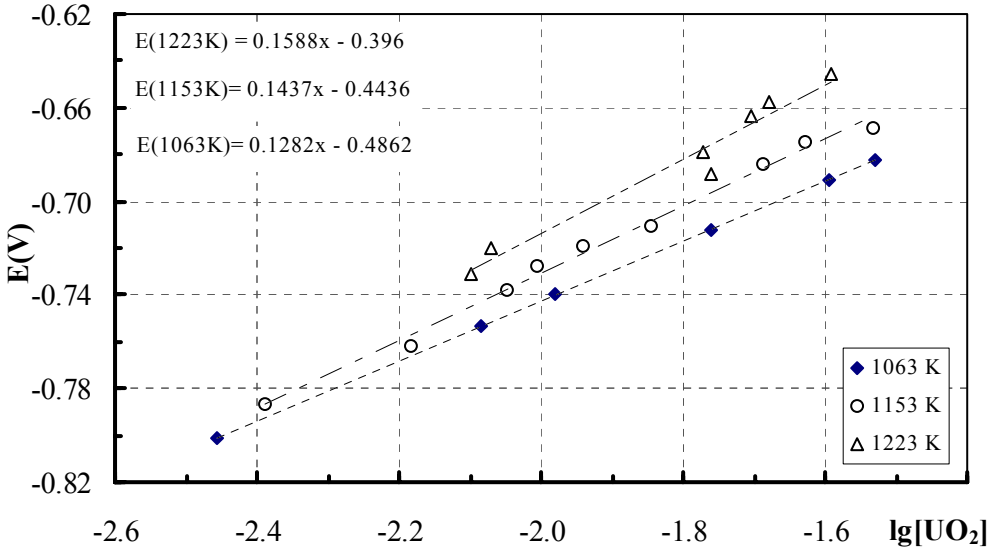

But the following values were calculated for the ***n*** from the Eq.(4.2.27) to (4.2.29).

n =1.64±0.01 (1063K), ***n*** =1.59±0.06 (1153K), ***n*** =1.53±0.13 (1223K)

These values indicate that there are UO_2^+ ions in the melt and Eq. (4.2.30) should be written as follows.

$$E = E_f(+/0) + \frac{2.303RT}{F}\log_{10}\left[UO_2^+\right] = E_f(2+/0) + \frac{2.303RT}{2F}\log_{10}\left[UO_2^{2+}\right] \quad (4.2.31)$$

There is a standard procedure to calculate the E_f by Smirnov [1].

Let's define the ratio of $[UO_2^+]$ to the total uranyl concentration $[UO_2]$;

$$X = [UO_2^+]/([UO_2^+]+[UO_2^{2+}]) = [UO_2^+]/[UO_2]$$

Then Eq.(4.2.31) becomes as follows.

$$E = E_f(+/0) + \frac{2.303RT}{F}\log_{10} X\left[UO_2\right] = E_f(2+/0) + \frac{2.303RT}{2F}\log_{10}(1-X)\left[UO_2\right] \quad (4.2.32)$$

Let's choose two total concentrations of UO_2 ions, say $[UO_2]_{(1)}$ = 0.5mol% and $[UO_2]_{(2)}$=2.0mol%, then the left half of Eq.(4.2.32) becomes as follows.

$$E_{(1)} = E_f(+/0) + \frac{2.303RT}{F}\log_{10} X_{(1)}\left[UO_2\right]_{(1)}$$

$$E_{(2)} = E_f(+/0) + \frac{2.303RT}{F}\log_{10} X_{(2)}\left[UO_2\right]_{(2)}$$

Then,

$$\log_{10}\frac{X_{(2)}}{X_{(1)}} = \frac{F}{2.303RT}\left(E_{(2)} - E_{(1)}\right) - \log_{10}\frac{[UO_2]_{(2)}}{[UO_2]_{(1)}}$$

or
$$\frac{X_{(2)}}{X_{(1)}} = \frac{[UO_2]_{(2)}}{[UO_2]_{(1)}} \exp\left\{\frac{F}{RT}\left(E_{(2)} - E_{(1)}\right)\right\} \tag{4.2.33}$$

The other equation can be obtained by the equilibrium constant K for the following reaction.

$$UO_2^{2+} + UO_2 \Leftrightarrow \quad 2UO_2^{+} \tag{4.2.34}$$

$$K = \frac{[UO_2^+]^2}{[UO_2^{2+}]} = \frac{X^2[UO_2]}{1-X} \tag{4.2.35}$$

Then,

$$\frac{X_{(1)}^2[UO_2]_{(1)}}{1-X_{(1)}} = \frac{X_{(2)}^2[UO_2]_{(2)}}{1-X_{(2)}} \tag{4.2.36}$$

By transforming Eq. (4.2.36),

$$X_{(1)} = \frac{\left(\frac{X_{(2)}}{X_{(1)}}\right)^2 \frac{[UO_2]_{(2)}}{[UO_2]_{(1)}} - 1}{\left(\frac{X_{(2)}}{X_{(1)}}\right)^2 \frac{[UO_2]_{(2)}}{[UO_2]_{(1)}} - \frac{X_{(2)}}{X_{(1)}}} \tag{4.2.37}$$

$X_{(1)}$ can be determined by substituting Eq.(4.2.33) into Eq.(4.2.37).

These calculations were shown in Table 4.2.6. The following correlations were made from the calculated formal potentials as shown in Fig.4.2.2.

$$E_f(+/0) = -0.7199 + 0.4673 \times 10^{-3}\ T \tag{4.2.38}$$

$$E_f(2+/0) = -1.0016 + 0.4601 \times 10^{-3}\ T \tag{4.2.39}$$

Temperature dependence of E_f

The formal potential is related to the free energy of formation by the following equation.

$$E_f = \frac{\Delta G_0}{Z_x \cdot F} + \frac{R \cdot T}{Z_x \cdot F} \ln \gamma_{salt} \tag{4.2.40}$$

where

ΔG_0: Standard free energy of formation of the chloride (J/mol)

Z_x : number of equivalents per mole.

Temperature dependence of the standard free energy is often expressed as follows.

$$\Delta G_0 = G_a + G_b \cdot T \tag{4.2.41}$$

The temperature dependence of the logarithm of activity coefficient is expected to be small so that the formal potential maybe approximated as follows.

$$E_f = \frac{G_a}{Z_x \cdot F} + \frac{1}{Z_x \cdot F}\left(G_b + R \cdot \ln \gamma_{salt}\right) \cdot T = a + b \cdot T \tag{4.2.42}$$

Table. 4.2.6 Calculation of formal potential of Ef(+/0) and Ef(2+/0) from measured electro-motive forces

T, K	$[UO_2]$, mol%	a	b	E (V vs. Cl_2)	$X_{(2)}/X_{(1)}$	$X_{(1)}$	Ef(+/0) (V vs Cl_2)	Ef(2+/0) (V vs Cl_2)
1063	0.50	-0.486	0.128	-0.781	0.580	0.451	-0.222	-0.510
1063	2.00	-0.486	0.128	-0.703				
1153	0.50	-0.444	0.144	-0.775	0.598	0.518	-0.184	-0.476
1153	2.00	-0.444	0.144	-0.689				
1223	0.50	-0.396	0.159	-0.762	0.620	0.586	-0.147	-0.436
1223	2.00	-0.396	0.159	-0.666				

Fig. 4.2.2. Fitting of Ef(+/0) and Ef(2+/0)

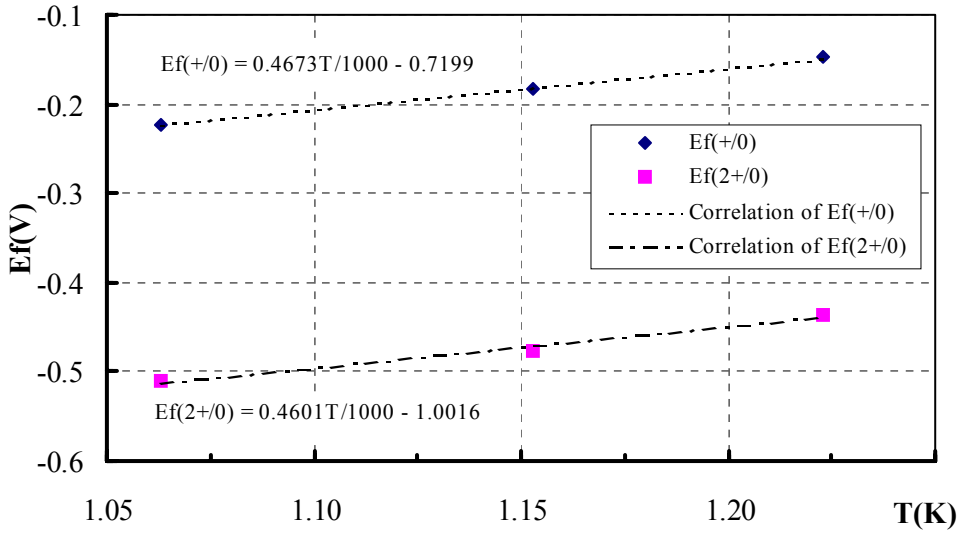

UO_2(2+/0) in NaCl-2CsCl

The parameters of Eq.(4.2.42) for UO_2(2+/0) are given in the upper part of Table 4.2.7 for KCl, RbCl, CsCl, 3LiCl-2KCl, and NaCl-KCl. Theses values were evaluated by the Institute of High Temperature Electrochemistry [5,6] in the same manner as described in the former section. The potentials at 650°C are also given in the Table. However, that of 2CsCl-NaCl is not given. Therefore, the following correlation [2] is used to obtain more universal equation.

$$a = a_0 + \frac{a_1}{r_{Me+}} \quad , \quad b = b_0 + \frac{b_1}{r_{Me+}} \tag{4.2.43}$$

where r_{Me+}: Ion radius of the salt (nm).

The following correlations are satisfactory as shown in the fitting results below (Fig. 4.2.3).

$$a = -1.6614 + \frac{0.0845}{r_{Me+}} \quad , \; b \cdot 1000 = 0.6519 - \frac{0.0219}{r_{Me+}} \qquad (4.2.44)$$

Table 4.2.7. Evaluation of Formal potential of $UO_2(2+/0)$ in NaCl-2CsCl

Experimental data						
Melt	r_{Me}^{+}(nm)	$1/r_{Me}^{+}$(nm)	T	a	$b \cdot 10^3$	Ef(vs. Cl)
KCl	0.133	7.519	923.15	-1.008	0.466	-0.578
RbCl	0.149	6.711	923.15	-1.085	0.500	-0.623
CsCl	0.165	6.061	923.15	-1.172	0.538	-0.675
NaCl-KCl	0.115	8.696	923.15	-0.920	0.463	-0.493
3LiCl-2KCl	0.095	10.526	923.15	-0.783	0.429	-0.387
New correlation						
NaCl-2CsCl	0.143	6.993	923.15	-1.070	0.499	-0.610

Fig. 4.2.3. Fitting of Ef parameters for $UO_2(2+/0)$
(Ef = a + b·T)

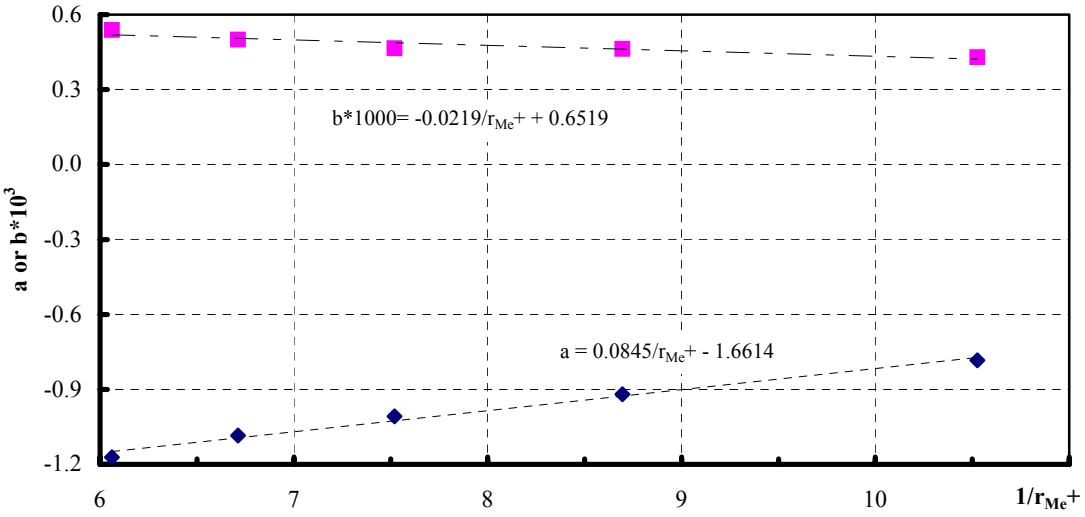

By substituting $r_{Me+} = 0.143$ nm in Eq.(4.2.44), the formal potential of $UO_2(2+/0)$ in 2CsCl-NaCl is given as follows.

$$E_f(2+/0) = -1.070 + 0.499 \times 10^{-3} \, T \qquad (4.2.45)$$

Then, the formal potential at 650°C becomes –0.61 V as shown in the bottom of Table 4.2.7.

UO_2(+/0) in NaCl-2CsCl

The formal potential of UO_2(+/0) in NaCl-2CsCl is evaluated by the same manner as UO_2(2+/0) as shown in Table 4.2.8. But the parameters for 3LiCl-2KCl were excluded from the correlation because their tendencies are so different from the linearity for other melts.

The following correlations are satisfactory as shown in the fitting results below Fig. 4.2.4.

$$a = -1.9493 + \frac{0.1633}{r_{Me+}} \quad , \tag{4.2.46}$$

Fig. 4.2.4. Fitting of Ef parameters for UO_2(+/0)

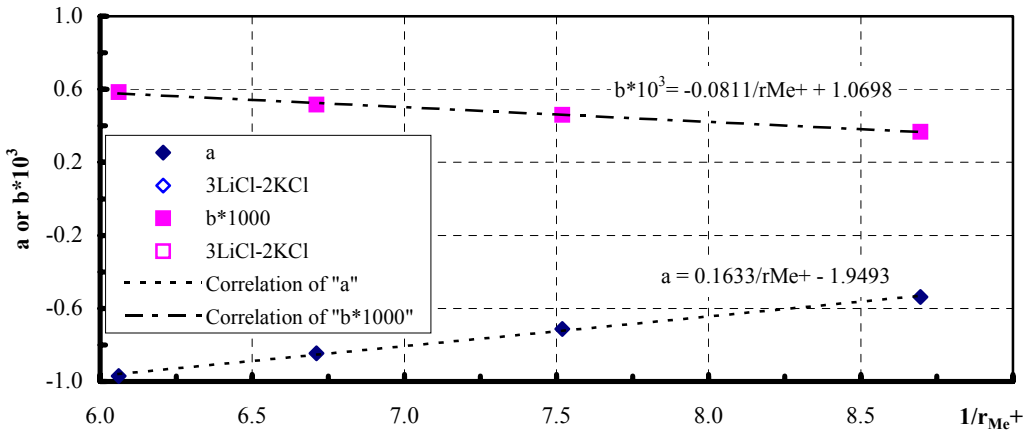

By substituting r_{Me+} = 0.143 nm in Eq.(4.2.46), the formal potential of UO_2(+/0) in 2CsCl-NaCl is given as follows.

$$E_f(+/0) = -0.807 + 0.503 \times 10^{-3}\ T \tag{4.2.47}$$

Then, the formal potential at 650°C becomes –0.343 V as shown in the bottom of Table 4.2.8.

UO2(2+/+) in NaCl-2CsCl

The formal potential of UO_2(2+/+) in NaCl-2CsCl can be calculated by using the following relation.

$$2E_f(2+/0) = E_f(2+/+) + E_f(+/0) \tag{4.2.48}$$

The results are shown in Table 4.2.9. The formal potential of UO_2(2+/+) in 2CsCl-NaCl is given as follows.

$$E_f(2+/+) = -1.334 + 0.495 \times 10^{-3}\ T \tag{4.2.49}$$

Then, the formal potential at 650°C becomes –0.877 V as shown in the bottom of Table 4.2.9.

Table 4.2.8. Evaluation of formal potential of UO_2(+/0) in NaCl-2CsCl

Experimental data						
Melt	r_{Me}^{+}(nm)	$1/r_{Me}^{+}$(nm)	T	a	$b \cdot 10^3$	Ef(vs. Cl)
KCl	0.133	7.519	923.15	-0.712	0.460	-0.287
RbCl	0.149	6.711	923.15	-0.846	0.517	-0.369
CsCl	0.165	6.061	923.15	-0.970	0.585	-0.430
NaCl-KCl	0.115	8.696	923.15	-0.537	0.367	-0.198
3LiCl-2KCl	0.095	10.526	923.15	-0.683	0.573	-0.154
New correlation						
NaCl-2CsCl	0.143	6.993	923.15	-0.807	0.503	-0.343

Table 4.2.9. Evaluation of formal potential of UO_2(2+/+) in NaCl-2CsCl

Calculated data by Eq.(4.2.48)						
Melt	r_{Me}^{+}(nm)	$1/r_{Me}^{+}$(nm)	T	a	$b \cdot 10^3$	Ef(vs. Cl)
KCl	0.133	7.519	923.15	-1.304	0.472	-0.868
RbCl	0.149	6.711	923.15	-1.324	0.483	-0.878
CsCl	0.165	6.061	923.15	-1.374	0.491	-0.921
NaCl-KCl	0.115	8.696	923.15	-1.303	0.559	-0.787
3LiCl-2KCl	0.095	10.526	923.15	-0.883	0.285	-0.620
New correlation						
NaCl-2CsCl	0.143	6.993	923.15	-1.334	0.495	-0.877

4.2.3. Kinetic of tetravalent uranium oxidation with oxygen

Tetravalent uranium can be oxidized with oxygen in the chloride melt by the following reaction

$$UCl_{4(melt)} + O_{2(gas)} = UO_2Cl_{2(melt)} + Cl_{2(gas)}. \quad (4.2.50)$$

Kinetics of tetravalent uranium oxidation reaction by oxygen has been studied by spectrophotometry method in NaCl-2CsCl melt [7].

Spectrophotometry lab facility allowed working with uranium and plutonium solutions in different molten salt electrolytes at the temperature of spectrophotometry cell from 350 to 800°C with the ±2° set-on accuracy. The heating block of the high temperature spectrophotometry facility is shown on Fig. 4.2.5.

Uranium tetrachloride absorption spectrum in near infrared region of spectra (800 – 2500 nm) is shown on Fig. 4.2.6.

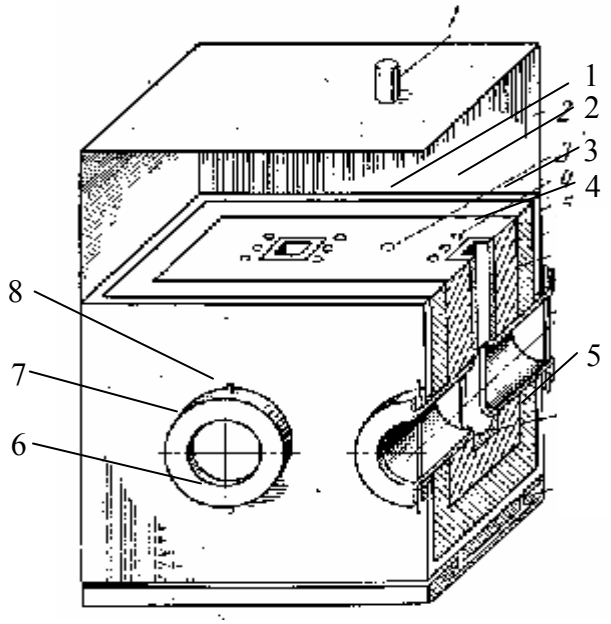

Fig. 4.2.5. Heating element for the spectrophotometer [8].
1 – seating slot for the thermocouple; 2 – apertures for a spiral; 3 - the block made from the heat-resisting steel; 4 – spectrophotometry cell holder; 5 – thermal insulation; 6 – jacket of cooling; 7 – windows cooling; 8 –

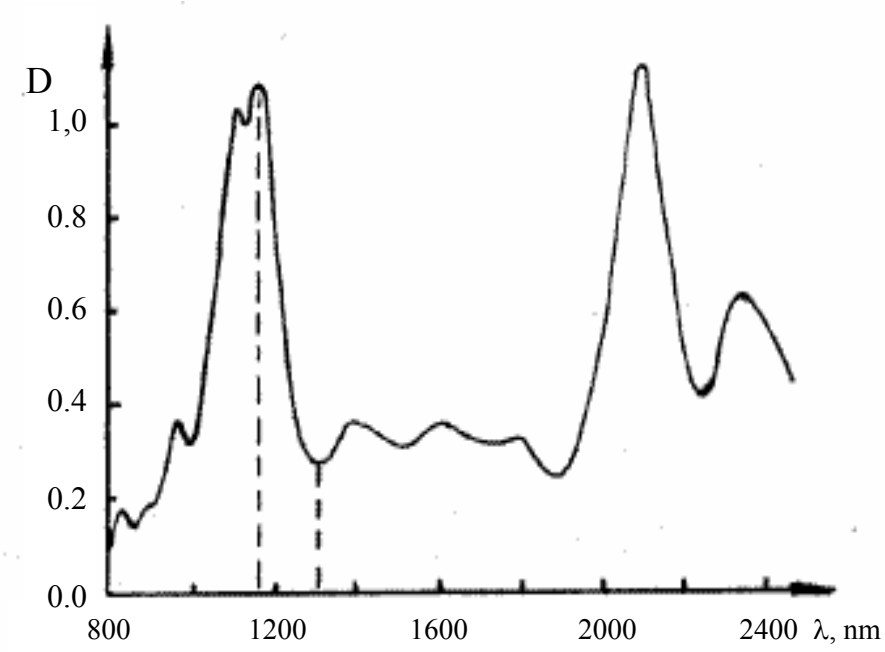

Fig. 4.2.6. Absorption spectrum of uranium (IV) in NaCl-2CsCl melt at 550°C. $C_{U(IV)}$ = 1.15·10-4 mole/cm^3 [7].

The 1 cm spectrophotometry cell made from optical grade quartz was used. During the reaction (4.2.50) the optical absorption of melt was measured at wavelength of 1165 nm, when [U (IV)] < $0.12 \cdot 10^{-3}$ mole/cm^3, and at wavelength of 1310 nm, when [U (IV)] > $0.12 \cdot 10^{-3}$ mole/cm^3. Uranium (VI) has no light-absorption in the wavelengths of 750 - 2500 nm. The absorption bands of uranium (V) were not found.

Values of the molar extinction coefficient of uranium (IV) in NaCl-2CsCl melt are presented in Table 4.2.10.

Table 4.2.10. Values of molar extinction coefficient of uranium (IV) in NaCl-2CsCl melt [7]

T, °C	ε^{1165}, cm^2/mole	ε^{1310}, cm^2/mole
550	$(9.3 \pm 0.2) \cdot 10^3$	$(2.3 \pm 0.1) \cdot 10^3$
650	$(8.5 \pm 0.2) \cdot 10^3$	$(2.5 \pm 0.1) \cdot 10^3$
750	$(7.9 \pm 0.2) \cdot 10^3$	$(2.7 \pm 0.1) \cdot 10^3$

Typical kinetic curve of uranium (IV) oxidation reaction with oxygen obtained at 550°C is shown on Fig. 4.2.7. Dependence of reaction rate on uranium (IV) concentration is show in Fig. 4.2.8. One can see, that at the [U(IV)] > $0.1 \cdot 10^{-3}$ mole/cm^3 the reaction kinetics can be described by the zeroth-order equation concerning uranium (IV) concentration, i.e.:

$$R = - \frac{d[U(IV)]}{d\tau} = k^*_0. \qquad (4.2.51)$$

At the [U(IV)] < $0.1 \cdot 10^{-3}$ mole/cm^3 the reaction kinetics may be described by equation:

$$R = - \frac{d[U(IV)]}{d\tau} = k^*_1 + k^*_2 \cdot [U(IV)]. \qquad (4.2.52)$$

At 650 and 750°C the reaction has the zeroth-order practically up to end.

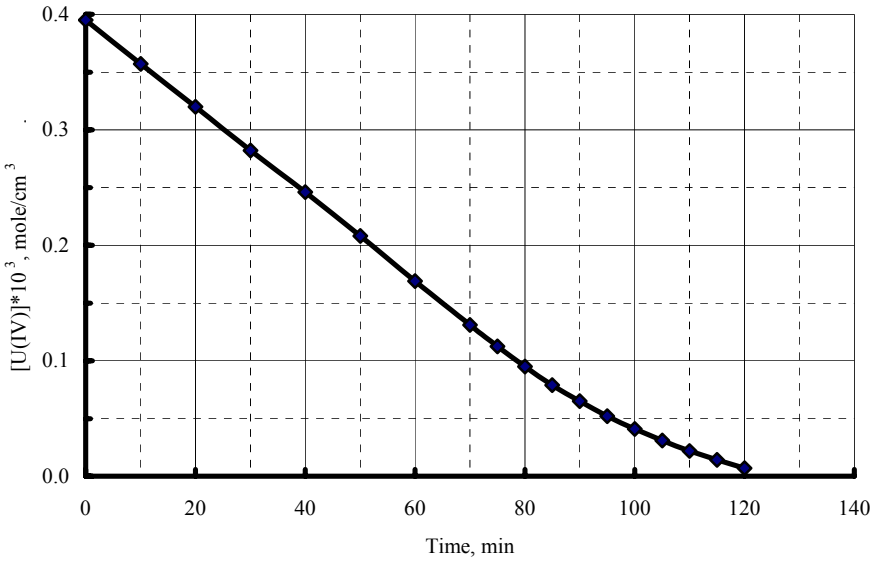

Fig. 4.2.7. Kinetic curve of U(IV) oxidation with oxygen in NaCl-2CsCl melt at 550°C. The specific "melt - gas" surface is equal 0.475 sm^{-1} [7].

Value of the specific "melt - gas" surface (a') was calculated by the following equation:

$$a' = [S_c + \pi \cdot (D_b^2 \cdot \alpha \cdot \tau_b \cdot w - D_t^2/4] \cdot d_m/P$$

where

S_c is the melt surface at gas bubbling in the spectrophotometry cell, S_c = 0.50cm^2;

D_b is diameter of gas babbles in melt, D_b= 0.40cm, measured with photography method;

α is the amount of bubbles arising in melt at passage of 1cm^3 of gas-reagent, α = 29cm^{-3};

τ_b is the bubble lifetime, $\tau_b = 3.7 \cdot 10^{-3}$min;

w is the gas flow, $w = 15 \div 31 cm^3/min$;

D_t is the internal diameter of the gas supply tube, $D_t = 0.41$cm;

d_m is the NaCl-2CsCl melt density, g/sm^3, $d_m = 3.175 - 10.01 \cdot 10^{-4} g/cm^3$;

P is the melt mass, P = 8.9g.

The specific "melt - gas" surface can be described by expressions (w is in cm^3/min):

550°C $a' = 0.148 + 0.0164 \cdot w$, cm^{-1};
650 °C $a' = 0.143 + 0.0157 \cdot w$, cm^{-1};
750 °C $a' = 0.137 + 0.0151 \cdot w$, cm^{-1}.

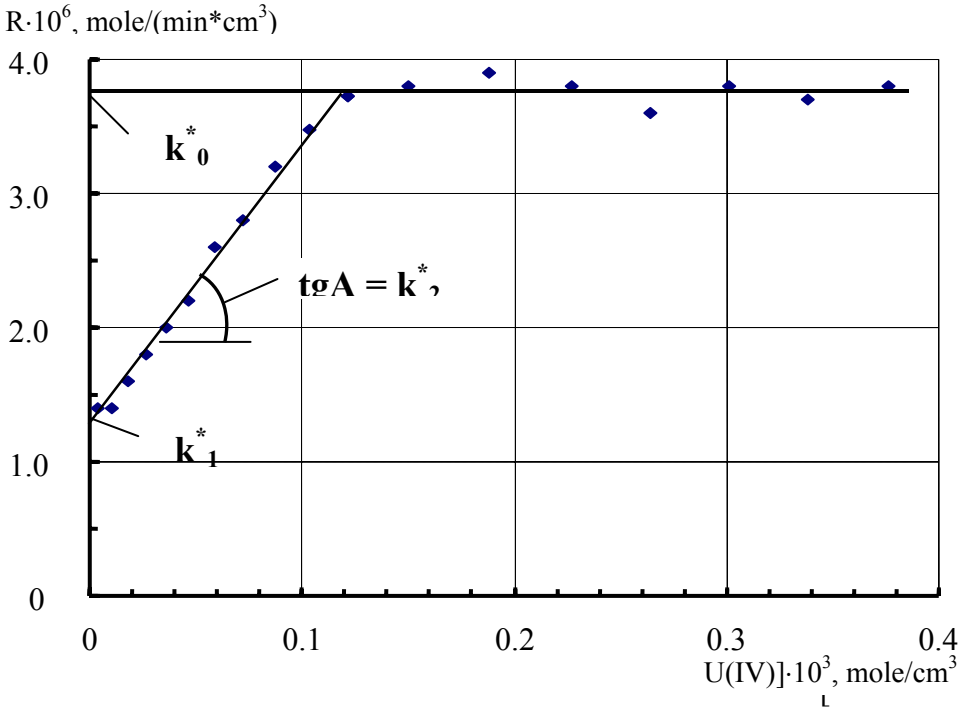

Fig. 4.2.8. Reaction rate dependence of uranium-IV oxidation by oxygen from U(IV) concentration in the NaCl-2CsCl melt at 550°C. (a = 0.475 cm^{-1}) [7]

The dependences of k^*_0, k^*_1 and k^*_2 parameters from a specific interphase surface "melt – gas" are shown in Fig. 4.2.9.

The Fig 4.2.9 data show that all kinetic parameters change proportionally to the value of specific interphase surface, i.e.:

$$k^*_0 = k_0 \cdot a'; \quad k^*_1 = k_1 \cdot a'; \quad k^*_2 = k_2 \cdot a';$$

and

$$R = R_0 \cdot a'.$$

Consequently, the all stages of reaction (4.2.27) take place on the melt surface or near it.

Fig. 4.2.10 demonstrates the influence of gas reagent composition on the reaction rate at high concentration of tetravalent uranium in the melt (the case when the reaction has the zeroth order concerning uranium (IV) concentration). The mixture of O_2 with He and O_2 with Cl_2 was used.

One can see two phenomena. The first (See Fig. 4.2.10, curves 1, 2 and 3), the rate reaction increases proportionally to partial pressure of oxygen in its mixture with helium:

$$R_0 = k_0 \cdot Po_2. \qquad (4.2.53)$$

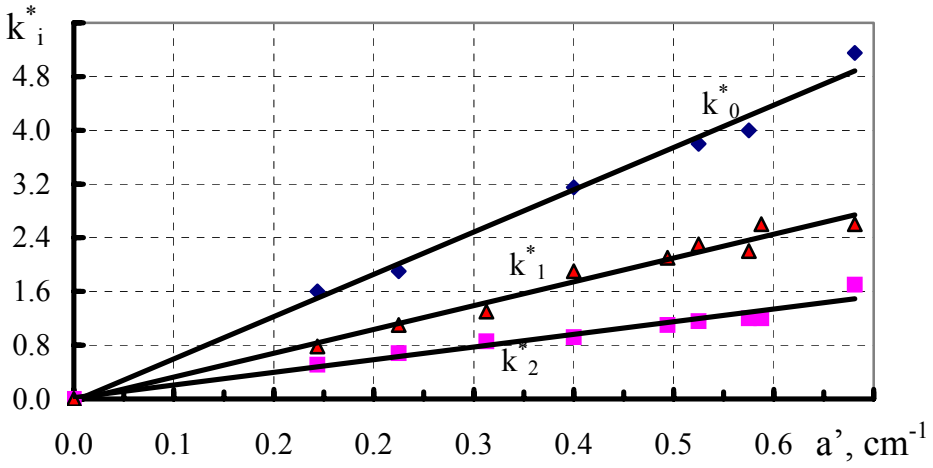

Fig. 4.2.9. Dependence of $k^*_0 \cdot 10^6$ (mole/min·cm^3), $k^*_1 \cdot 10^6$ (mole/min·cm^3) and $k^*_2 \cdot 10^2$ (cm/min) from specific interphase surface a' [7].
T = 550°C, $Po_2 = 1.0 \cdot 10^{-5}$Pa.

The second (See Fig. 4.2.10, curves 1', 2' and 3'), the chlorine gas reduces the rate reaction at all temperature.

The treatment of experimental data allowed finding the equation describing relationship between the reaction rate and the chlorine gas content in its mixture with oxygen:

$$\frac{k_0 \cdot Po_2}{R} = kCl_2 \cdot P_{Cl_2}^{1/2} + 1 \qquad (4.2.54)$$

In coordinates "Po_2/R - $P_{Cl_2}^{1/2}$", the experimental data can be approximated by straight lines. (See Fig. 4.2.11).

So, the kinetics of tetravalent uranium oxidation reaction with oxygen can be described by following empirical equation:

$$R = a' \cdot \frac{k_0 \cdot Po_2}{kCl_2 \cdot P_{Cl_2}^{1/2} + 1} \qquad (4.2.55)$$

where R is the rate of U(IV) oxidation reaction with oxygen, mole/(cm^2·min); a' is the specific interphase surface "melt – gas", cm^2/cm^3; k_0 is the parameter at the oxygen partial pressure, mole/(cm^2·Pa·min); kCl_2 is the parameter at the chlorine gas partial pressure, Pa$^{-1/2}$.

The following equations describe the temperature dependence of k_0 and kCl_2 parameters:

$$Log k_0 = -5.03 - 3680/T \pm 0.04, \qquad (4.2.56)$$

$$Log kCl_2 = -0.80 - 1500/T \pm 0.06. \qquad (4.2.57)$$

On the basis of analysis of the experimental data obtained by studying of the kinetics of tetravalent uranium oxidation reaction by oxygen, it is possible to conclude that chemical absorption process of oxygen by the melt is limiting the reaction rate.

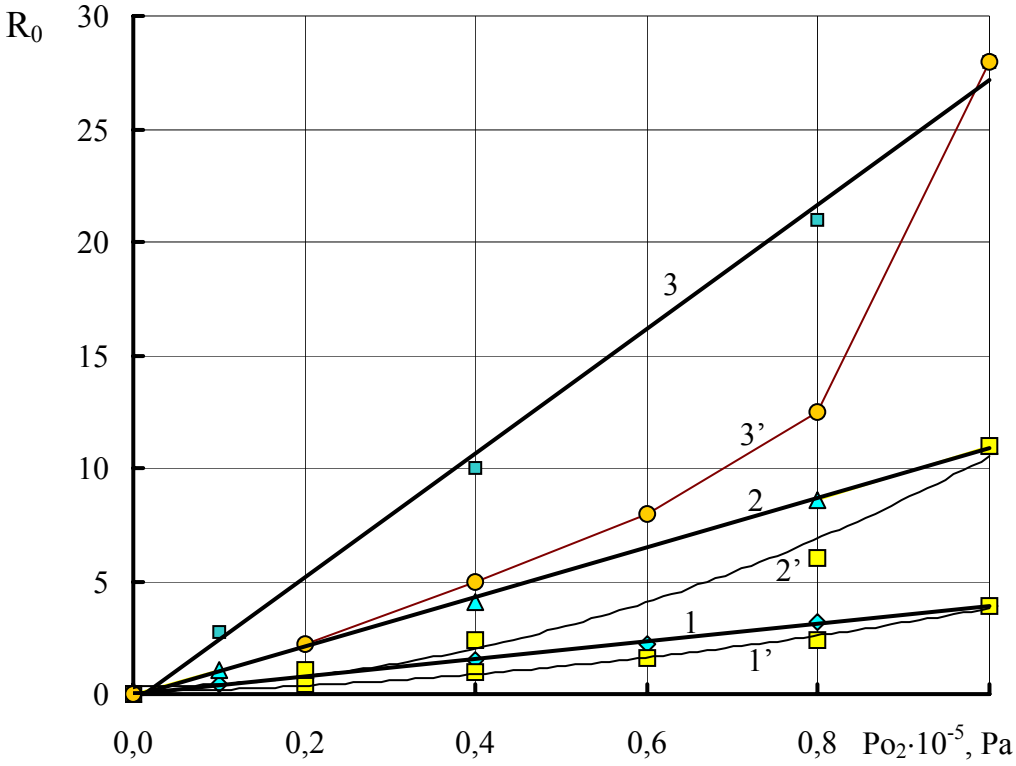

Fig. 4.2.10. Dependence of $R_0 \cdot 10^{-6}$ (mole/min·cm^3) from the gas reactant composition. 1, 2, 3 – gas reactant is O_2-He mixture; 1', 2', 3' – gas reactant is O_2-Cl_2 mixture [7]. 1, 1' – 550°C, a' = 0.475 cm^{-1}; 2, 2' – 650°C, a' = 0.457 cm^{-1}; 3, 3' – 750°C, a' = 0.439 cm^{-1}.

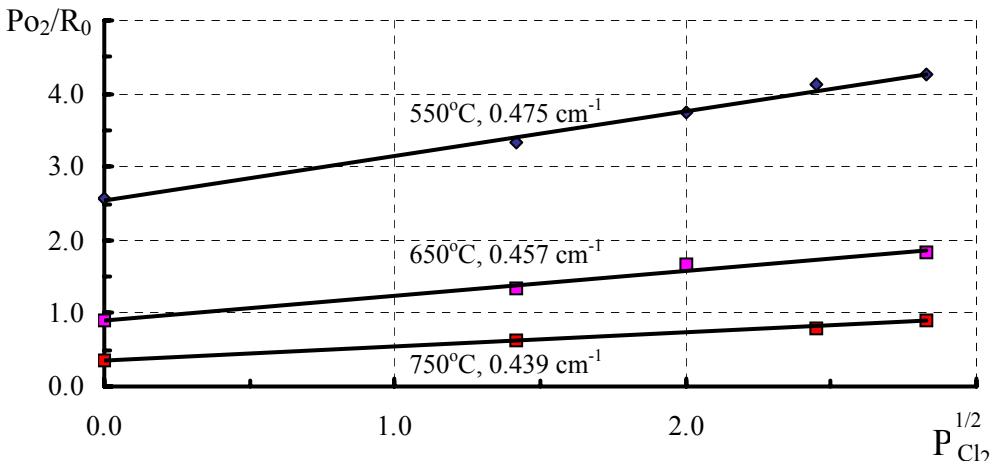

Fig. 4.2.11. "Po_2/R - $P_{Cl_2}^{1/2}$" dependence.

The following reactions of oxygen and it ions were taken into account at the development of the mechanism of reaction of tetravalent uranium oxidation with oxygen [7]:

$$\begin{aligned}
&1 \quad O_{2(gas)} + Cl^-_{(melt)} \underset{k_1^-}{\overset{k_1^+}{\rightleftharpoons}} O_2^-{}_{(melt)} + 1/2\ Cl_{2(gas)} \\
&2 \quad O_2^-{}_{(melt)} + Cl^-_{(melt)} \underset{k_2}{\overset{k_2^+}{\rightleftharpoons}} O_2^{2-}{}_{(melt)} + 1/2\ Cl_{2(gas)} \\
&3 \quad O_2^{2-}{}_{(melt)} + 2Cl^-_{(melt)} \overset{k_3^+}{\rightleftharpoons} 2\ O^{2-}{}_{(melt)} + Cl_{2(gas)}
\end{aligned} \qquad (4.2.58)$$

The most satisfactory interpretation of the experiment results was achieved by the following assumptions:

- Direct reaction of stage 1, i.e. the reaction

$$O_{2(gas)} + Cl^-_{(melt)} \rightarrow O_2^-{}_{(melt)} + 1/2\ Cl_{2(gas)},$$

is the slowest and it limits the rate of the tetravalent uranium oxidation process with oxygen as a whole;

- Peroxide anions oxidize tetravalent uranium on reaction

$$O_2^{2-}{}_{(melt)} + U^{4+}_{(melt)} \rightarrow UO_2^{2+}{}_{(melt)}.$$

This reaction is irreversible and has the rate exceeding the rate of the peroxide anions diffusion into the melt bulk.

Some comments to the kinetic data interpretation

There is a case of the momentary irreversible reaction.

The specific rate of the momentary irreversible reaction (R_0) can be described by equation, which is taking into account the diffusion processes. Using "the film model" of the "gas-liquid reactions" [9], the equation have been obtained

$$R_0 = \frac{D_{O_2^{2-}}}{\delta} \cdot [O_2^{2-}] + \frac{D_{U^{4+}}}{\delta} \cdot [U^{4+}]. \qquad (4.2.59)$$

According to the reaction scheme (4.2.58) the accumulation rate of peroxide anions on the melt surface ($V_{O_2^{2-}}$) can be described by the equation

$$V_{O_2^{2-}} = \frac{k'^{+}_1 \cdot P_{O_2}}{(k'^{-}_1/k'^{+}_2) \cdot P_{Cl_2}^{1/2} + 1} + (k'^{-}_2 \cdot P_{Cl_2}^{1/2} + k'^{+}_3) \cdot [O_2^{2-}]. \qquad (4.2.60)$$

The quasi-stationary concentration method for the oxygen anions was used [10].

In the stationary state the specific rate of the peroxide anions accumulation on the melt is equal to the rate of the uranium (IV) oxidation reaction with oxygen, i.e. $R_0 = V_{O_2^{2-}}$. Due to that, the following equations describing the peroxide anions concentration on the melt surface ($[O_2^{2-}]$) and the specific uranium (IV) oxidation rate with oxygen (R_0), were obtained.

$$[O_2^{2-}] = \frac{\dfrac{k'^{+}_1 \cdot P_{O_2}}{(k'^{-}_1/k'^{+}_2) \cdot P_{Cl_2}^{1/2} + 1} - \dfrac{D_{U^{4+}}}{\delta} \cdot [U^{4+}]}{\dfrac{D_{O_2^{2-}}}{\delta} + k'^{-}_2 \cdot P_{Cl_2}^{1/2} + k'^{+}_3} \qquad (4.2.61)$$

$$R_0 = \frac{\frac{Do_2^{2-}}{\delta} \cdot \frac{k'^{+}_1 \cdot P_{O_2}}{(k'^{-}_1/k'^{+}_2) \cdot P_{Cl_2}^{1/2} + 1} + (k'^{-}_2 \cdot P_{Cl_2}^{1/2} + k'^{+}_3) \cdot [U^{4+}]}{\frac{Do_2^{2-}}{\delta} + k'^{-}_2 \cdot P_{Cl_2}^{1/2} + k'^{+}_3} \qquad (4.2.62)$$

There is possibility to separate three states, which it is better to consider with diagram of the concentrations profile of uranium (IV) and peroxide anions presented on Fig. 4.2.12.

At first, if in numerator of equation (4.2.61) the members are equal among themselves, i.e.:

$$\frac{k'^{+}_1 \cdot P_{O_2}}{(k'^{-}_1/k'^{+}_2) \cdot P_{Cl_2}^{1/2} + 1} = \frac{D_U^{4+}}{\delta} \cdot [U^{4+}]$$

the concentrations of uranium (IV) and peroxide anions on the melt surface are zero. In this state the uranium (IV), diffusing across the laminar film, reaches the melt surface in the chemical equivalent amounts with the peroxide anions forming on reaction of oxygen with chloride anions.

Secondly, when $\frac{k'^{+}_1 \cdot P_{O_2}}{(k'^{-}_1/k'^{+}_2) \cdot P_{Cl_2}^{1/2} + 1} < \frac{D_U^{4+}}{\delta} \cdot [U^{4+}]$, the equation (4.2.62) does not work.

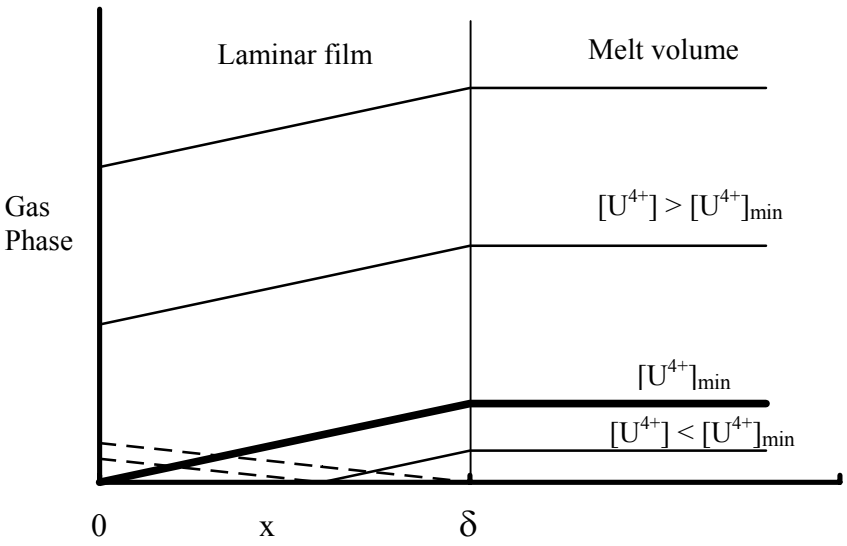

Fig. 4.2.12. Profile of the uranium (IV) (——) and O_2^{2-}anions (– – –) concentration in laminar film near the surface of the melt.

In this state, according to equation (4.2.60), the reaction rate of uranium (IV) oxidation with oxygen is equal to the reaction rate of peroxide anion formation on the melt surface:

$$R_0 = \frac{k'^{+}_1 \cdot P_{O_2}}{(k'^{-}_1/k'^{+}_2) \cdot P_{Cl_2}^{1/2} + 1}$$

And finally, if $\frac{k'^{+}_1 \cdot P_{O_2}}{(k'^{-}_1/k'^{+}_2) \cdot P_{Cl_2}^{1/2} + 1} > \frac{D_U^{4+}}{\delta} \cdot [U^{4+}]$, the equation (4.2.62) describes the kinetics of the studied reaction.

A lot of attention has been paid to the reaction mechanism of the tetravalent uranium oxidation by oxygen, since kinetic laws describing the oxidation process of tetravalent

uranium by oxygen extend to the oxidation process of reduced plutonium forms by oxygen. Therefore it is clear, what they are meaning for the MOX fuel preparation by the electrolysis and for the plutonium dioxide preparation by the volume precipitation method.

4.2.4. Estimation of diffusion coefficients for U^{3+}, U^{4+} and UO_2^{2+}

4.2.4.1. Experimental data

Diffusion coefficients of U^{3+}, U^{4+} and UO_2^{2+} in NaCl-2CsCl and 3LiCl-KCl are estimated from existing coefficients in other melts. The following correlations are derived [11-14].

(1) NaCl-2CsCl U^{3+}: $Log_{10}D(cm^2/s) = - 2.6533 - 1949.8/T(K)$

U^{4+}: $Log_{10}D(cm^2/s) = - 2.2438 – 2564.1/T(K)$

UO_2^{2+}: $Log_{10}D(cm^2/s) = - 2.8087 – 1834.9/T(K)$

(2) 3LiCl-2KCl. U^{3+}: $Log_{10}D(cm^2/s) = - 2.5651 – 1739.2/T(K)$

U^{4+}: $Log_{10}D(cm^2/s) = - 2.3255 – 2103.6/T(K)$

As for UO_2^{2+}, the following correlation is accepted.

UO_2^{2+}: $Log_{10}D(cm^2/s) = - 2.88 – 1640/T(K)$

Specific values are calculated as follows (Table 4.2.11).

Table 4.2.11. Estimated diffusion coefficients in NaCl-2C and 3LiCl-2KCl melts

Ions	In NaCl-2CsCl at 650°C	In 3LiCl-2KCl at 500°C
U^{3+}	$1.72 \cdot 10^{-5}$	$1.53 \cdot 10^{-5}$
U^{4+}	$9.51 \cdot 10^{-6}$	$8.99 \cdot 10^{-6}$
UO_2^{2+}	$1.60 \cdot 10^{-5}$	$9.97 \cdot 10^{-6}$

As for other actinides such as Pu, Np and Am, it will be appropriate to use the D of U for other actinides when there is no reliable data.

The most extensive experimental data for the diffusion coefficients (D) in various melt are summarized in Table 4.2.12 [11 - 14] where,

$$Log_{10}D(cm^2/s) = a + b/T(K) \quad (4.2.63)$$

Diffusion coefficients (cm^2/sec) of uranium ions in various salt electrolytes may be calculated with the help of the equations given in [14]. It is accepted to count the diffusion coefficient of UO_2^+ cations is proximally twice more than $D_{UO_2^{2+}}$.

No coefficient is provided for U^{3+} and U^{4+} in 3LiCl-KCl in the Table 4.2.12. It was indicated that those values in NaCl-2CsCl are calculated but there is no explanation on how the values

were calculated. Therefore, it will be worthwhile to study more general correlations for various melts so that the coefficients in 3LiCl-KCl and NaCl-2CsCl can be estimated.

Table 4.2.12. Diffusion coefficient of uranium ions [11-14]

Melt	$LgDU^{3+} = a + b/T$		$LgDU^{4+} = a' + b'/T$		$LgDUO_2^{2+} = a'' + b''/T$	
	- a	- b	- a'	- b'	- a''	- b''
NaCl	2.66	1690	2.42	2040	-	-
KCl	2.61	1940	2.51	2200	2.79	1815
RbCl	2.69	1970	2.18	2700	2.79	1855
CsCl	2.73	2010	1.80	3190	2.84	1870
3LiCl-2KCl	-	-	-	-	2.88	1640
NaCl-KCl	2.48	1920	2.02	2580	2.79	1790
NaCl-2CsCl*	2.65	1960	2.32	2480	2.79	1840

* - calculated data.

Correlation study: Dependence of the coefficients "a" and "b" to ion radius of the melts

(1) U^{3+}

The coefficients "-a" and "-b/1000" for U^{3+} in Table 4.2.11 are plotted vs. the inverse of ion radius of the melts; $1/R_{Me}^{+}$(nm) in Fig. 4.2.13 and Fig.4.2.14. The following correlations are obtained.

$$-a = 2.8448 - 0.0269/R_{Me}^{+} \quad (4.2.64)$$

$$-b/1000 = 2.4624 - 0.0711/R_{Me}^{+} \quad (4.2.65)$$

The R^2 values of correlations are generally small; the dependence to $1/R_{Me}^{+}$ is not so strong.

Fig. 4.2.13. –a vs. $1/R_{Me}^{+}$ for U(3+)

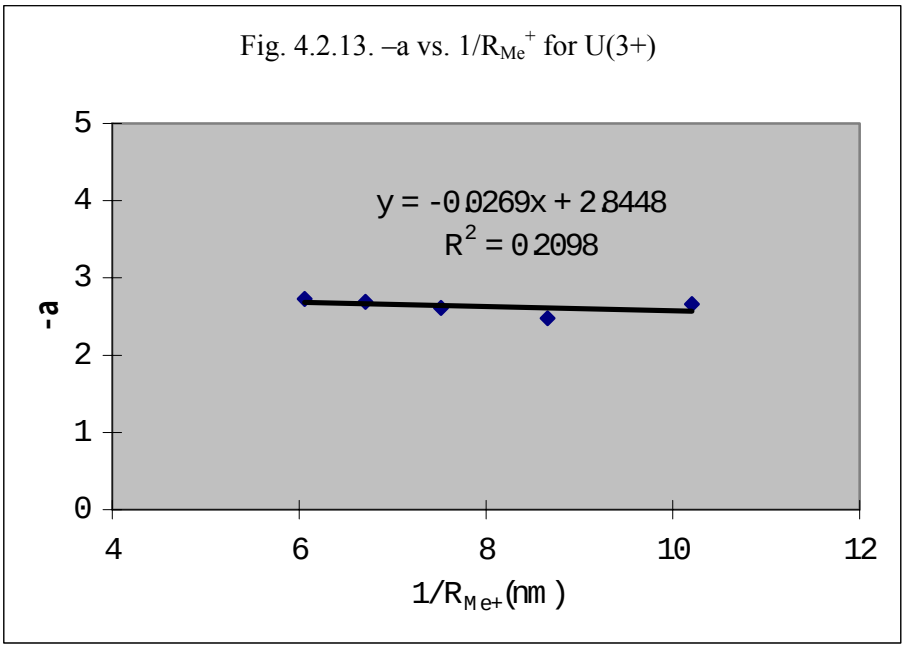

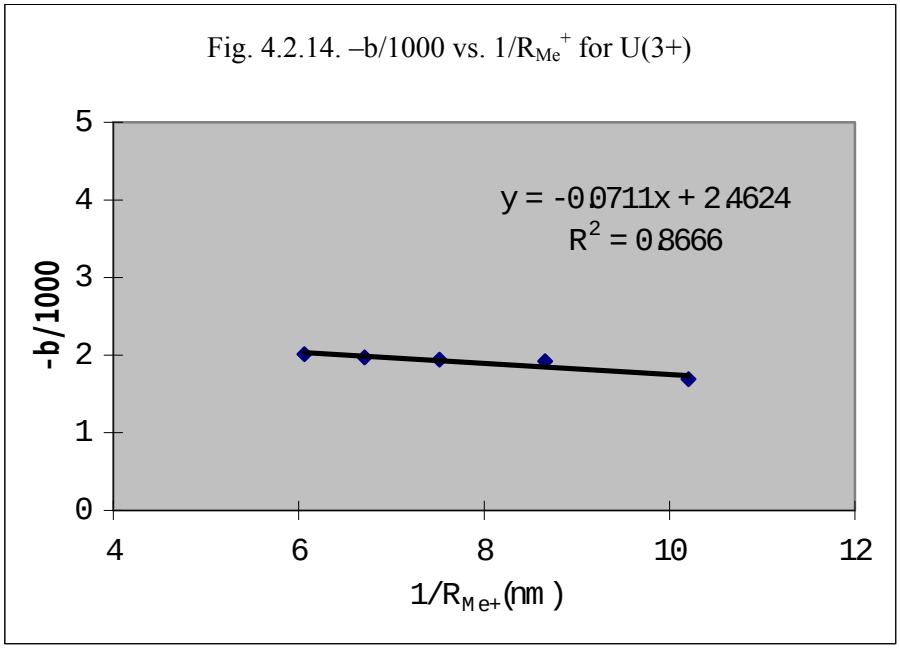

Fig. 4.2.14. –b/1000 vs. $1/R_{Me}^{+}$ for U(3+)

(2)U^{4+}

The coefficients "-a" and "-b/1000" for U^{4+} in Table 4.2.11 are plotted vs. the inverse of ion radius of the melts; $1/R_{Me}^{+}$(nm) in Fig. 4.2.15 and Fig.4.2.16. The following correlations are obtained.

$$-a = 1.456 + 0.0932/R_{Me}^{+} \quad (4.2.66)$$

$$-b/1000 = 4.2655 - 0.2201/R_{Me}^{+} \quad (4.2.67)$$

The R^2 values of correlations are generally small; the dependence to $1/R_{Me}^{+}$ is not so strong.

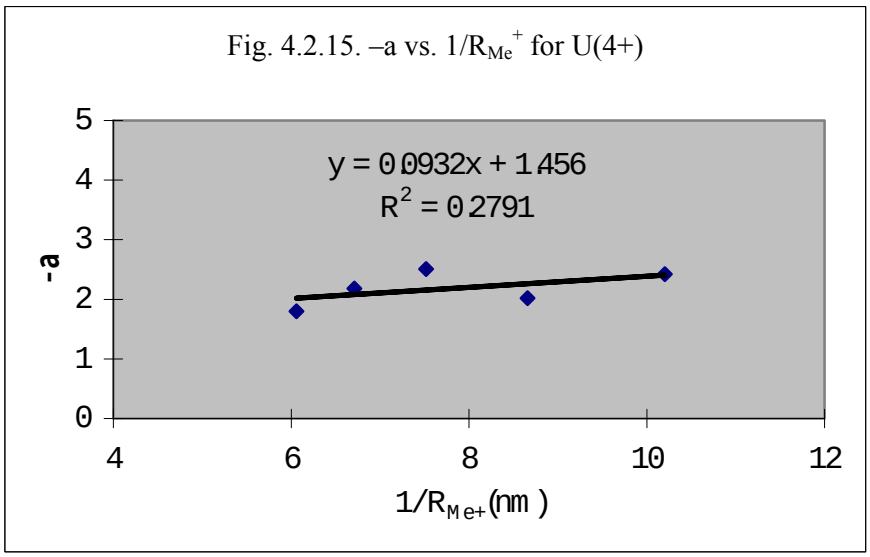

Fig. 4.2.15. –a vs. $1/R_{Me}^{+}$ for U(4+)

Fig. 4.2.16. –b/1000 vs. $1/R_{Me}^{+}$ for U(4+)

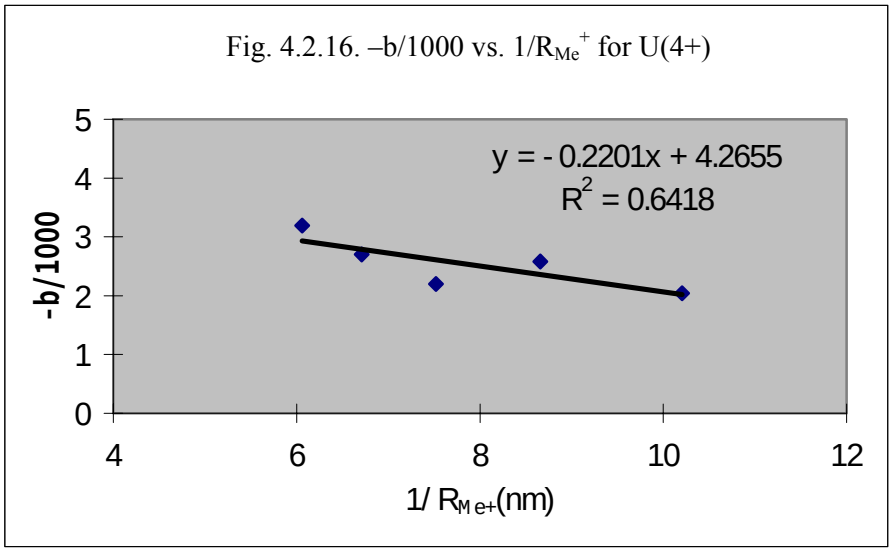

(3) UO_2^{2+}

The coefficients "-a" and "-b/1000" for UO_2^{2+} in Table 4.2.11 are plotted vs. the inverse of ion radius of the melts; $1/R_{Me}^{+}$(nm) in Fig.4.2.17 and Fig.4.2.18. The following correlations are obtained.

$$-a = 2.7255 + 0.0117/R_{Me}^{+} \quad (4.2.68)$$

$$-b/1000 = 2.1865 - 0.0496/R_{Me}^{+} \quad (4.2.69)$$

The R^2 values of correlations are generally small; the dependence to $1/R_{Me}^{+}$ is not so strong.

Fig. 4.2.17. –a vs. $1/R_{Me}^{+}$ for UO_2(2+)

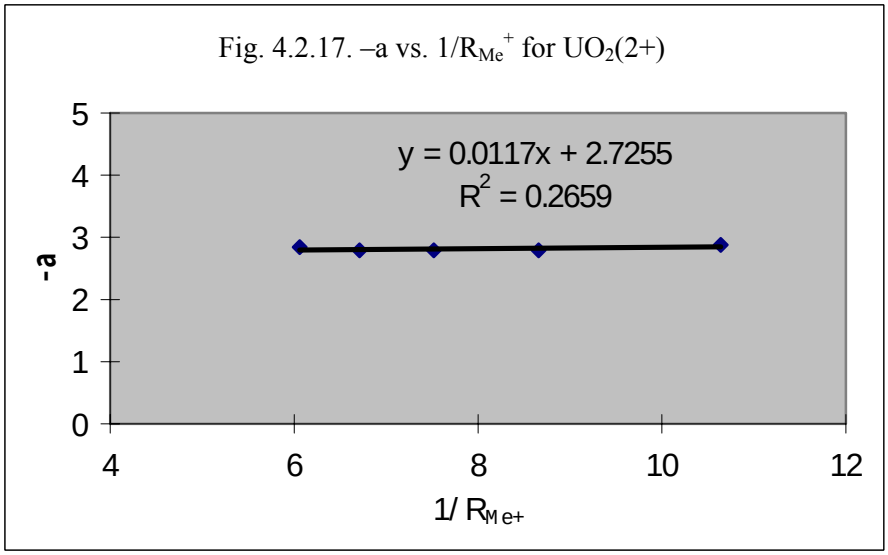

Fig. 4.2.18. –b/1000 vs. $1/R_{Me}^{+}$ for $UO_2(2+)$

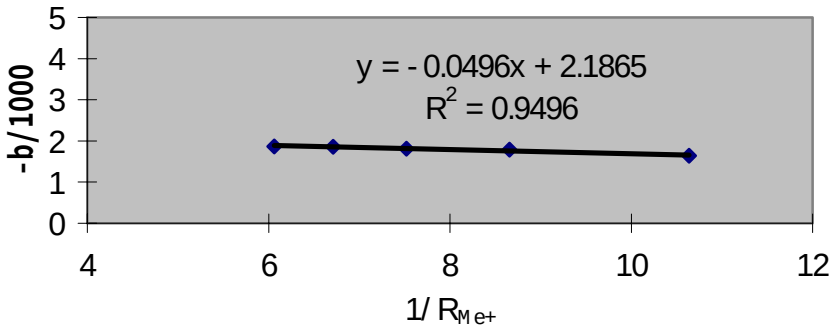

Dependence of D vs. ion radius

Dependence of D to inverse of ion radius of the melts is plotted for U^{3+}, U^{4+} and UO_2^{2+} at 650°C in Fig. 4.2.19 to Fig. 4.2.21. The R^2 values are close to one; the correlations are reliable. Note that the Arrhenius correlations of Table 4.2.11 are extrapolated to sub cooled melt; D is calculated below the melting temperature of each melt corresponding to $1/R_{Me}^{+}$.

Fig. 4.2.19. D vs. $1/R_{Me}^{+}$ for U(3+) at 650°C

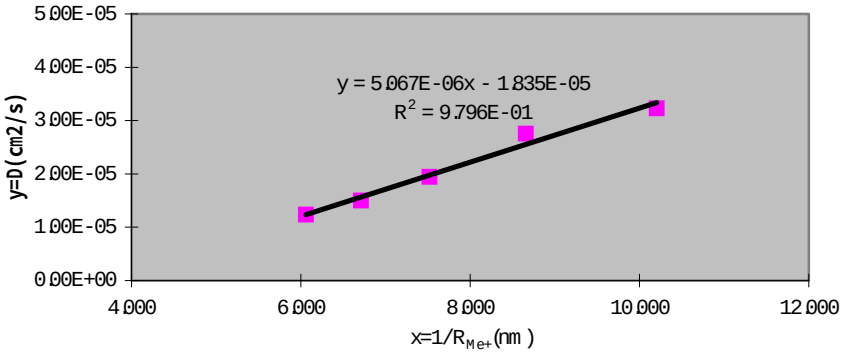

Fig. 4.2.20. D vs. $1/R_{Me}^{+}$ for U(4+) at 650°C

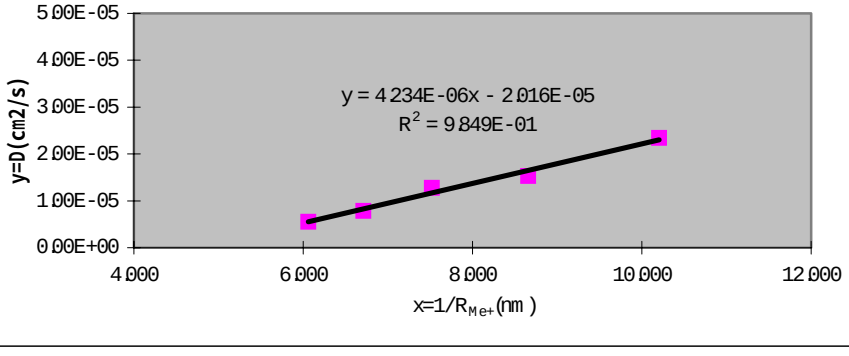

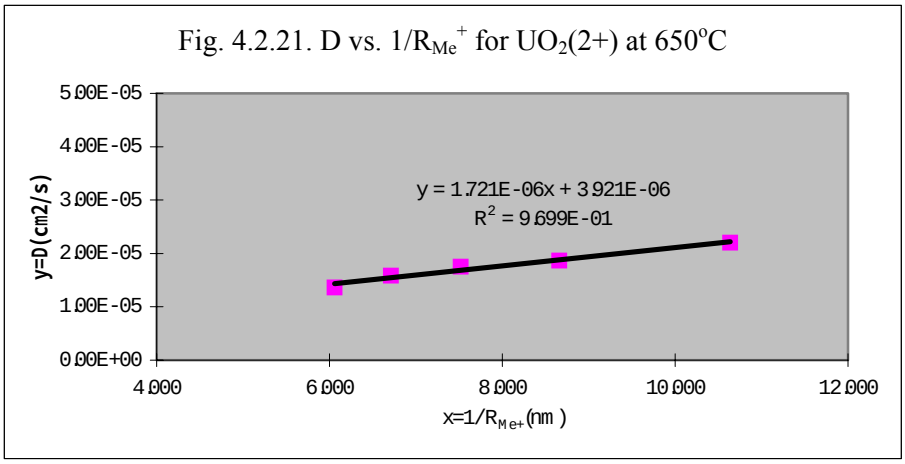

Fig. 4.2.21. D vs. $1/R_{Me}^{+}$ for $UO_2(2+)$ at 650°C

4.2.4.2. Diffusion coefficients in NaCl-2CsCl

(1) Diffusion coefficient of U^{3+}

It was shown that Diffusion coefficient of U^{3+} at 650°C in NaCl-2CsCl can be estimated by the correlation in Fig.4.2.19. Coefficients at 500°C, 550°C, 600 °C, and 650 °C are also estimated in the same manner. Arrhenius plot of the estimated diffusion coefficients is shown in Fig. 4.2.22, which gives the following correlation for U^{3+}. The R^2 value suggests that the correlation is very reliable.

$$Log_{10}D(cm^2/s) = - 2.6533 - 1949.8/T(K) \qquad (4.2.70)$$

The coefficients are similar to the ones in Table 4.2.11.

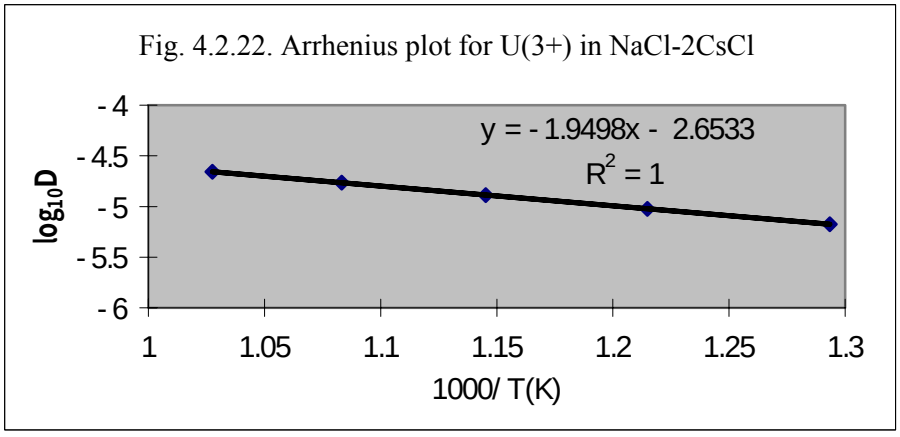

Fig. 4.2.22. Arrhenius plot for U(3+) in NaCl-2CsCl

(2) Diffusion coefficient of U^{4+}

It was shown that Diffusion coefficient of U^{4+} at 650 °C in NaCl-2CsCl can be estimated by the correlation in Fig.4.2.20. Coefficients at 500 °C, 550 °C, 600 °C, and 650 °C are also evaluated in the same manner. Arrhenius plot of the estimated diffusion coefficients is shown in Fig. 4.2.23, which gives the following correlation for U^{4+}. The R^2 value suggests that the correlation is very reliable.

$$Log_{10}D(cm^2/s) = -2.2438 - 2564.1/T(K) \quad (4.2.71)$$

The coefficients are similar to the ones in Table 4.2.11.

Fig. 4.2.23. Arrhenius plot for U(4+) in NaCl-2CsCl

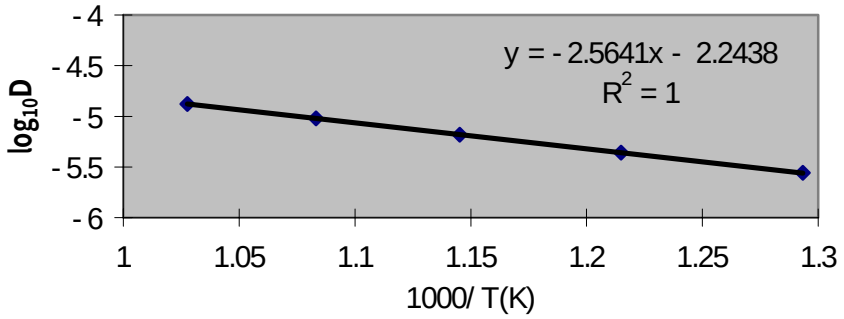

(3) Diffusion coefficient of UO_2^{2+}

It was shown that Diffusion coefficient of UO_2^{2+} at 650 °C in NaCl-2CsCl can be estimated by the correlation in Fig.4.2.21. Coefficients at 500°C, 550°C, 600°C, and 650°C are also evaluated in the same manner. Arrhenius plot of the estimated diffusion coefficients is shown in Fig. 4.2.24, which gives the following correlation for UO_2^{2+}. The R^2 value suggests that the correlation is very reliable.

$$Log_{10}D(cm^2/s) = -2.8087 - 1834.9/T(K) \quad (4.2.72)$$

The coefficients are similar to the ones in Table 4.2.11.

Fig. 4.2.24. Arrhenius plot for UO_2(2+) in NaCl-2CsCl

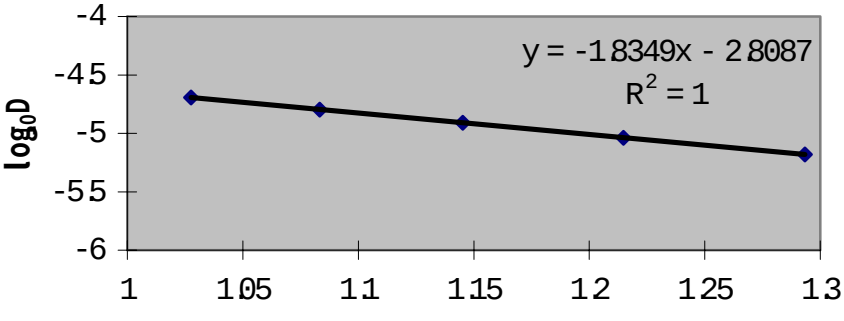

4.2.4.3. Diffusion coefficients in 3LiCl-2KCl

(1) Diffusion coefficient of U^{3+}

It was shown that Diffusion coefficient of U^{3+} at 650 °C in 3LiCl-2KCl can be estimated by the correlation in Fig.4.2.19. Coefficients at 500 °C, 550 °C, 600 °C, and 650 °C are also estimated in the same manner. Arrhenius plot of the estimated diffusion coefficients is shown in

Fig. 4.2.25, which gives the following correlation for U^{3+}. The R^2 value suggests that the correlation is very reliable.

$$\log_{10}D(cm^2/s) = -2.5651 - 1739.2/T(K) \quad (4.2.73)$$

Fig. 4.2.25. Arrhenius plot for U(3+) in 3LiCl-2KCl

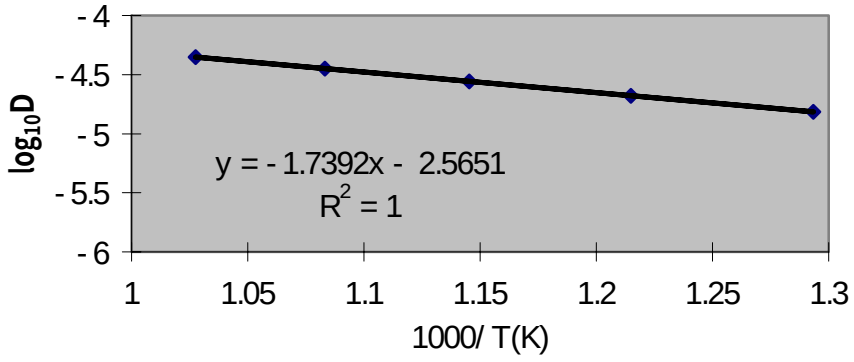

(2) Diffusion coefficient of U^{4+}

It was shown that Diffusion coefficient of U^{4+} at 650 °C in NaCl-2CsCl can be estimated by the correlation in Fig.4.2.20. Coefficients at 500°C, 550°C, 600 °C, and 650 °C are also evaluated in the same manner. Arrhenius plot of the estimated diffusion coefficients is shown in Fig. 4.2.26, which gives the following correlation for U^{4+}. The R^2 value suggests that the correlation is very reliable.

$$Log_{10}D(cm^2/s) = -2.3255 - 2103.6/T(K) \quad (4.2.74)$$

Fig. 4.2.26. Arrhenius plot for U(4+) in 3LiCl-2KCl

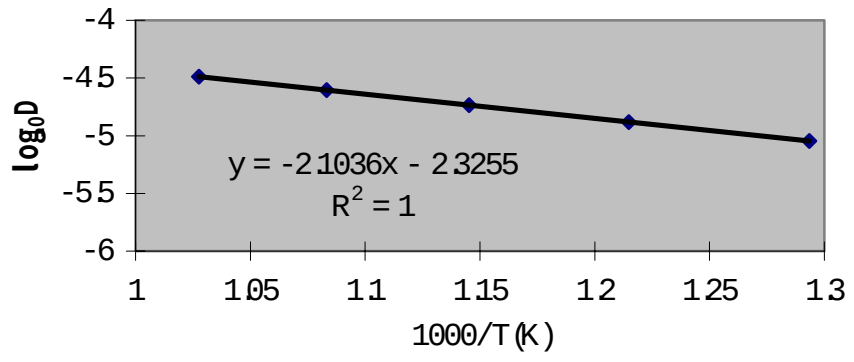

4.2.4.4. Comparison of diffusion coefficients

The estimated diffusion coefficients at 650°C are plotted in Fig. 4.2.27. The dependence of the coefficient to the inverse of the ion radius of the melts is similar for U^{3+} and U^{4+} but somewhat smaller for UO_2^{2+}.

Fig. 4.2.27. Comparison of diffusion coefficients at 650°C

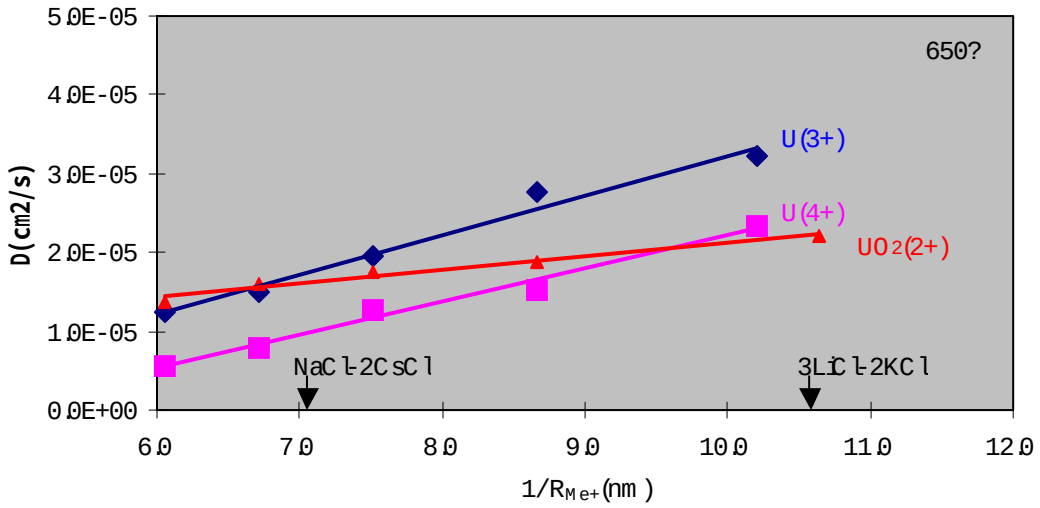

2.2.4.5. Diffusion coefficients of other actinides

Correlations of Diffusion coefficients in KCl-NaCl are summarized in Table 4.2.13. Dr. Lebedev [2, p. 131] cites the following correlations by using the moment of ion "n/r" where n is number of valence and r is radius of the ion.

$$D = \left[\frac{107.57 - 84630/T + (5.56 - 5280/T)\cdot n/r}{1 + (0.77 - 470/T)\cdot n/r} \pm 0.67 \right] \cdot 10^{-5} \qquad (4.2.75)$$

Table 4.2.13. Diffusion coefficient of ions in KCl-NaCl [2]

Ions	n	r_{Me}^{n+}(nm)	1/r	n/r	-a	-b	$-\mathrm{Log}_{10}D(T=1000)$
1	2	3	4	5	6	7	8
Ag^{+}	1	0.133	7.519	7.519	2.89	1240	4.13
Ag^{+}	1	0.133	7.519	7.519	2.72	1400	4.12
Mg^{2+}	2	0.074	13.514	27.027	2.45	1890	4.31
Mg^{2+}	2	0.074	13.514	27.027	2.43	1820	4.25
Zn^{2+}	2	0.083	12.048	24.096	2.34	1950	4.29
Cd^{2+}	2	0.099	10.101	20.202	2.52	1800	4.32
Pb^{2+}	2	0.132	7.576	15.152	2.56	1880	4.44
Zr^{2+}	2	0.1	10.000	20.000	1.99	2540	4.53
Zr^{2+}	2	0.1	10.000	20.000	2.09	2366	4.44
Nb^{2+}	2	0.095	10.526	21.053	2.16	2080	4.24
Mo^{3+}	3	0.073	13.699	41.096	2.18	2360	4.54
Nb^{3+}	3	0.088	11.364	34.091	2.36	2290	4.65
U^{3+}	3	0.103	9.709	29.126	2.55	1920	4.47
U^{3+}	3	0.103	9.709	29.126	2.63	1810	4.44

1	2	3	4	5	6	7	8
Pu^{3+}	3	0.1	10.000	30.000	3.01	1510	4.52
Zr^{4+}	4	0.082	12.195	48.780	2.35	2230	4.58
Hf^{4+}	4	0.082	12.195	48.780	2.08	2610	4.69
W^{4+}	4	0.07	14.286	57.143	1.94	2770	4.71
U^{4+}	4	0.095	10.526	42.105	2.02	2580	4.60
U^{4+}	4	0.095	10.526	42.105	2.46	2120	4.58
Th^{4+}	4	0.099	10.101	40.404	1.76	2790	4.55
Th^{4+}	4	0.099	10.101	40.404	2.13	2420	4.55

At 1000 K, $\log_{10}D$ are plotted vs. n/r in Fig. 4.2.28. This plot indicates that the diffusion coefficient of other actinides are not so different from that of U as their moment n/r are close to that of U (U^{3+}: n/r = 29.1; Am^{3+}: n/r = 30.6; Cm^{3+}: n/r = 30.9). Therefore, it will be appropriate to use the D of U for other actinides when there is no reliable data.

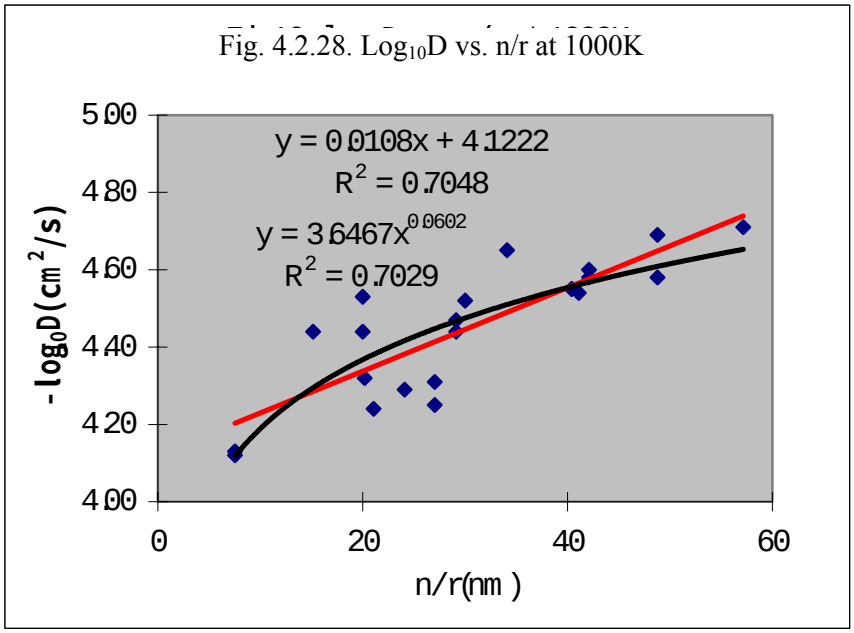

Fig. 4.2.28. $Log_{10}D$ vs. n/r at 1000K

4.2.5. Uranium dioxide electric conductivity

Uranium dioxide is a good conductor of the electric current and it can participate in electrode processes like a metal electrode. The uranium dioxide electric conductivity is equal to 0.02 ÷ 0.002 1/(Ω·m) at 923 K.

It is very important that the uranium dioxide electric conductivity is lower than that of salt-electrolyte [χ_{NaCl} = 3.54 1/(Ω·m) at 1078 K, and χ_{CsCl} = 1.14 1/(Ω·m) at 933 K]. Due to this difference, the uniform continuous deposits of UO_2 with the perfect crystal structure can be prepared by electrolysis of chloride melts. There are no strong restrictions for the thickness of deposits.

Dioxides of the other elements have very poor electric conductivity. However, there is possibility of their codeposition with uranium dioxide during the melt electrolysis. In this case, neptunium and plutonium partly co-deposit into crystal structure of uranium dioxide, forming the solid solutions. But mainly, their dioxides form the small crystals around the big crystals of uranium dioxide.

4.3. Plutonium chemistry

The plutonium is the unique element among the actinides due to its redox properties. It is the only element that can exist simultaneously in the four valent states (Pu(III), Pu(IV), Pu(V) and Pu(VI)) at the specific conditions both in the water solutions and in the chloride melts.

Oxygen-free form of P(III) is the most stable plutonium state in the chloride melts. In these systems, the plutonium (IV) can exists at the extreme positive values of the oxidizing potentials. The oxygen-free chloride compounds of penta- and hexavalent plutonium are not known.

Oxygen anions stabilize the high-oxidized states of plutonium. But, the chloride compounds of plutonium having the oxidized state more than three are unstable and they are decomposing at high temperature.

The melts of alkali metal chlorides, which are good complexing agents, increase the stability of oxidized states of plutonium. Nevertheless, the stability of the oxidized states of plutonium is essentially less than that of the uranium. This is the reason why the traditional investigations methods are not suitable for studying the thermodynamic properties of the plutonium in the chloride melts. The spectrophotometry method gives the most reliable results to directly measure the concentration of plutonium valent forms in the melt. But this method has own restrictions; the deficiency of intensive absorption bands for the all plutonium valent forms.

4.3.1. Reactions of production and mutual transformation of plutonium valent forms

The stability regions of Pu(III), Pu(IV), Pu(V) and Pu(VI) plutonium valent form in the melts of chloride alkali metals are shown in the "Potential - pO^{2-}" diagram (Fig. 4.3.1a and b) [15]. The tri- and tetravalent plutonium form the oxygen-free Pu^{3+} and Pu^{4+} ions. At high temperature, tetravalent plutonium forms oxygen-contained PuO^{2+} ions Fig. 4.3.1b). The penta- and hexavalent plutonium form the oxygen-containing PuO_2^{+} and PuO_2^{2+} ions.

Trivalent plutonium can be prepared by:

dissolution of plutonium trichloride:

$$PuCl_{3(solid)} + Melt = PuCl_{3(melt)}; \quad (4.3.1)$$

anodic dissolution of metal plutonium:

$$Pu_{(solid,\ liquid)} - 3e^- + 3Cl^-_{(melt)} = PuCl_{3(melt)}, \quad \text{(anodic process)} \quad (4.3.2)$$

$$Cl_{2(gas)} + 2e^- = 2Cl^-_{(melt)}; \quad \text{(cathodic process)} \quad (4.3.3)$$

chlorination of metal plutonium:

$$Pu_{(solid,\ liquid)} + 3/2Cl_{2(gas)} + Melt = PuCl_{3(melt)}; \quad (4.3.4)$$

dioxide plutonium chlorination in the presence of reducers

$$PuO_{2(solid)} + 3/2Cl_{2(gas)} + C_{(solid)} = PuCl_{3(melt)} + CO_{2(gas)}; \quad (4.3.5)$$

reduction of oxygen-containing plutonium compounds:

$$PuO_2Cl_{(melt)} + 4HCl_{(gas)} = PuCl_{3(melt)} + 2H_2O_{(gas)} + Cl_{2(gas)}, \quad (4.3.6)$$

$$PuO_2Cl_{2(melt)} + CCl_{4(gas)} = PuCl_{3(melt)} + CO_{2(gas)} + 3/2Cl_{2(gas)}. \quad (4.3.7)$$

In molten salts, plutonium trichloride forms the $PuCl_6^{3-}$ complex ions.

Pure plutonium trichloride can be obtained by chlorination of plutonium dioxide with carbon tetrachloride at 650°C on reaction

$$PuO_{2(solid)} + CCl_{4(gas)} = PuCl_{3(solid)} + CO_{2(gas)} + 1/2\ Cl_{2(gas)}. \quad (4.3.8)$$

Plutonium tetrachloride cannot be prepared as pure compound. This is very unstable compound in molten chlorides too. It can be obtained by the chlorination method of trivalent plutonium with chlorine gas on reversible reaction

$$PuCl_{3(melt)} + 1/2Cl_{2(gas)} \rightleftarrows PuCl_{4(melt)}. \quad (4.3.9)$$

In the melt the tetravalent plutonium forms complex ions $PuCl_6^{2-}$.

Several binary compounds of plutonium tetrachloride are known. Cs_2PuCl_6 can be prepared adding CsCl to plutonium (IV) solution in HCl. Cs_2PuCl_6 is not hygroscopic compound and it can be used as initial material for preparing the solutions of plutonium chlorides in the molten salts.

During plutonium dioxide chlorination with chlorine gas, the oxygen-containing plutonium compounds are formed at the first stage of the process:

$$PuO_{2(solid)} + 1/2\ Cl_{2(gas)} + Melt \rightleftarrows PuO_2Cl_{(melt)}, \quad (4.3.10)$$

$$PuO_{2(solid)} + Cl_{2(gas)} + Melt \rightleftarrows PuO_2Cl_{2(melt)}. \quad (4.3.11)$$

In accordance with the reversibility of (4.3.10) and (4.3.11) reaction they lost oxygen and reduced up to the tri- and tetravalent states.

The penta- and hexavalent plutonium can be obtained by:

Oxidation of tri- and tetravalent plutonium with oxygen:

$$PuCl_{3(melt)} + O_{2(gas)} \rightleftarrows PuO_2Cl_{(melt)} + Cl_{2(gas)}, \quad (4.3.12)$$

$$PuCl_{4(melt)} + O_{2(gas)} \rightleftarrows PuO_2Cl_{2(melt)} + Cl_{2(gas)}, \quad (4.3.13)$$

The penta- and hexavalent plutonium compounds are in the state of equilibrium

$$PuO_2Cl_{(melt)} + 1/2Cl_{2(gas)} \rightleftarrows PuO_2Cl_{2(melt)} \quad (4.3.14)$$

and the relation of their concentrations depends on the chlorine partial pressure over the melt.

The compounds PuO_2Cl and PuO_2Cl_2 can exist in the chloride melts in the form of $PuO_2Cl_4^{3-}$ and $PuO_2Cl_4^{2-}$ complex groups.

The distribution of oxygen-free ($PuCl_3$, $PuCl_4$) and oxygen-containing (PuO_2Cl, PuO_2Cl_2) plutonium forms is determined by equilibrium of reaction (4.3.12) and (4.3.14) and depends on the chlorine and oxygen partial pressure over the melt.

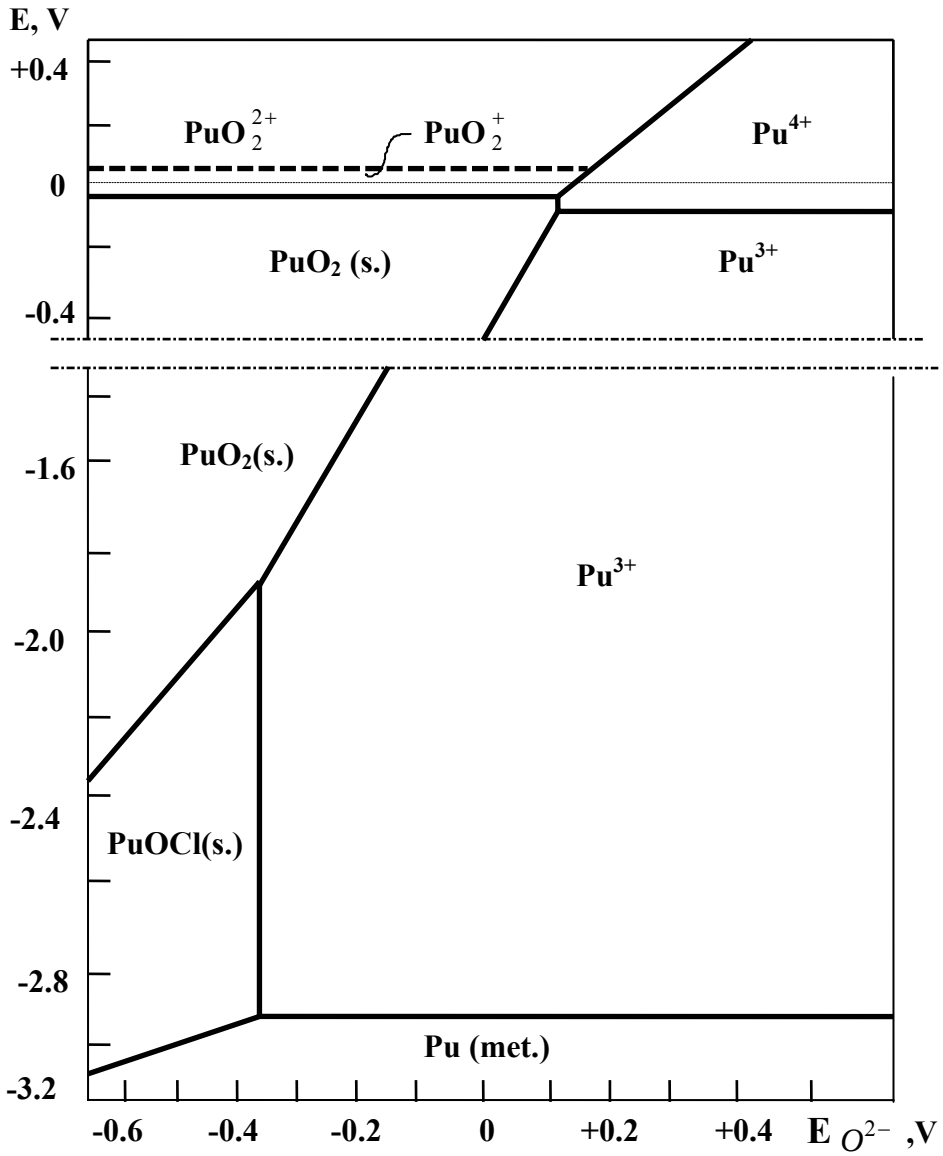

Fig. 4.3.1a. Potential/pO^{2-} (or potential of oxygen electrode) diagrams of plutonium in NaCl-2CsCl melt at 863 K [15].
[Pu(III)] = [Pu(IV)] = PuO_2(V)] = PuO_2(VI)] = 0.01 mole /l

PuO_2Cl and PuO_2Cl_2 compounds are reduced by the tetravalent uranium

$$PuO_2Cl_{2(melt)} + UCl_{4(melt)} = PuCl_{4(melt)} + UO_2Cl_{2(melt)}, \quad (4.3.15)$$

and by carbon in the presence of chlorine

$$PuO_2Cl_{2(melt)} + C_{(solid)} + Cl_{2(gas)} = PuCl_{4(melt)} + CO_{2(gas)}. \quad (4.3.16)$$

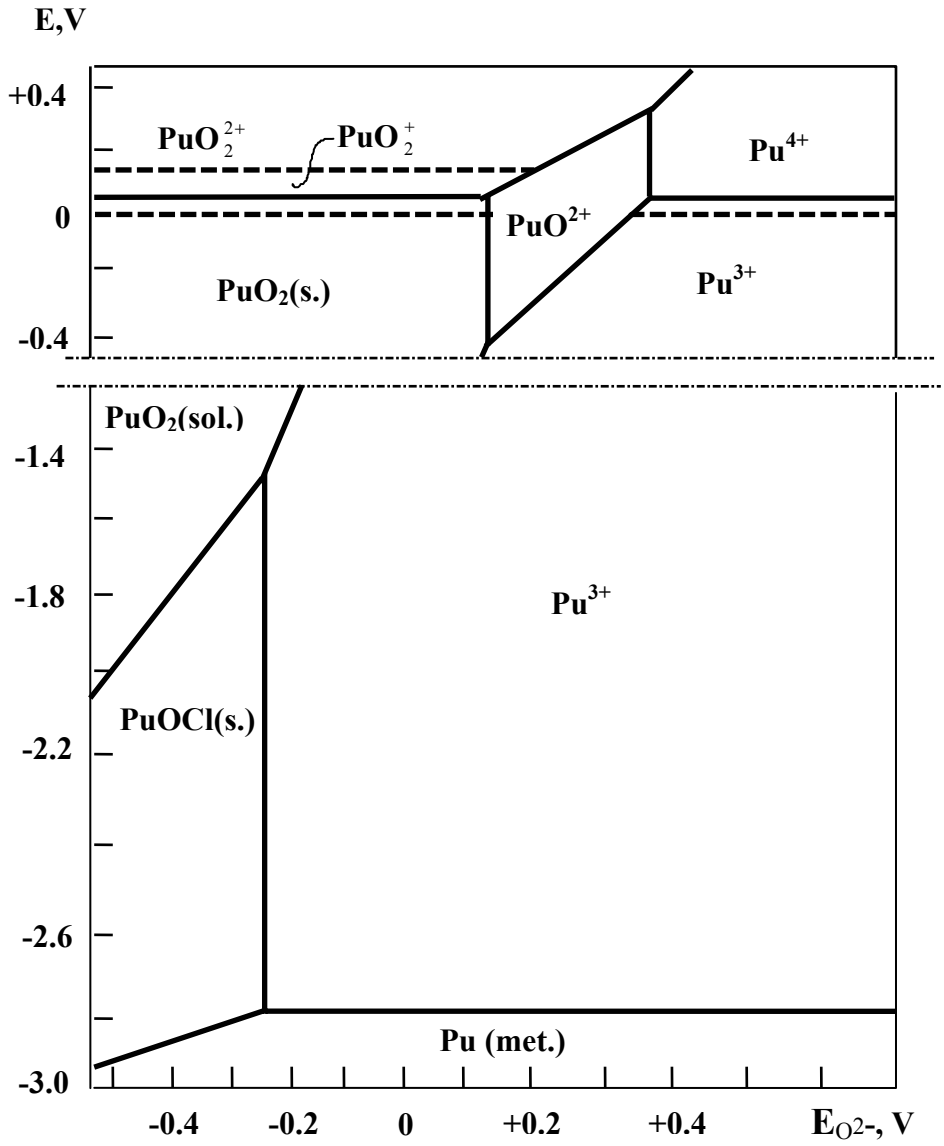

Fig. 4.3.1b. Potential/pO^{2-} (or potential of oxygen electrode) diagrams of plutonium in NaCl-2CsCl melt at 1043 K [15].
[Pu(III)] = [Pu(IV)] = PuO_2(V)] = PuO_2(VI)] = 0.01 mole / l

The cations of PuO_2Cl_2 and PuO_2Cl compounds are reduced into plutonium dioxide in the cathode process:

$$PuO_2^{n+}(melt) + ne^- = PuO_2(cath.) \quad (n = 1 \text{ or } 2) \qquad (4.3.17)$$

Unlike uranium dioxide, plutonium dioxide has very low electrical conductivity and passivates the cathode surface. However, in the electrolysis of melt containing oxygen compounds of uranium and plutonium, the deposits with 50 % mass portion of plutonium can be obtained at the cathode. The cathodic deposition of plutonium dioxide is also caused by the (4.3.17) reaction and exchange reaction

$$PuO_2Cl_2(melt) + nUO_2(solid) = PuO_2 \cdot (n-1)UO_2(solid) + UO_2Cl_2(melt). \qquad (4.3.18)$$

The ability for cathodic reduction of PuO_2^{n+} ions to plutonium dioxide served as the basis for MOX fuel production and reprocessing by electrochemical technology.

The PuO_2Cl and PuO_2Cl compounds are not stable in the chloride melts. By decreasing the partial pressure of chlorine, they are reduced to plutonium dioxide

$$PuO_2Cl_{2(melt)} \rightleftarrows PuO_2Cl_{(melt)} + 1/2Cl_{2(gas)}, \quad (4.3.19)$$

$$PuO_2Cl_{(melt)} \rightleftarrows PuO_{2(solid)} + 1/2Cl_{2(gas)}. \quad (4.3.20)$$

The oxychloride ions of plutonium promote the formation and growth of plutonium dioxide crystals. The reactions (1.19) and (1.20) served as the basis for the process of granulated plutonium dioxide production by the volume precipitation method.

4.3.2. Thermodynamic and electrochemical characteristics of plutonium reactions

In general, the chemical behavior of plutonium in the chloride melts can be described by the following reactions:

$$Pu_{(liquid)} + 3/2\ Cl_{2(gas)} + melt = PuCl_{3(melt)}, \quad (4.3.21)$$

$$PuCl_{3(melt)} + 1/2\ Cl_{2(gas)} \rightleftarrows PuCl_{4(melt)}, \quad (4.3.22)$$

$$PuCl_{4(melt)} + O_{2(gas)} \rightleftarrows PuO_2Cl_{2(melt)} + Cl_{2(gas)}, \quad (4.3.23)$$

$$PuO_2Cl_{(melt)} + 1/2\ Cl_{2(gas)} \rightleftarrows PuO_2Cl_{2(melt)}, \quad (4.3.24)$$

$$PuO_2Cl_{(melt)} \rightleftarrows PuO_{2(solid)} + 1/2\ Cl_{2(gas)}. \quad (4.3.25)$$

The formation process of the plutonium (III) solutions in chloride melts is presented by reaction (4.3.21). Other reactions describe the mutual transformations among the different plutonium valent forms. All reactions are reversible.

$Pu_{(liquid)} + 3/2\ Cl_{2(gas)} + melt = PuCl_{3(melt)}$ reaction

Gibbs' energy of formation of the pure liquid plutonium trichloride from the initial element by the reaction

$$Pu_{(liquid)} + 3/2Cl_{2(gas)} = PuCl_{3(liquid)} \quad (4.3.26)$$

changes with temperature in accordance with equation

$$\Delta G^o_{PuCl_3} = - 911 + 0.174 \cdot T,\ kJ/mole.$$

Thermodynamics of the formation of the diluted solutions of the plutonium trichloride in alkali metal chloride melts by reaction (4.3.21) had been studied with the electro moving forces (EMF) method [16]. The most reliable and regular data on $PuCl_3$ formation in several alkali chlorides have been obtained in RIAR.

Experimental equations for the formal standard potential of metal plutonium and Gibbs's energy of the diluted solutions formation of $PuCl_3$ from elements are presented in Table 4.3.1.

These parameters can be described by the following common equations:

$$E^*_{Pu^{3+}/Pu} = - 4.24 + 0.67/r^*_{Me^+} + (13.3 - 3.6/ r^*_{Me^+}) \cdot 10^{-4}T \pm 0.02\ V, \quad (4.3.27)$$

$$\Delta G^*_{PuCl_3} = -1227 + 194/r^*_{Me^+} + (0.385 - 0.104/ r^*_{Me^+})\cdot T \pm 5.8 \text{ kJ/mole.} \quad (4.3.28)$$

Checking of the equation (4.3.27) for $E^*_{Pu^{3+}/Pu}$ with the Excel program shows the difference of coefficients. There are two possible reasons. At first, at that time the authors used the hand calculator method for treatment of the experimental results. Secondly, usually, Russian uses the all of experimental points obtained for various temperature and ion radiuses instead of the making correlations for each temperature at certain radius or vice versa.

Table 4.3.1. Electrochemical and thermodynamic characteristics of reaction $Pu_{(liquid)} + 3/2\ Cl_{2(gas)} + melt = PuCl_{3(melt)}$ [16,4]

Melt	r_{Me^+}, Å	T, K	$E^*_{Pu^{3+}/Pu} = a + b\cdot T$, V		$\Delta G^*_{PuCl_3} = \Delta H^*_{PuCl_3} - T\Delta S^*_{PuCl_3}$	
			a	$b\cdot 10^3$	$\Delta H^*_{PuCl_3}$, kJ/mole	$-\Delta S^*$, kJ/(mole·K)
LiCl	0.68	958 – 1028	- 3.46	0.94	1002	0.272
NaCl	0.98	1083 – 1143	- 3.60	0.98	1042	0.284
KCl	1.33	1083 – 1143	- 3.76	1.08	1089	0.313
CsCl	1.65	928 – 983	- 3.87	1.16	1121	0.336
NaCl-KCl	1.15	983 – 1107	- 3.58	0.93	1037	0.269
NaCl-2CsCl**	1.42		- 3.80	1.11	1100	0.321

** - calculated data

Besides, the authors used the value 0.78 A for the Li^+ ion radius, whereas the value of 0.68 A is more prevailing. Somehow, new equations was formulated by Excel when value of 0.68 A for r_{Li}+ was used:

$$E^*_{Pu^{3+}/Pu} = -4.07 + 0.44/r^*_{Me^+} + (12.3 - 2.2/ r^*_{Me^+})\cdot 10^{-4}T \pm 0.02 \text{ V,} \quad (4.3.29)$$

$$\Delta G^*_{PuCl_3} = -1180 + 130/r^*_{Me^+} + (0.356 - 0.64/ r^*_{Me^+})\cdot T \pm 0.02 \text{ kJ/mole.} \quad (4.3.30)$$

Difference of the $E^*_{Pu^{3+}/Pu}$ values calculated with help of both (4.3.27) and (4.3.29) equations do not exceeds the error of the original data. Nevertheless, (4.3.29) and (4.3.30) equations are more correct, and they must be recommended for practical calculations.

$PuCl_{3(melt)} + 1/2\ Cl_{2(gas)} = PuCl_{4(melt)}$ reaction

Equilibrium of reaction

$$PuCl_{4(melt)} \rightleftarrows PuCl_{3(melt)} + 1/2\ Cl_{2(gas)} \quad (4.3.31)$$

in chloride melts had been studied at RIAR by the high temperature spectrophotometry method [17,18].

Spectra of the NaCl-2CsCl melt containing the equilibrium mixture of Pu^{3+} and Pu^{4+} ions are presented on Fig. 4.3.2 [17].

Different authors applied two methods of spectrum treatment. First of them is the method of "base line" (See additional lines on Fig. 4.3.2). At the second case, the optical density had been

calculated by using of the pure melt spectrum as a reference point. Data obtained with the second method will be discussed below.

The presence of isopiestic points near 6000 and 7700 cm^{-1} (See Fig. 4.3.2) is evidence that there are only two spectral forms of plutonium in the melt.

Absorption bands at wave numbers 5200 cm^{-1} and 7200cm^{-1} were used for the determination of the Pu^{4+} and Pu^{3+} concentration in the melt, respectively. The extinction coefficient of Pu^{3+} at wave numbers 5300 and 7200 cm^{-1} was measured directly because it is possible to prepare its pure solutions. The extinction coefficient of Pu^{4+} at these wave numbers was calculated. It is not difficult to find the equation showing the relationship among the optical density (D), total plutonium concentration ([Pu]), extinction coefficients (ε^{ν}), reaction 4.3.31 equilibrium constant ($K^{*}_{4.3.311}$) and chlorine gas partial pressure under melt (PCl_2).

$$\frac{D}{L} = [Pu]\cdot \frac{\varepsilon^{\nu}_{Pu(III)} + \varepsilon^{\nu}_{Pu(IV)}\cdot K^{*}_{4.3.31}\cdot P_{Cl_2}^{1/2}}{1 + K^{*}_{4.3.31}\cdot P_{Cl_2}^{1/2}}$$

Here L is the length of spectrophotometry cell (L = 1 cm).

Using the experimental data, the Pu(III) and Pu(IV) absorption coefficients at waves length of 5200 and 7200 cm^{-1} (See Table 4.3.2) and the reaction (4.3.11) equilibrium constant were calculated (See Table 4.3.3).

According to Lambert-Beer Law, the dependence of the optical density from the total Pu content in melt must be linear. Experiments had confirmed this assumption (See Fig. 4.3.3).

Data of Table 4.3.2 indicate the intensity of the light-absorption by Pu^{3+} and Pu^{4+} ions depending on the temperature and the melt composition.

Parallel with RIAR data, the data of other authors are shown in Table 4.3.3. One can see that the data obtained by spectrophotometry method, marked by *, are in good agreement.

Values of the relative concentrations of the Pu^{3+} and Pu^{4+} ions in some electrolytes in equilibrium with the atmosphere containing the chlorine gas are given in Table 4.3.4. These data show clearly how the plutonium (IV) stability changes with the temperature and the composition of the melt.

It is impossible to study experimentally the thermodynamics of the formation reaction of the $PuCl_4$ in diluted solutions of chloride melts because the plutonium, being in equilibrium with metal plutonium, can exist in form Pu^{3+} only. But the $\Delta G^{*}_{PuCl_4}$ value can be calculated by assuming the reaction

$$Pu_{(sol.,liq,)} + 2\ Cl_{2(gas)} + melt = PuCl_{4(melt)} \qquad (4.3.32)$$

as summation of the next two reactions:

$$Pu_{(liquid)} + 3/2\ Cl_{2(gas)} + melt = PuCl_{3(liquid)}, \qquad (4.3.33)$$

$$PuCl_{3(melt)} + 1/2\ Cl_{2(gas)} \rightleftarrows PuCl_{4(melt)}. \qquad (4.3.34)$$

Then $\Delta G^*_{PuCl_4} = \Delta G^*_{PuCl_3} + \Delta G^*_{PuCl_4/\,PuCl_3}$,

where $\Delta G^*_{PuCl_4/\,PuCl_3} = -2.3RT\log_{10}K^*_{2.4} - 1/2 \cdot 2.3RT \cdot \log_{10}1.0133 \cdot 10^5$.

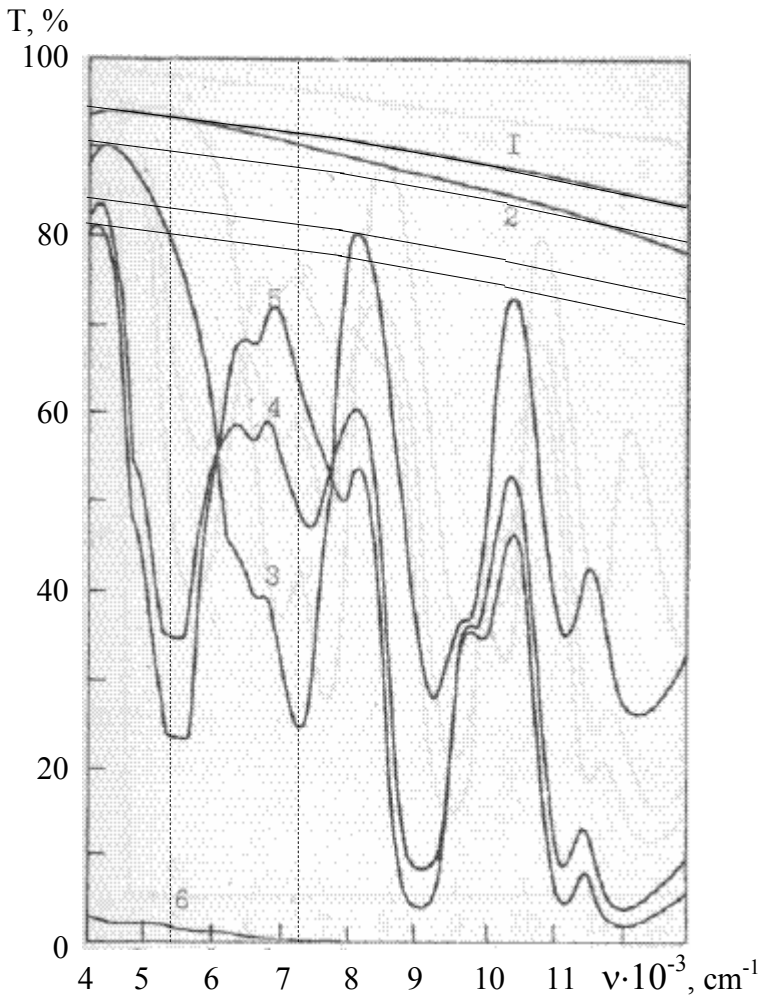

Fig. 4.3.2. Absorption spectra of Pu(III) and Pu(IV) in NaCl-2CsCl melt at 823 K [17]
[Pu] = 0: 1 – He ($PCl_2 = 0$); 2 – $PCl_2 = 1.013 \cdot 10^5$ Pa;
[Pu] = $0.14 \cdot 10^{-3}$ mole/cm^3: 3 – $PCl_2 = 0$; 4 – $PCl_2 = 0.203 \cdot 10^5$ Pa; 5 – $PCl_2 = 1.013 \cdot 10^5$ Pa;
6 – melt irradiation.

Calculated values of the $\Delta G^*_{PuCl_4}$ parameter are given in Table 4.3.5.

Gibbs' energy of the formation of the liquid plutonium tetrachloride from the pure element

$$Pu_{(sol.,liq.)} + 2\,Cl_{2(gas)} = PuCl_{4(liq.)}$$

changes with temperature in according with equations:

$\Delta G^o_{PuCl_4} = -880 + 0.200 \cdot T$, kJ/mole (857 – 913 K),

$\Delta G^o_{PuCl_4} = -888 + 0.211 \cdot T$, kJ/mole (913 – 1111 K).

Table 4.3.2. Calculated values of the Pu(III) and Pu(IV) extinction coefficients, (cm^2/mole) [17,18]

Melt	T, C	ν = 5200 cm^{-1}		ν = 7200 cm^{-1}	
		$\varepsilon^{\nu}_{Pu(III)} \cdot 10^3$	$\varepsilon^{\nu}_{Pu(IV)} \cdot 10^3$	$\varepsilon^{\nu}_{Pu(III)} \cdot 10^3$	$\varepsilon^{\nu}_{Pu(IV)} \cdot 10^3$
CsCl	700	0.34±0.06	6.9±0.4	4.07±0.03	0.3±0.2
	770	0.35±0.02	8.1±0.7	4.25±0.03	0.3±0.4
	850	0.36±0.02	10.8±1.5	4.35±0.04	-0.3±0.3
NaCl-2CsCl	550	0.50±0.05	5.3±0.2	4.28±0.04	0.3±0.2
	650	0.50±0.05	6.3±0.2	4.43±0.05	0.3±0.2
	750	0.50±0.05	8.7±0.8	4.63±0.05	0.4±0.4
KCl	820	0.24±0.03	10.3±0.5	5.21±0.03	-
	870	0.24±0.03	12.1±0.7	5.25±0.04	-
	920	0.24±0.03	12.5±1.1	5.31±0.05	-
4LiCl-3CsCl	500	0.50±0.05	3.8±0.2	5.40±0.05	-
	630	0.50±0.05	7.0±0.4	5.60±0.05	-
	800	0.50±0.05	10.2±0.2	6.10±0.05	-
NaCl-KCl	720	0.25±0.05	11.0±0.8	6.10±0.10	-
	780	0.25±0.05	12.4±1.5	6.10±0.10	-
	840	0.25±0.05	14.0±2.6	6.10±0.10	-
3LiCl-2KCl	420	0.14±0.06	7.1±0.2	6.52±0.04	0.1±0.2
	500	0.14±0.06	7.7±0.3	6.23±0.04	0.5±0.5
	600	0.14±0.06	8.8±0.6	6.09±0.04	0.6±0.7
LiCl	670	-	-	7.50±0.05	-
	770	-	-	7.46±0.05	-

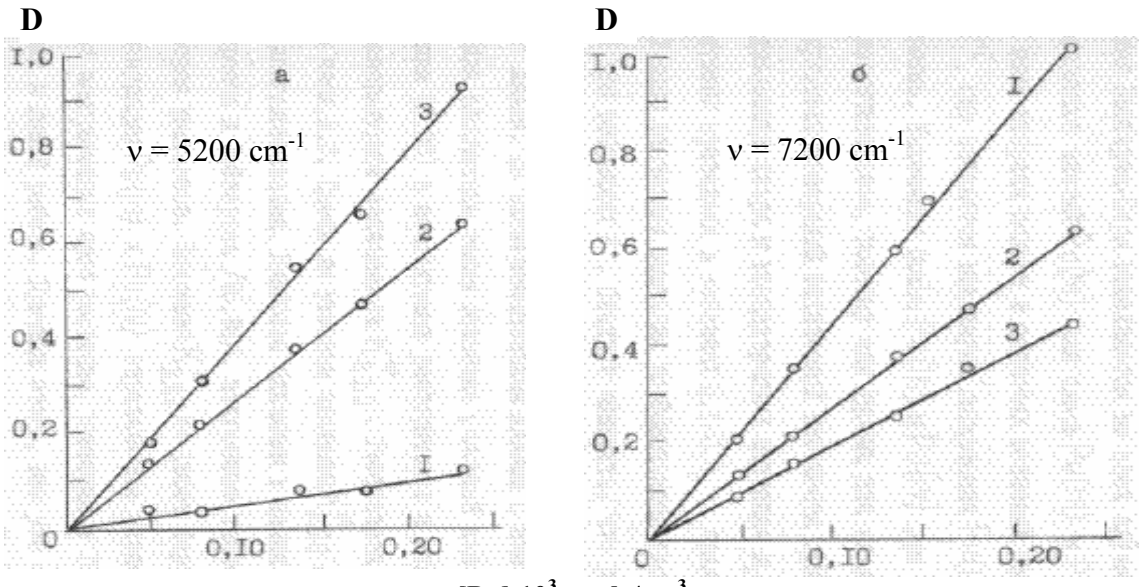

Fig. 4.3.3. Dependence of the optical density of the Pu(III) and Pu(IV) absorption bands from the total plutonium concentration in NaCl-2CsCl at 650°C [17]
1 – P_{Cl_2} = 0; 2 – P_{Cl_2} = 0.203·10^5 Pa; 3 – P_{Cl_2} = 1.013·10^5 Pa

Table 4.3.3. Values of formal equilibrium constant of reaction
$PuCl_{4(melt)} \rightleftarrows PuCl_{3(melt)} + 1/2\ Cl_{2(gas)}$ [17, 18]

Melt	T, °C	$K^* \cdot 10^2$, $Pa^{-1/2}$		$Lg\ K^* = a + b/T \pm \delta$		
		RIAR	Other	- a	b	δ
CsCl	700 770 850	0.33±0.03 0.20±0.03 0.10±0.02		6.36	3790	0.08
NaCl-2CsCl	550 600 650 700 750	1.03±0.10 1.37±0.18[18] 0.77±0.09[18] 0.46±0.03 0.54±0.07[18] 0.40±0.05[18] 0.17±0.02 0.31±0.04[18]	4.2 2.4	5.96 5.12[18]	3290 2652[18]	0.07 0.04[18]
KCl	820 870 920	0.066±0.003 0.047±0.003 0.038±0.003		6.09	3180	0.06
4LiCl-3CsCl	500 630 800	1.35±0.09 0.48±0.04 0.11±0.01	1.9±0.6 [19]	5.72	3000	0.05
NaCl-KCl	720 780 840	0.072±0.006 0.050±0.005 0.035±0.004	0.8±0.2 (750°C)	5.95	2790	0.05
3LiCl-2KCl	420 500 600	0.64±0.04 0.35±0.03 0.14±0.01	0.32±0.04 [20,21]	5.44	2270	0.6
LiCl	670 770	0.0160.003 0.009±0.003		-	-	-

The formal standard mixing energy of the $PuCl_4$ and the melt-solvent with the diluted solution formation ($\Delta G_{mix}PuCl_4$) can be calculated as $\Delta G_{mix}PuCl_4 = \Delta G^*_{PuCl_4} - \Delta G^o_{PuCl_4}$:

$$\Delta G_{mix}PuCl_4 = - 610 + 0.502T + (477 - 0.433T)/ r^*_{Me^+}\ kJ/mole\ (857 - 913\ K),$$

$$\Delta G_{mix}PuCl_4 = - 602 + 0.491T + (477 - 0.433T)/ r^*_{Me^+}\ kJ/mole\ (913 - 1111\ K),$$

where the value of 913 K is melting point of plutonium metal.

Table 4.3.4. Relative concentrations of the Pu^{3+} and Pu^{4+} ions (%) in equilibrium with the atmosphere containing the chlorine gas

Melt	T, °C	$K^*_{4.3.31}\cdot10^2$, $Pa^{-1.2}$	P_{Cl_2}, Pa					
			$0.1\cdot10^5$		$0.6\cdot10^5$		$1.0\cdot10^5$	
			Pu^{3+}	Pu^{4+}	Pu^{3+}	Pu^{4+}	Pu^{3+}	Pu^{4+}
CsCl	700	0.33	75	25	55	45	49	51
	770	0.20	83	17	67	33	61	39
	850	0.10	91	9	80	20	76	24
NaCl-2CsCl	550	1.37	42	58	23	77	19	81
	600	0.77	56	44	35	65	29	71
	650	0.54	65	35	43	57	37	63
	700	0.40	71	29	51	49	44	56
	750	0.31	76	24	57	43	50	50
KCl	820	0.066	94	6	86	14	83	17
4LiCl-3CsCl	500	1.35	43	57	23	77	19	81
	630	0.48	68	32	46	54	40	60
	800	0.11	90	10	79	21	74	26
NaCl-KCl	720	0.072	97	3	85	15	81	19
3LiCl-2KCl	420	0.64	61	39	39	61	33	67
	500	0.35	74	26	54	46	47	53
	600	0.14	88	12	74	26	69	31
LiCl	670	0.016	98	2	96	4	95	5
	770	0.009	99	1	98	2	97	3

Table 4.3.5. Calculated values of formal standard Gibbs' Energy for reaction $Pu_{(sol.,liq.)} + 2\ Cl_{2(gas)} + melt = PuCl_{4(melt)}$ [17]

Melt	$\Delta G^*_{PuCl_3}$, kJ/mole	$\Delta G^*_{PuCl_4/\ PuCl_3}$, kJ/mole	$\Delta G^*_{PuCl_4}$, kJ/mole
CsCl	– 1121 + 0.336T	– 72.6 + 0.080T	– 1193 + 0.410T
KCl	– 1089 + 0.213T	– 60.9 + 0.069T	– 1150 + 0.382T
NaCl-KCl	– 1037 + 0.269T	– 53.4 + 0.066T	– 1090 + 0.335T
3LiCl-2KCl	– 938 + 0.193T	– 43.5 + 0.056T	– 981 + 0.249T
LiCl	– 714 (1043K)	+ 30.4 (1043K)	– 684 (1043K)

$\Delta G^*_{PuCl_4} = - 1490 + 0.702T/r^*_{Me^+} + (477 – 0.433T)/r^*_{Me^+} \pm 7$ kJ/mole

$PuCl_{4(melt)} + O_{2(gas)} = PuO_2Cl_{2(melt)} + Cl_{2(gas)}$ reaction

Chloride ions of plutonium can be oxidized by oxygen up to oxychloride plutonium forms. There are two plutonium oxychloride forms: PuO_2Cl and PuO_2Cl_2. It was told before that both plutonium chloride forms and both plutonium oxychloride forms are in equilibrium among themselves. The interaction of the plutonium tetrachloride with oxygen by the reaction

$$PuCl_{4(melt)} + O_{2(gas)} \rightleftarrows PuO_2Cl_{2(melt)} + Cl_{2(gas)} \quad \text{(See 4.3.23)}$$

had been studied in the NaCl-2CsCl melt by the high temperature spectrophotometry method and in NaCl-KCl and 3LiCl-2KCl melts by the heterogeneous equilibrium method [15].

Results of these investigations are presented in Table 4.3.6. One can see that the equilibrium of reaction (4.3.23) is strongly directed to the formation of plutonium oxychloride compounds.

Apparently, the most reliable data had been obtained in the NaCl-2CsCl melt by the high temperature spectrophotometry method, and they can be taken for the subsequent calculations.

Table 4.3.6. Equilibrium constant of reaction
$PuCl_{4(melt)} + O_{2(gas)} \rightleftarrows PuO_2Cl_{2(melt)} + Cl_{2(gas)}$ [15]

Melt	T, K	$K^* \cdot 10^{-3}$	$Log_{10}K^* = a + b/T$
NaCl-2CsCl	863	0.34	$Log_{10}K^* = 4.31 - 1540/T$
	963	0.52	
	1043	0.69	
NaCl-KCl	973	0.78	$Log_{10}K^* = 2.42 + 460/T$
	1043	0.74	
	1113	0.68	
3LiCl-2KCl	873	0.55	$Log_{10}K^* = 2.74$
	973	0.55	
	1053	0.55	

$PuO_2Cl_{(melt)} + 1/2\ Cl_{2(gas)} \rightleftarrows PuO_2Cl_{2(melt)}$ reaction

Spectrophotometric experimental observations show that in the oxidation of the plutonium containing melts by the chlorine-oxygen gas mixtures, it is possible to come to the state when all plutonium exist as PuO_2^+ or PuO_2^{2+} ions. This state can be achieved when the stability limits of the PuO_2^+ and PuO_2^{2+} ions were not exceeded. Otherwise, the part of plutonium will be precipitated as the plutonium dioxide where spectrophotometry method cannot applicable.

In this connection, the melts having the cesium chloride in their composition are the most acceptable in the research of equilibrium between the plutonium oxygen containing ions.

The equilibrium of reaction

$$PuO_2Cl_{2(melt)} \rightleftarrows PuO_2Cl_{(melt)} + 1/2\ Cl_{2(gas)} \quad (4.3.35)$$

had been studied in the NaCl-2CsCl melt at RIAR [15,22].

The spectra of the NaCl-2CsCl melt containing the equilibrium concentrations of PuO_2^+ and PuO_2^{2+} ions are shown on Fig. 4.3.4. As it follows from Fig 4.3.4, the intensity of the absorption band with a maximum at wave number 7040 of the cm^{-1}, belonging to the six-valent plutonium spectrum, decreases with dropping of the chlorine contents in the gas reagent. At the same time the intensity of the absorption band with a maximum at wave number 9090 of the cm^{-1},

corresponding to the five-valent plutonium absorption spectrum, grows. The absorption bands of three and tetravalent plutonium are not found out.

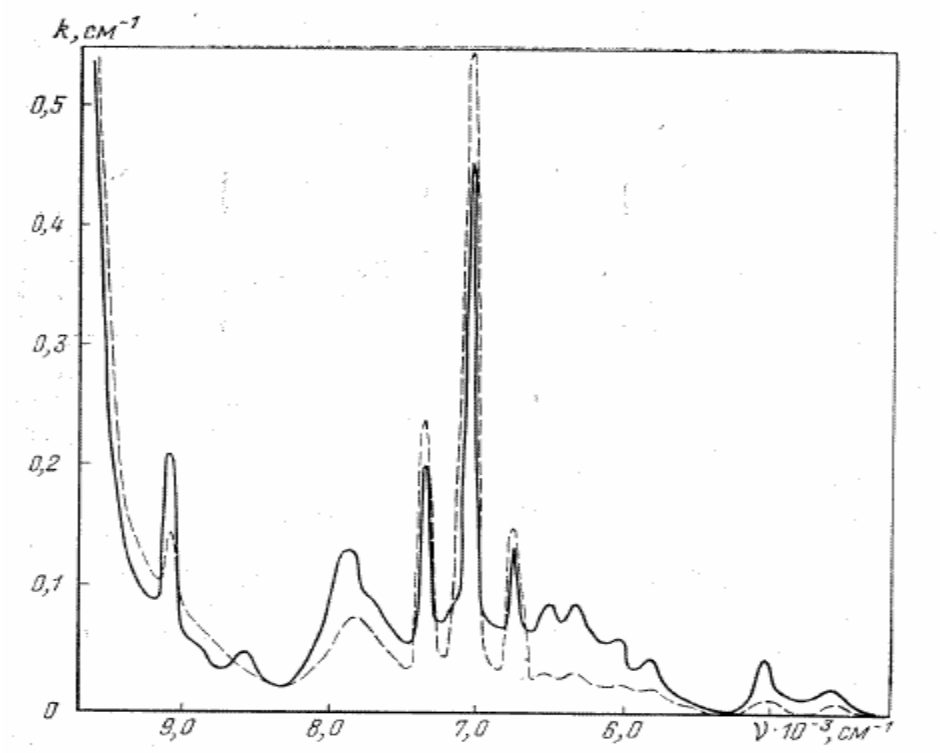

Fig. 4.3.4. Spectra of NaCl-2CsCl melt containing the equilibrium mixture of plutonium (V) and plutonium (VI) [22]
$T = 550^{o}C$; $[PuO_2^{n+}] = 0.192$ mole/l.
———— $P_{Cl_2} = 0.1 \cdot 10^5$Pa; – – – – – – $P_{Cl_2} = 1.0 \cdot 10^5$Pa.

It is not possible to prepare the pure solutions of plutonium (V) or plutonium (VI). However, if the Lambert-Beer's law is correct for the absorption bands with the maximums at 9090 and at 7040 cm^{-1} that the concentration of plutonium (V) and plutonium (VI) can be described by the next equations:

$$[PuO_2^{+}] = k^{9.0}/\varepsilon_5;\ [PuO_2^{2+}] = k^{7.0}/\varepsilon_6,$$

were $[PuO_2^{+}]$ and $[PuO_2^{2+}]$ are the concentration of plutonium (V) and plutonium (VI), mole/l; $k^{9.0}$ and $k^{7.0}$ are the melt absorption coefficients at the wave numbers 9090 and 7040 cm^{-1}, cm^{-1}; ε_5 and ε_6 are the molar absorption coefficients of plutonium (V) and plutonium (VI) at the wave numbers 9090 and 7040 cm^{-1}, l/(mole·cm).

Total plutonium concentration is equal to:

$$[PuO_2^{n+}] = [PuO_2^{+}] + [PuO_2^{2+}] = k^{9.0}/\varepsilon_5 + k^{7.0}/\varepsilon_6. \quad (4.3.36)$$

Transformation of equation (4.3.16) gives a new equation

$$k^{9.0}/\varepsilon_5/[PuO_2^{n+}] = \varepsilon_5 - (\varepsilon_5/\varepsilon_6)\cdot k^{7.0}/[PuO_2^{n+}], \quad (4.3.37)$$

that allows to calculate values of ε_5 and ε_6.

The following equation

$$Log_{10}([PuO_2^{+}]/ [PuO_2^{2+}] = \log_{10}K^{*} - 1/2\log_{10}P_{Cl_2} \quad (4.3.38)$$

was used for the calculation of the reaction (4.3.35) equilibrium constant, and the unit of P_{Cl_2} is Pa.

Graphical checking of equation (4.3.37) (See Fig. 4.3.5) confirms the correctness of the Lambert-Beer's law for both absorption bands.

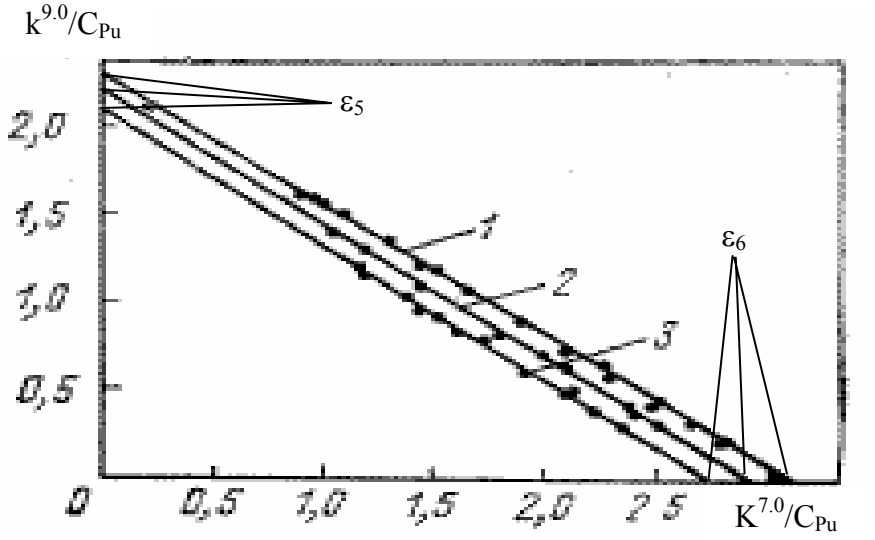

Fig. 4.3.5. Graphical checking of equation 4.3.37 [22]
1 – 550°C; 2 – 650 °C; 3 – 750 °C.

The received molar absorption coefficients have been used for calculation of equilibrium concentration of plutonium (V) and plutonium (VI). The graphic charts allowing to calculate the value of an exponent at chlorine partial pressure in a gaseous reagent and the $\log K^{*}_{4.3.35}$ are presented on Fig. 4.3.6.

Experimental values of the extinction coefficients of plutonium (V) (ν=9090 cm^{-1}) and plutonium (VI) (ν=7040 cm^{-1}) as well as the equilibrium constant of reaction (4.3.35) are shown in Table 4.3.7. (To obtain a non-dimensional value of the equilibrium constant the relative chlorine partial pressure was used at calculation.) These data have been obtained with help of two treatment methods of spectra and of experimental results. The first method (marked by $^{(1)}$) has been described before. This method allows the checking of the material balance in each experimental point and the finding of the stoichiometric coefficient at chlorine in reducing reaction of the plutonium (VI). In the second one (marked by $^{(2)}$) the absorption band of plutonium (VI) only was used for the calculation of equilibrium constant. In this case, it was

declared that the stoichiometric coefficient at chlorine in reaction of the plutonium (VI) reducing (4.3.35) equals to 1/2.

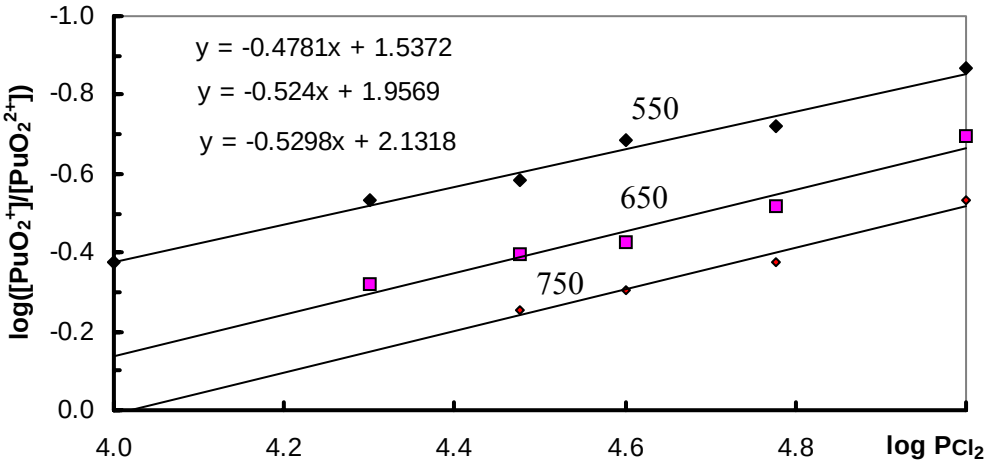

Fig. 4.3.6. Dependence of the $\log([PuO_2^+]/[PuO_2^{2+}])$ on $\log P_{Cl_2}$ at different temperature [22]

The temperature dependence of the equilibrium constant of reaction (4.3.35) can be described by two original equations:

$$Log_{10}K^*_{4.3.35} = 2.42 - 1900/T \pm 0.05, [22]$$

$$Log_{10}K^*_{4.3.35} = 5.03 - 2690/T \pm 0.07 [15].$$

Data on the formal standard potential of the PuO_2^{2+}/PuO_2^+ couple are presented in Table 4.3.8 and Fig. 4.3.7. One can see that the standard potential of the PuO_2^{2+}/PuO_2^+ couple is significantly more positive than the standard potential of the UO_2^{2+}/UO_2^+ couple.

Table 4.3.7. Experimental values of the extinction coefficients of the Pu(V) and Pu(VI) absorption bands and the equilibrium constant of $PuO_2Cl_{2(melt)} + 1/2\ Cl_{2(gas)} \rightleftarrows PuO_2Cl_{(melt)}$ reaction [15, 22]

T, °C	m*	$\varepsilon \cdot 10^3$, cm²/mole		Exponent at P_{Cl_2}	$K^* \cdot 10^{-2}$	$-\log K^*$
		ε_5 (ν=9090 cm^{-1})	ε_6 (ν=7040 cm^{-1})			
550	24[18]	2.3±0.1	3.1±0.2	0.48**	0.135±0.016	0.87±0.05
	10[11]	-	3.3±0.2	0.50***	0.18±0.02	0.75±0.05
650	18[18]	2.2±0.2	2.9±0.2	0.52**	0.225±0.04	0.65±0.04
	8[11]	-	3.3±0.2	0.50***	0.43±0.04	0.37±0.04
750	12[18]	2.1±0.2	2.7±0.2	0.53**	0.380±0.040	0.41±0.04
	5[11]	-	3.3±0.4	0.50***	0.79±0.13	0.11±0.07

*m is the number of experimental points;
**The parameter value was measured experimentally;
*** The parameter value was taken from the chemical equation (4.3.35).

Table 4.3.8. Formal standard potential of the PuO_2^{2+}/PuO_2^{+} couple in NaCl-2CsCl and LiCl-CsCl (45 mole %) melts [15,22].

Melt	Method	$E^*_{PuO_2^{2+}/PuO_2^{+}} - E_{Cl_2/Cl^-} = 2.3RT/nF \cdot \log K^*_{4.3.35}$			
		500°C	550°C	650°C	750°C
NaCl-2CsCl (r^+_{Me} = 1,42)	[22]	-0,159	-0,145	-0,117	-0,089
	[15]	-0,145	-0,120	-0,070	-0,020
	Average	-0,149	-0,130	-0,090	-0,050
LiCl-CsCl (45 mole %) (r^{*+}_{Me} = 1,17) [23]		-0.116	-0.106	-0.081	-0.056

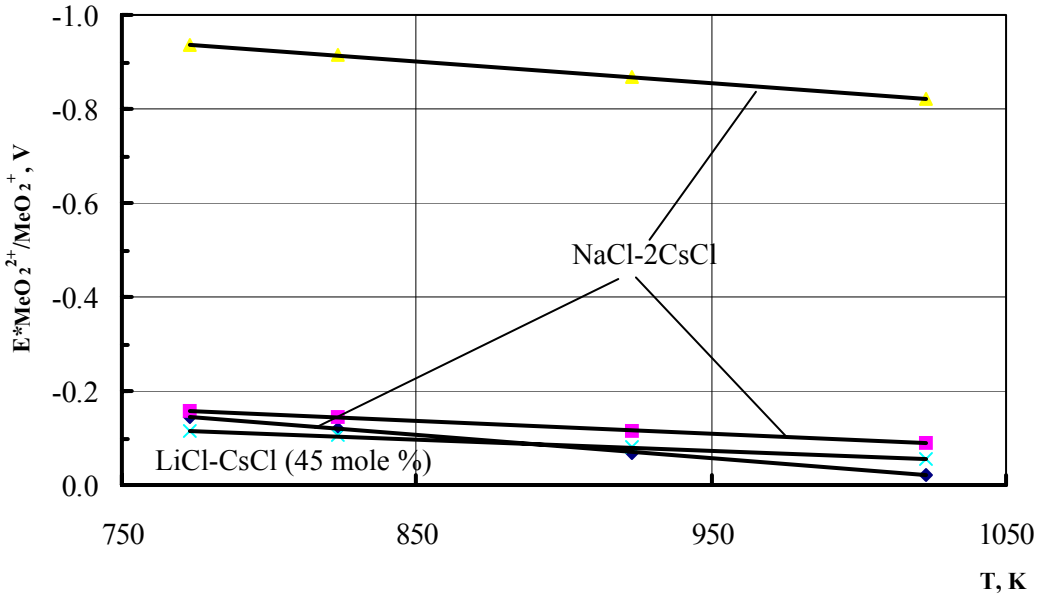

Fig. 4.3.7. Temperature dependence of the conventional formal potentials of UO_2^{2+}/UO_2^{+} and PuO_2^{2+}/PuO_2^{+}couples in NaCl-2CsCl and LiCl-CsCl (45 mole %) melts. [15,22,23]

4.3.3. Evaluation of electrochemical characteristics of plutonium

The most important electrochemical characteristics of plutonium valent transformations for the salt processes of the nuclear oxide fuel production and reprocessing are summarized in Table 4.3.9. In the lower part of Table 4.3.9 the extrapolation coefficients for each case are given. These coefficients can be recommended for calculations of the electrochemical and thermodynamic characteristics of the corresponding plutonium valent transformations and reactions. They can have some difference from coefficients of cited above equations, but they are the result of the complex analysis of the "plutonium – alkali metal chloride melts" system as a whole.

Table 4.3.9. Formal standard and oxidative potentials of the main plutonium valent transformations in the molten chlorides of alkali metals [2,15-18,22]

$E^* = a + b \cdot T$

Melt	r_{Me}^+, A	$E^*_{Pu^{3+}/Pu}$		$E^*_{Pu^{4+}/Pu^{3+}}$		$E^*_{Pu^{4+}/Pu}$		$E^*_{PuO_2^+/PuO_2}$		$E^*_{PuO_2^{2+}/PuO_2}$		$E^*_{PuO_2^{2+}/PuO_2^+}$	
		a	$b \cdot 10^3$	a	$b \cdot 10^3$	a	$b \cdot 10^3$	a	$b \cdot 10^3$	a	$b \cdot 10^3$	a	$b \cdot 10^3$
CsCl	1.65	-3.87	1.16	-0.752	0.765	-3.09	1.06	-0.347	0.802	-0.495	0.675	-0.643	0.548
KCl	1.33	-3.76	1.08	-0.631	0.713	-2.98	0.99	-0.268	0.807	-0.374	0.643	-0.480	0.478
NaCl	0.98	-3.60	0.98	-0.465	0.599	-2.61	0.71	-0.123	0.821	-0.151	0.585	-0.179	0.349
LiCl	0.68	-3.46	0.94	-0.171	0.433	-2,03	0,30	+0.121	0.843	+0.224	0.487	+0.327	0.131
NaCl-2CsCl	1.42	-3.80	1.11	-0.653	0.686	-3.01	1.00	-0.294	0.805	-0.414	0.654	-0.534	0.502
4LiCli3CsCl	1.17	3.67	1.06	-0.595	0.638	-2.83	0.86	-0.212	0.813	-0.290	0.621	-0.367	0.429
NaCl-KCl	1.15	-3.58	0.93	-0.553	0.684	-2.82	0.87	-0.206	0.813	-0.279	0.618	-0.351	0.422
3LiCl-2KCl	0.95	-3.61	1.00	-0.451	0.584	-2.54	0.65	-0.103	0.823	-0.121	0.579	-0.139	0.331
Extrapolation coefficients		$a = -4.085 + 0.4543/r^*_{Me}{}^+$		$a = -1.1314 + 0.6521/r^*_{Me}{}^+$		$a = -3.9026 + 1.2702/r^*_{Me}{}^+$		$a = -0.6756 + 0.542/r^*_{Me}{}^+$		$a = -1.008 + 0.8331/r^*_{Me}{}^+$		$a = -1.3256 + 1.124/r^*_{Me}{}^+$	
		$b \cdot 10^3 = 1.2511 - 2.385/r^*_{Me}{}^+$		$b \cdot 10^3 = 0.9769 - 0.3702/r^*_{Me}{}^+$		$b \cdot 10^3 = 1.6448 - 0.9165/r^*_{Me}{}^+$		$b \cdot 10^3 = 0.7712 - 0.0488/r^*_{Me}{}^+$		$b \cdot 10^3 = 0.8068 - 0.2172/r^*_{Me}{}^+$		$b \cdot 10^3 = 0.8417 - 0.4835/r^*_{Me}{}^+$	

Evaluation formal potentials of PuO_2 ions

Formal potentials of PuO_2 ions are the most fundamental parameters for the Oxide pyroprocess. In Japan, these values have been arbitrary quoted from various research papers or RIAR's report without any critical point of view. Therefore, authors review these values from the original papers. People tend to misunderstand that these potentials are directly measured by electrochemical method. In the following section, we will describe how these potentials are calculated by the equilibrium constants measured by the high temperature spectrophotometry method. As the result, new correlations are recommended for NaCl-2CsCl melt.

The formal potential can be calculated from the equilibrium constant $K_{2+/+}$ for the following reaction.

$$PuO_2Cl_2 = PuO_2Cl + 1/2\ Cl_2 \tag{4.3.39}$$

This reaction divided into the following half reactions at any point of the melt.

$$Cl^- = 1/2\ Cl_2 + e^- \tag{4.3.40}$$

$$PuO_2^{2+} + e^- = PuO_2^{+} \tag{4.3.41}$$

Potentials of these reactions can be calculated by the following Nernst equations.

$$E\left(Cl^- / Cl_2\right) = E_f\left(Cl^- / Cl_2\right) + \frac{R \cdot T}{F} \ln P_{cl2}^{1/2} \tag{4.3.42}$$

$$E\left(PuO_2^{2+} / PuO_2^{+}\right) = E_f\left(PuO_2^{2+} / PuO_2^{+}\right) + \frac{R \cdot T}{F} \ln \frac{[PuO_2^{2+}]}{[PuO_2^{+}]} \tag{4.3.43}$$

where

$E\ (Cl\text{-}/Cl_2)$: Equilibrium potential of Cl^-/Cl_2, (V vs. Cl^-/Cl_2),

$E(PuO_2^{2+}/PuO_2^{+})$: Equilibrium potential of PuO_2^{2+}/PuO_2^{+}(V vs. Cl^-/Cl_2)

$E_f(Cl^-/Cl_2)$: Formal potential of Cl^-/Cl_2 =0,

$E_f(PuO_2^{2+}/PuO_2^{+})$: Formal potential of PuO_2^{2+}/PuO_2^{+},

P_{Cl_2}: Chlorine partial pressure (relative to 1 atom)

$[PuO_2^{2+}]$: Molar concentration of PuO_2^{2+} ion (mole fraction)

$[PuO_2^{+}]$: Molar concentration of PuO_2^{+} ion (mole fraction)

There will be no electro-motive force at the equilibrium, i.e. $E(Cl^-/Cl_2) = E(PuO_2^{2+}/PuO_2^{+})$.

Then, the formal potential can be calculated from $K_{2+/+}$ as follows.

$$\begin{aligned} E_f\left(PuO_2^{2+} / PuO_2^{+}\right) &= \frac{R \cdot T}{F} \ln \frac{[PuO_2^{+}] \cdot P_{cl2}^{1/2}}{[PuO_2^{2+}]} = \frac{R \cdot T}{F} \ln K_{2+/+} \\ &= 2.303 \frac{R \cdot T}{F} \log_{10} K_{2+/+} \end{aligned} \tag{4.3.44}$$

The most reliable equilibrium constant in NaCl-2CsCl is the following one evaluated by the electro-photometry method [22]:

$$\lg K_{2+/+} = 1.42\ (+2.5 \text{ if } P_{Cl_2} \text{ is in Pa}) - 1900/T \tag{4.3.45}$$

The formal potential can be calculated by substituting Eq.(7) into Eq.(4.3.44) ;

$$E_f(PuO_2^{2+}/PuO_2^{+}) = -0.3689 + 2.757\times10^{-4}\cdot T\ (K) \tag{4.3.46}$$
$$= -0.114\ (V)\ \text{at } 923\ K$$

Evaluation of the formal potential of PuO_2^+/PuO_2 in NaCl-2CsCl melt

The formal potential of PuO_2^+/PuO_2 can be calculated by the equilibrium constant of the following reaction.

$$PuO_2Cl = PuO_2 + 1/2\ Cl_2 \tag{4.3.47}$$

$$K_{+/0} = \frac{P_{cl2}^{1/2}}{[PuO_2^+]} \tag{4.3.48}$$

This reaction is divided into the following half reactions at the place of melt and oxide at contact.

$$Cl^- = 1/2\ Cl_2 + e^- \tag{4.3.49}$$

$$PuO_2^+ + e^- = PuO_2 \tag{4.3.50}$$

Potentials of these electrodes can be calculated by the following Nernst equations.

$$E\left(Cl^-/Cl_2\right) = E_f\left(Cl^-/Cl_2\right) + \frac{R\cdot T}{F}\ln P_{cl2}^{1/2} \tag{4.3.51}$$

$$E\left(PuO_2^{\ +}/PuO_2\right) = E_f\left(PuO_2^{\ +}/PuO_2\right) + \frac{R\cdot T}{F}\ln[PuO_2^+] \tag{4.3.52}$$

Then, the following equation holds in the equilibrium.

$$E_f\left(PuO_2^{\ +}/PuO_2\right) = \frac{R\cdot T}{F}\ln\frac{P_{cl2}^{1/2}}{[PuO_2^+]} = \frac{R\cdot T}{F}\ln K_{+/0}$$
$$= 2.303\frac{R\cdot T}{F}\log_{10} K_{+/0} \tag{4.3.53}$$

If $K_{2+/+}$ is given by Eq.(4.3.45), $K_{+/0}$ can be calculated as follows.

$$[Pu_{ox}] = [PuO_2^{2+}] + [PuO_2^+] = \frac{P_{cl2}^{1/2}\cdot[PuO_2^+]}{K_{2+/+}} + [PuO_2^+] = \left(\frac{P_{cl2}^{1/2}}{K_{2+/+}} + 1\right)\cdot\frac{P_{cl2}^{1/2}}{K_{+/0}} \tag{4.3.54}$$

Then, the following equation holds.

$$K_{+/0} = \left(\frac{P_{cl2}^{1/2}}{K_{2+/+}} + 1\right)\cdot\frac{P_{cl2}^{1/2}}{[Pu_{ox}]} \tag{4.3.55}$$

$[Pu_{ox}]$ and P_{cl2} are measured [24] as shown in the left columns of Table 4.3.10. $K_{2+/+}$ and $K_{+/0}$ can be calculated by Eq. (4.3.45) and Eq. (4.3.54) respectively as shown in the right columns of Table 4.3.10.

Table 4.3.10. Evaluation of equilibrium constant $K_{+/0}$ in NaCl-2CsCl

T, K	1/T, K^{-1}	PCl_2 (relative)	[Pu]= [Pu^{3+}] +[Pu^{4+}] (mole fraction)	$K_{2+/+}$	$K_{+/0}$	$\log_{10}K_{+/0}$
823.15	0.001215	0.3001	0.01178	0.1294	243.50	2.3865
863.15	0.001159	0.3001	0.00779	0.1655	303.23	2.4818
923.15	0.001083	0.3001	0.00439	0.2301	421.55	2.6248
963.15	0.001038	0.3001	0.00380	0.2801	426.56	2.6300

The logarithm of $K_{+/0}$ is plotted vs. 1/T in Fig.4.3.8 and their correlation equation is given as follows.

$$Log_{10}K_{+/0} = -1470.3/T + 4.183 \quad (4.3.56)$$

Now, the formal potential for PuO_2^{+}/PuO_2 can be calculated as follows.

$$E_f(PuO_2^{+}/PuO_2)=-0.292 + 8.302\times10^{-4}T=0.474\ (V)\ \text{at}\ 923\ K \quad (4.3.57)$$

Fig. 4.3.8. Evaluated equilibrium constant K+/0

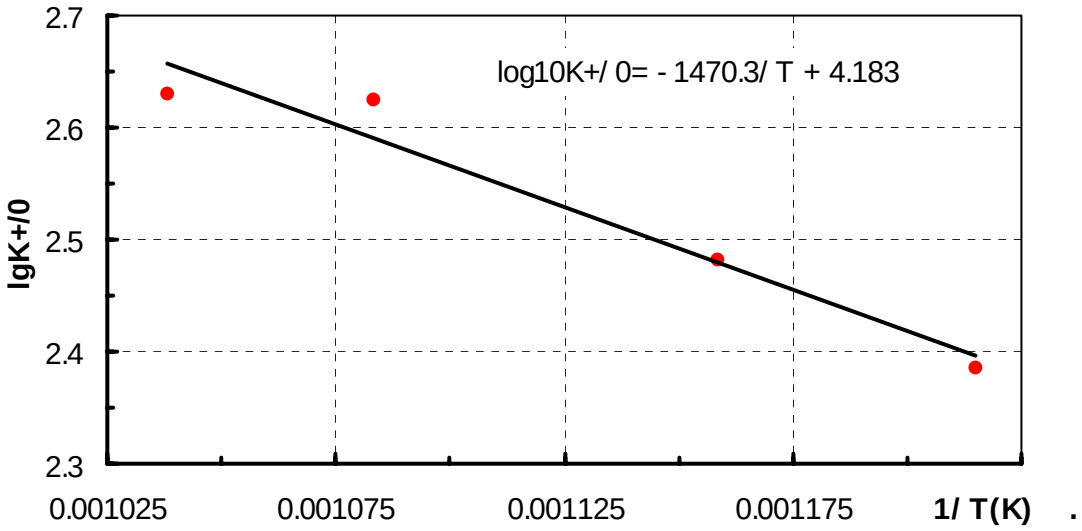

Evaluation of the formal potential of PuO_2^{2+}/PuO_2 in NaCl-2CsCl melt

It is very difficult to measure the potential of PuO_2^{2+}/PuO_2 couple, as PuO_2 is an insulator. At equilibrium, $E_f(PuO_2^{2+}/PuO_2)$ can be calculated by $E_f(PuO_2^{2+}/PuO_2^{+})$ and $E_f(PuO_2^{+}/PuO_2)$ by the using following equation.

$$2\,E_f(PuO_2^{2+}/PuO_2) = E_f(PuO_2^{2+}/PuO_2^{+}) + E_f(PuO_2^{+}/PuO_2) \quad (4.3.58)$$

Then, the following correlation is given for the formal potential.

$$E_f(PuO_2^{2+}/PuO_2) = -0.3305 + 5.530\times10^{-4}T = 0.18 \text{ (V) at 923 K} \qquad (4.3.59)$$

Comparison of the potentials with literature data

The formal potentials are calculated for various temperatures in Table 4.3.11. The corresponding values are also calculated by RIAR's correlation in Table 4.3.12. These values are compared in Fig. 4.3.9. The difference is largest at higher temperature for PuO_2(+/0), which is less than 0.05V. The agreement is better for PuO_2(2+/0) as the result of the coincident cancellation of the other potentials.

Table 4.3.11. Evaluated formal potential for PuO_2 ions in NaCl-2CsCl vs. Cl^-/Cl_2

Temperat. / Couples	550°C	600°C	650°C	700°C	Coefficient	
	823.15K	873.15K	923.15K	973.15K	a	b
PuO_2^{2+}/PuO_2	0.125	0.152	0.180	0.208	-0.3305	$5.53\cdot10^{-4}$
PuO_2^{2+}/PuO_2^{+}	-0.142	-0.128	-0.114	-0.101	-0.3689	$2.76\cdot10^{-4}$
PuO_2^{+}/PuO_2	0.391	0.433	0.474	0.516	-0.292	$8.30\cdot10^{-4}$

Table 4.3.12. Evaluated formal potential for PuO_2 ions in NaCl-2CsCl vs. Cl^-/Cl_2

Temperat. / Couples	550°C	600°C	650°C	700°C	Coefficient	
	823.15K	873.15K	923.15K	973.15K	a	b
PuO_2^{2+}/PuO_2	0.124	0.157	0.190	0.208	-0.414	$6.54\cdot10^{-4}$
PuO_2^{2+}/PuO_2^{+}	-0.121	-0.096	-0.071	-0.101	-0.534	$5.02\cdot10^{-4}$
PuO_2^{+}/PuO_2	0.369	0.409	0.449	0.516	-0.294	$8.05\cdot10^{-4}$

Fig. 4.3.9 Comparison of Formal potentials

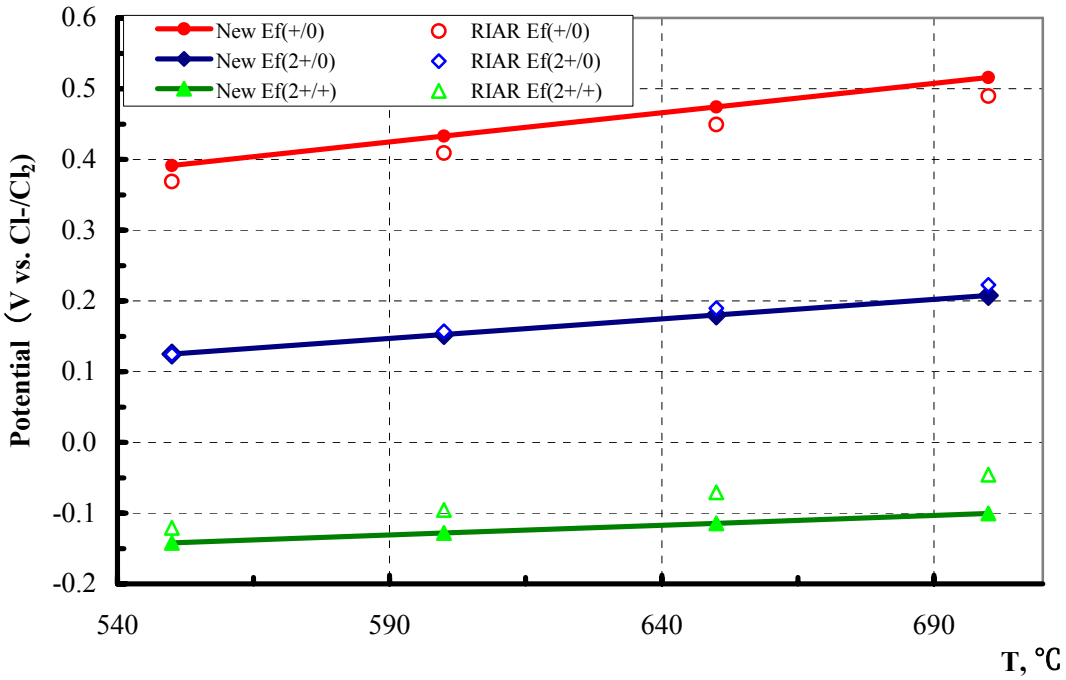

4.3.4. Kinetics of the plutonium redox reactions

The kinetics of the plutonium redox reactions had been studied by the high temperature spectrophotometry method. The absorption band of plutonium (IV) with wave number 5300cm^{-1} was used at the examination in course of reactions. Other plutonium forms have not any absorption bands at this wave number.

Reaction of oxidation of reduced plutonium forms with oxygen

Oxidation of reduced plutonium forms can be presented by following equation

$$PuCl_{n(melt)} + O_{2(gas)} = PuO_2Cl_{m(melt)} + (n\text{-}m)/2Cl_{2(gas)} \qquad (4.3.60)$$

where n and m are the averaged valency of reduced and oxidized plutonium forms. The temperature and the chlorine gas partial pressure influence the values of n and m in compliance with the equilibrium of reaction (4.3.21) and (4.3.35).

The change of the plutonium (IV) concentration in course of the oxidation of Pu(III), Pu(IV) and of theirs equilibrium mixture with oxygen at 550^{o}C is shown on Fig. 4.3.10 (See curves 1 – 4) [24]. The "melt – gas" specific interphase was equal 1 cm^2 per 1 cm^3 of melt. The oxygen-chlorine gas mixture was used as the gas reagent.

Due to the low stability of plutonium (IV), there is little possibility of preparing its pure solutions. At first, the Pu(III)-Pu(IV) equilibrium mixtures were obtained at the pure chlorine atmosphere. Chlorine gas content in the oxidative gas reagent was always less than its content at

the initial solution. Therefore, the curve (1) shows the change of the Pu(IV) concentration in melt in the course of the following two reactions:

$$PuCl_{4(melt)} + O_{2(gas)} \rightarrow PuO_2Cl_{2(melt)} + Cl_{2(gas)}; \quad (4.3.61)$$

$$PuCl_{4(melt)} \rightarrow PuCl_{3(melt)} + 1/2\ Cl_{2(gas)}. \quad (4.3.62)$$

In 40 minutes, the reaction (4.3.62) comes to equilibrium, and oxidation of the Pu(III)-Pu(IV) equilibrium mixture take place.

Initial solution of Pu(III) had been prepared by reducing the oxidized plutonium forms by hydrogen chloride followed by washing the HCl in the melt by inert gas.

The curve (2) shows the change of the plutonium (IV) concentration in melt in course of reaction

$$PuCl_{3(melt)} + O_{2(gas)} = PuO_2Cl_{(melt)} + Cl_{2(gas)}. \quad (4.3.63)$$

One can see that the oxidation of Pu(III) up to Pu(IV) by chlorine gas occurs at first

$$PuCl_{3(melt)} + 1/2\ Cl_{2(gas)} = PuCl_{4(melt)}. \quad (4.3.64)$$

In 10 minutes, the reaction (4.3.64) comes to equilibrium, and the oxidation of the Pu(III)-Pu(IV) equilibrium mixture take place again.

The curve (3) shows the change of the plutonium (IV) concentration in melt in the course of oxidation reaction of Pu(III)-Pu(IV) equilibrium mixture (reaction 4.3.60).

In this case, the initial solutions of Pu(III)-Pu(IV) equilibrium mixture had been prepared by oxidizing the Pu(III) by the chlorine – inert gas mixture having the same chlorine content as in the chlorine – oxygen mixture, which was used at following oxidation. In that way, the reactions (4.3.62) and (4.3.64) were excluded.

Using the reaction (4.3.31) equilibrium constant, we can calculate the change of the total concentration of the reduced plutonium forms. It is shown by the curve (4).

It was shown in section 4.2.3 that at certain conditions the kinetics of reaction

$$UCl_{4(melt)} + O_{2(gas)} = UO_2Cl_{2(melt)} + Cl_{2(gas)}.$$

can be described by equation:

$$- d[U^{4+}]/dt = k_o \cdot Po_2/\{1 + kCl_2 \cdot (PCl_2)^{1/2}\}. \quad (4.3.65)$$

Process of the formation of peroxide anions is the stage, which limits the rate of whole reaction . If the plutonium forms do not change strongly the properties of melt surface, it is possible to suppose that the kinetics of reaction (4.3.60) also can be described by equation (4.3.65).

For uranium at 550°C the value of parameter k_o (see equation 4.3.65) equals $(8.2\pm0.6)\cdot10^{-11}$ mole/(min·Pa·cm^2), and the value of parameter kCl_2 equals $(2.3\pm0.1)\cdot10^{-3}$ Pa$^{-1/2}$. (It is necessary to note that the investigations of the oxidation reactions both the uranium and plutonium had been carried out in the same geometry.) The calculated kinetic curve for the uranium oxidation

(See curve 5 on Fig. 4.3.10) agrees with the kinetic curve (4) obtained from experimental data for plutonium.

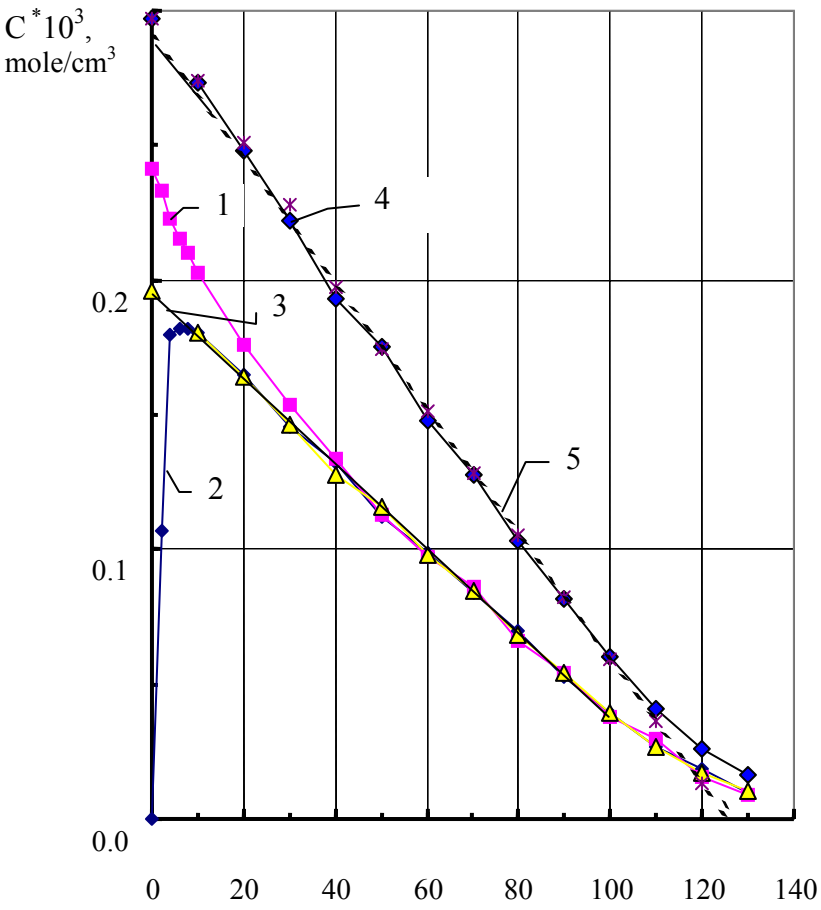

Fig. 4.3.10. Change of the Pu(IV) concentration at the oxygen oxidation of (1) Pu(IV), (2) Pu(III), (3) Pu(III) and Pu(IV) equilibrium mixture [24]. (4) - change of the Pu total concentration in course of (1), (2) and (3) reactions. Gas reagent: O_2 – 80 vol.%; Cl_2 – 20 vol.%. T = 550°C; a' – 0.475 cm^{-1}. (5) –kinetics curve for the U(IV) oxidation.

This agreement demonstrates that there exists a common process determining the oxidation rate of uranium and plutonium.

Reduction reaction of plutonium oxidized forms with chlorine

Reaction (4.3.60) is reversible. The oxygen-contained plutonium forms can be reduced by chlorine up to oxygen-free plutonium forms by the following reaction

$$PuO_2Cl_{m(melt)} + (n\text{-}m)/2Cl_{2(gas)} \rightarrow PuCl_{n(melt)} + O_{2(gas)}. \qquad (4.3.66)$$

The experimental kinetic curves of reaction (4.3.66), obtained at the chlorine partial pressure of 1 atmosphere ($1.01 \cdot 10^5$Pa), are presented on Fig. 4.3.11 [24]. In semi-logarithmic coordinates,

they can be transformed into straight lines. That is argument for describing the reaction (4.3.45) kinetics by equation of first order for the oxidized plutonium forms, i.e.:

$$- d[PuO_2^{m+}]/dt = a' \cdot k_{red} \cdot P_{Cl_2} \cdot [PuO_2^{m+}].$$

where k_{red} is kinetic constant, cm/min; a' is specific "gas-melt" surface, cm^{-1} (or cm^2/cm^3).

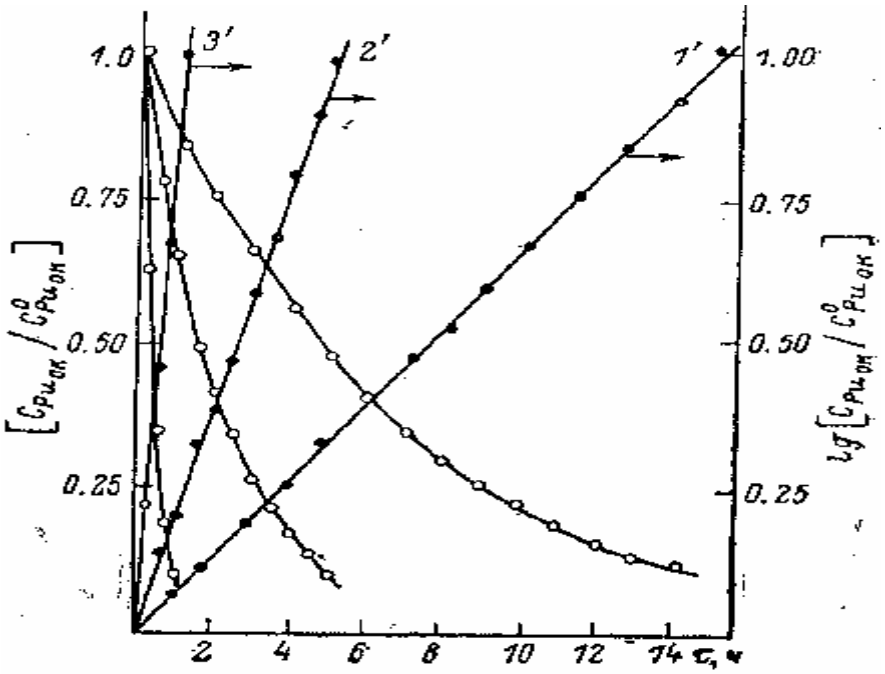

Fig. 4.3.11. Experimental kinetic curves of reaction (4.3.45) in NaCl-2CsCl melt at: 1 – 550; 2 – 650; 3 – 750°C. $P_{Cl_2} = 1.0 \cdot 10^5$ Pa., $a' = 0.475$ cm^{-1} [24]

It was found that

$$Log_{10}k_{red} = - 0.491 - 7642/T \pm 0.08.$$

Influence of the chlorine partial pressure on the kinetics of reaction (4.3.45) has not been investigated.

So, the next equations can be recommended for kinetic calculations:

$$- \frac{d[Pu^{n+}]}{dt} = a' \cdot \left(\frac{k_o \cdot P_{O_2}}{1 + k_{Cl_2} \cdot (P_{Cl_2})^{1/2}} - k_{red} \cdot P_{Cl_2} \cdot [PuO_2^{m+}] \right)$$

$$- \frac{d[U^{4+}]}{dt} = a' \cdot \frac{k_o \cdot P_{O_2}}{1 + k_{Cl_2} \cdot (P_{Cl_2})^{1/2}} \qquad (4.3.67)$$

$$\log_{10}k_0 = - 5.623 - 3676/T \pm 0.04 \quad (k_0 \text{ dimension is } [\text{mole}/(\text{min} \cdot \text{cm}^2 \cdot \text{Pa}]),$$

$$\log_{10}k_{Cl_2} = - 0.80 - 1500/T \pm 0.02 \quad (k_{Cl_2} \text{ dimension of is } [\text{Pa}^{1/2}]),$$

$$\log_{10}k_{red} = - 0.491 - 7642/T \pm 0.08 \quad (k_{red} \text{ dimension of is } [\text{cm}/(\text{min} \cdot P_{Cl_2}]),$$

where the unit of plutonium content in melt has to be in $mole/cm^3$, time min, and temperature Kelvin.

It's necessary to remember that all data were obtained in a small melt volume of 4 cm^3 with spectrophotometry method. These data can only used for the basic understanding of plutonium redox reactions.

Mechanism of the plutonium redox reaction

The kinetic law of reaction (4.3.60) can be presented by the equation (4.3.67). Obtained kinetic behaviour of plutonium can be explained on the assumption of the following reversible reactions [24]:

$$\left.\begin{array}{ll} \text{I} & O_{2(gas)} + Cl^-_{(melt)} \rightleftarrows O_2^-{}_{(melt)} + 1/2\ Cl_{2(gas)}, \\ \text{II} & O_2^-{}_{(melt)} + Cl^-_{(melt)} \rightleftarrows O_2^{2-}{}_{(melt)} + 1/2\ Cl_{2(gas)}, \\ \text{III} & Pu^{4+}(Pu^{3+}) + O_2^{2-}{}_{(melt)} \rightleftarrows PuO_2^{2+}(\ PuO_2^{+})_{(melt)}, \end{array}\right\} \qquad (4.3.68)$$

where the forwarding stage of the reaction (I) and the back stage of reaction (III) are slow.

Thus, oxygen oxidizes the ions U^{4+}, Pu^{3+} and Pu^{4+} into the ions UO_2^{2+}, PuO_2^{+} and PuO_2^{2+} in chloride melts by the identical mechanism, which includes the following stages:

- Formation of O_2^- ions;
- Formation of O_2^{2-} ions;
- Oxidation of Me^{n+} by O_2^{2-} ions.

Formation of O_2^- ions is the slowest stage, which proceeds on the "gas – melt" interface. Other stages take place in the melt directly interface.

There is a difference between interaction of ions O_2^{2-} with ions U^{4+}, and ions Pu^{3+} and Pu^{4+}. Due to the high stability of ions UO_2^{2+}, interaction of ions U^{4+} with anions O_2^{2-} is irreversible practically, and content of anions O_2^{2-} in melt (in presence of ions U^{4+}) is very low. On the contrary, due to low stability of ions PuO_2^{+} and PuO_2^{2+}, interaction of ions Pu^{3+} and Pu^{4+} with anions O_2^{2-} is reversible, i.e., the content of anions O_2^{2-} in melt (in presence of ions Pu^{3+} and Pu^{4+}) is enough to provide high rate of anions O_2^{2-} interaction with chlorine dissolved in melt.

4.4. Minor actinides chemistry in molten chloride systems

Neptunium. Similar to U Pu, in molten chlorides of alkali metals neptunium presents in the oxygen-free and oxygen-containing state. Np(III) and Np(IV) are realized as the Np^{3+} and Np^{4+} cations, and Np(V) and Np(VI) as the NpO_2^{+} and NpO_2^{2+} cations [25].

The stability regions of various neptunium valency forms are shown in Fig. 4.4.1 [26-28].

The neptunium ions have the form of complexes similar to the appropriate uranium and plutonium ones: $NpCl_6^{3-}$, $NpCl_6^{2-}$, $NpO_2Cl_4^{3-}$ and $NpO_2Cl_4^{2-}$.

Various valency forms of neptunium can be obtained in the melts by the methods previously described for uranium and plutonium.

Actually, the same reactions are characteristic of the neptunium chemistry:

$$Np_{(solid)} - 3e^- + 3Cl^-_{(melt)} = NpCl_{3(melt)};\quad \text{- anodic process,} \quad (4.4.1)$$

$$NpCl_{3(melt)} + 1/2Cl_{2(gas)} \rightleftarrows NpCl_{4(melt)}, \quad (4.4.2)$$

$$NpCl_{4(melt)} + O_{2(gas)} = NpO_2Cl_{(melt)} + 3/2Cl_{2(gas)}, \quad (4.4.3)$$

$$NpO_2Cl_{(melt)} + 1/2Cl_{2(gas)} \rightleftarrows NpO_2Cl_{2(melt)}, \quad (4.4.4)$$

$$NpO_2Cl_{2(melt)} + CCl_{4(gas)} = NpCl_{4(melt)} + CO_{2(gas)} + Cl_{2(gas)}, \quad (4.4.5)$$

$$NpO_2Cl_{(melt)} = NpO_{2(solid)} + 1/2Cl_{2(gas)}, \quad (4.4.6)$$

$$NpO_2Cl_{n(melt)} + ne^- = NpO_{2(solid)} + nCl^-_{(melt)}, \quad (n = 1 \text{ or } 2). \quad (4.4.7)$$

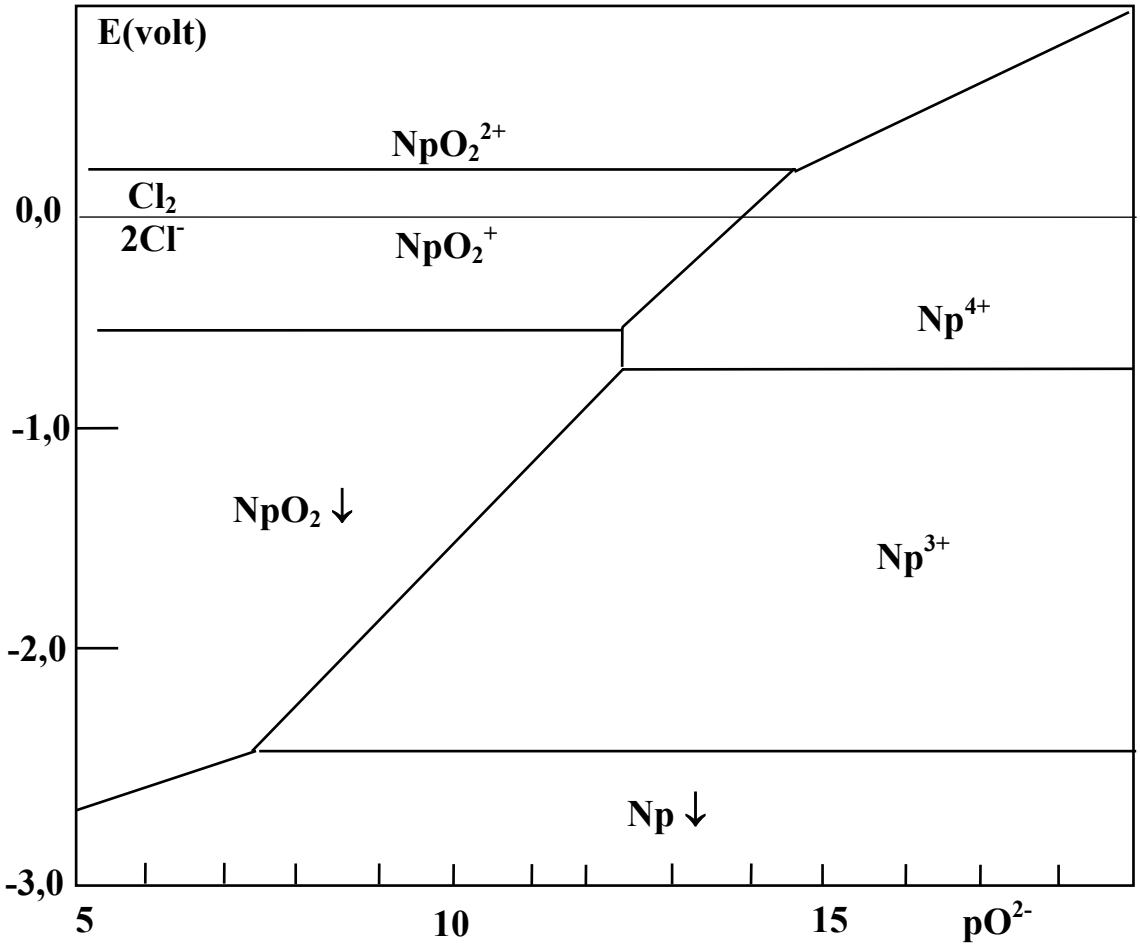

Fig. 4.4.1. Potential-pO^{2-} diagram of neptunium in molten Li-K)Cl at 450°C: $[Np^{3+}] = [Np^{4+}] = [NpO^+_2] = 10^{-2}$ mol/l [26].

The main valency transformations of neptunium in molten chlorides of alkali metals have the reversible character, but the highest oxidation degrees of neptunium are more stable compared with plutonium.

The most important thermodynamic characteristics of neptunium reactions for the nuclear oxide fuel production and reprocessing in molten salts are summarized in Table 4.4.1(Calculated of [3,21-30] data).

Table 4.4.1. Thermodynamic characteristics of neptunium reactions [4,25-30]

Reaction	Melt	Thermodynamic characteristics
$NpCl_3 + 1/2Cl_2 \rightleftarrows NpCl_4$	NaCl-KCl	lg K = -5.55 + 2790/T ± 0.05
$NpCl_4 + O_2 = NpO_2Cl_2 + Cl_2$	RbCl-CsCl	Lg K = - 0.58 (923 K)
$NpO_2 + 1/2\ Cl_2 \rightleftarrows NpO_2Cl$	3LiCl-2KCl	Lg K = - 1.63 (673 K)
-"-	LiCl- KCl	Lg K = - 1.72 (723 K)
-"-	LiCl- KCl	Lg K = - 1.82 (773 K)
$NpO_2Cl + 1/2\ Cl_2 \rightleftarrows NpO_2Cl_2$	3LiCl-2KCl	Lg K = 0.89 (673 K)

The main electrochemical characteristics of neptunium valency transformations in the molten chlorides of alkali metals are presented in Table 4.4.2 (Calculated of [4,25-34] data).

Table 4.4.2. Formal standard and oxidative potentials of Np transformation [4,25-34]

Transformation	Melt	Temperature relation of the formal standard potential, V
$Np(III) \rightarrow Np$	3LiCl-2KCl	$-2.805 + 0.00064_*T$
-"-	(Li.....Cs)Cl	$- 4.35+(0.79/r^*_{Me^+})+(14.89-5.60/ r^*_{Me^+})\cdot 10^{-4}*T$
$Np(IV) \rightarrow Np(III)$	3LiCl-2KCl	$-2.10 + 0.00076\cdot T \pm 0.003$
$NpO_2(VI) \rightarrow NpO_2(V)$	(Li.....Cs)Cl	$- 1.25+(1.11/r^*_{Me^+})+(9.19-3.81/ r^*_{Me^+})\cdot 10^{-4}*T$
$NpO_2(V) \rightarrow NpO_2$	(Li.....Cs)Cl	$- 0.006+(0.58/r^*_{Me^+})+(3.90-0.12/ r^*_{Me^+})\cdot 10^{-4}{}_*T$

r_{M^+} is average radius of alkali metal cations.

Americium. In molten chlorides of alkali metals, americium exhibits the stable form of trivalent oxygen-free state [4,29,35-38] that can be obtained by:

anodic dissolution of metal by the reaction

$$Am_{(solid)} - 3e^- + 3Cl^-_{(melt)} = AmCl_{3(melt)}; \quad (4.4.8)$$

metal chlorination with chlorine by the reaction

$$Am_{(solid)} + 3/2Cl_{2(gas)} = AmCl_{3(melt)}; \quad (4.4.9)$$

dioxide chlorination with chlorine, carbon tetrachloride or other chlorinating reagents, for example:

$$AmO_{2(solid)} + 3/2Cl_{2(gas)} = AmCl_{3(melt)} + O_{2(gas)}, \quad (4.4.10)$$

$$AmO_{2(solid)} + CCl_{4(gas)} = AmCl_{3(melt)} + CO_{2(gas)} + 1/2\ Cl_{2(gas)}. \quad (4.4.11)$$

Americium in equilibrium with metal exists as Am(II). The formal standard potential of the pair Am(II)/Am relative to the chlorine reference electrode in molten 3LiCl-2KCl eutectic at 773 K is equal to -3.05V [38].

Americium can be incorporated into the MOX fuel due to its capability to form AmOCl by the reaction [4]

$$AmCl_{3(melt)} + 1/2O_{2(gas)} = AmOCl_{(melt)} + Cl_{2(gas)}. \quad (4.4.12)$$

The following cathodic processes can present uranium and americium co-deposition:

$$\left.\begin{array}{l} AmO^{+} + e^{-} = \\ UO_2^{2+} + 2\,e^{-} = \end{array}\right| = (U,Am)O_{2-x}(\text{cath.}). \qquad (4.4.13)$$

Compound AmOCl is not stable in chloride melts. Therefore, americium fraction in the cathodic deposit obtained by electrolysis does not exceed several percents.

Curium. In molten chlorides of alkali metals curium exists only as Cm(III). It can be obtained by:

anodic dissolution of metal

$$Cm_{(solid)} - 3e^{-} + 3Cl^{-}_{(melt)} = CmCl_{3(melt)}; \qquad (4.4.14)$$

metal chlorination by chlorine

$$Cm_{(solid)} + 3/2Cl_{2(gas)} = CmCl_{3(melt)}; \qquad (4.4.15)$$

oxide chlorination by chlorine, carbon tetrachloride or other chlorinating reagents, for instance:

$$Cm_2O_{3(solid)} + 3/2Cl_{2(gas)} = CmCl_{3(melt)} + 3/2\ O_{2(gas)}, \qquad (4.4.16)$$

$$Cm_2O_{3(solid)} + CCl_{4(gas)} = CmCl_{3(melt)} + CO_{2(gas)} + CO_{(gas)} + Cl_{2(gas)}. \qquad (4.4.17)$$

The formal standard potential of Cm in molten NaCl-KCl exists in the range from -2.85 to -2.95 V relative to the chlorine reference electrode within the temperature from 973 up to 1023 K [27,39].

There is no information about oxygen containing ions of curium in molten salts.

Comparison of electrochemical properties of actinides

The electrochemical characteristics of actinide valency transformations of some electrolytes are presented in Table 4.4.3. The Table shows the position of actinide formal standard and formal redox potentials relative to the chlorine reference electrode.

Table 4.4.3. Formal standard and redox potentials of actinide in molten chlorides of alkali metals

Me(n)/Me(m)	$E^{*}_{Me(n)/Me(m)}$, V		
	3LiCl-2KCl (773 K)	NaCl-KCl (1000 K)	NaCl-2CsCl (873 K)
Am(II)/Am(0)	- 3.05 [38]	-	-
Cm(III)/Cm(0)	-	- 2.90 [29]	-
Pu(III)/Pu(0)	- 2.82 [16]	- 2.64 [16]	- 2.83 [16]
Np(III)/Np(0)	- 2.32 [30]	-	-
U(III)/U(0)	- 2.31 [1]	- 2.19 [1]	- 2.39 [1]
Pu(IV)/Pu(III)	+ 0.01 [17]	+ 0.09 [17]	- 0.05 [17,18]
Np(IV)/Np(III)	- 1.51 [32]	-	-
U(IV)/U(III)	- 1.40 [4]	- 1.39 [4]	- 1.45 [4]
PuO_2(VI)/PuO_2	+ 0.32 [15]	+ 0.33 [15]	+ 0.149 [15]
NpO_2(VI)/NpO_2	+ 0.61 [4]*	+0,59 [4]*	+ 0,42 [4]*
UO_2(VI)/UO_2	- 0.50 [5]	- 0.40 [5]	- 0.65 [5]

* Data calculated with using the generalized equations.

4.5. Chemistry of fission products

Gamma activity of the nuclear materials after the fuel irradiation in the fast reactor is very high. Preliminary calculations show that if the decontamination factor equals to 600, the gamma activity of fission products impurity will about 30% of the recovered fuel materials' gamma activity. Apparently, there is no necessity for increasing the decontamination factor because it is necessary to work with the regenerated fuel in "hot" cells on automated remote controlled equipment in any case.

Not more than 25 elements make 99 % of total fission products mass and the activity of theirs isotopes makes 99 % of total activity of all radioisotopes. Zr, Mo, Tc, Ru, Rh, Pd, Ag, J, Ce, Pr, Nd, Pm, Sm, Eu elements are the «dangerous» fission products from the viewpoint of the fast reactor physics. To obtain the nuclear-physical properties of regenerated fuel, the decontamination coefficient for these elements should be at least 30. Decontamination factor of fission materials for other elements should be at least 10. Some isotopes of Nb, Sb, Ba, Cs, La as well as Cr, Mn, Fe, Ni, Co steel components are also "hazardous" from the viewpoint of radiation safety when handling reprocessed fuel. With respect to the fuel element cladding, Te is also paid attention for its corrosive nature. The behavior of these impurities in molten chlorides of alkali metals was taken into consideration in the development of the spent nuclear fuel regeneration technology.

Let's consider them separately..

Zirconium, niobium and hafnium. The main states of Zr, Nb, and Hf in chloride melts are Zr (II, IV), Nb (IV, V) and Hf (II, IV).

The formal standard potentials of zirconium can be described by the following equations [1]:

$$E^*_{Zr(II)/Zr} = -3.32 + 0.77/r^*_{Me}{}^{+} + (10.3 + 3.3/r^*_{Me}{}^{+})\cdot 10^{-4}T, \quad (4.5.1)$$

$$E^*_{Zr(IV)/Zr} = -3.36 + 0.75/r^*_{Me}{}^{+} + (9.6 + 2.80/r^*_{Me}{}^{+})\cdot 10^{-4}T, \quad (4.5.2)$$

where r_R^+ is the ion radius of the cations of the melt in nm.

The formal standard potentials of hafnium can be described by the following equations [1]:

$$E^*_{Hf(II)/Hf} = -3.33 + 0.755/r^*_{Me}{}^{+} + (10.84 + 4.13/r^*_{Me}{}^{+})\cdot 10^{-4}T, \quad (4.5.3)$$

$$E^*_{Hf(IV)/Hf} = -3.57 + 0.84/r^*_{Me}{}^{+} + (10.66 + 3.0/r^*_{Me}{}^{+})\cdot 10^{-4}T. \quad (4.5.4)$$

The temperature dependence of the formal standard potentials of niobium are known in NaCl-KCl melt [40]:

$$E^*_{Nb(II)/Nb} = -1.842 + 0.00067*T, V \ (973\text{-}1253K), \quad (4.5.5)$$

$$E^*_{Nb(III)/Nb} = -2.374 + 0.00124*T, V \ (973\text{-}1173K). \quad (4.5.6)$$

Zirconium and niobium chlorides have the appreciable vapor pressure over NaCl-KCl melt. Small zirconium concentration is stable in melt. Niobium chlorides are fully sublimated from NaCl-KCl-$NbCl_5$ melt. The volatile niobium oxychlorides ($NbOCl_3$ type) can be formed.

Zirconium and niobium tetra chlorides in interaction with oxygen or other oxide ions form the following oxides:

$$ZrCl_{4(melt)} + O_{2(gas)} = ZrO_{2(solid)}\ [41], \quad (4.5.7)$$

$$2NbCl_{5(melt)} + 5/2O_{2(gas)} = Nb_2O_{5(solid)} + 5Cl_{2(gas)}\ [42]. \quad (4.5.8)$$

Zirconium oxychloride can be formed in the melt too:

$$ZrCl_{4(melt)} + ZrO_{2(solid)} = 2ZrOCl_{2(melt)}\ [43]. \quad (4.5.9)$$

$$K_{eq} = (1.7\pm0.6)\cdot10^{-3}, \text{ mole at 1000 K.}$$

The spectrophotometric investigations showed the possible formation of "bridge" type structures such as -Zr-O-Zr-O or -U-O-Zr-O-U that was confirmed by a partial dissolution of ZrO_2 (to 0.1 mass%) in NaCl-KCl-UCl_4 melt (4.7mass%).

Niobium forms the NbO^{2+} and NbO_2^+ oxygen-containing ions, which are reduce on the cathode at -(0.6-0.8) V.

The laboratory tests showed that $ZrCl_4$ interacts with UO_2 in NaCl-KCl melts high rate according to the following reaction [44]

$$ZrCl_{4(melt)} + UO_{2(solid)} = UCl_{4(melt)} + ZrO_{2(solid)}. \quad (4.5.10)$$

$$\lg K_{22} = 0.116 + 1850/T.$$

Interaction of the highest niobium chlorides with uranium dioxide forms the following solid solution [44]

$$5UO_{2(solid)} + 4NbCl_{5(melt)} = 2Nb_2O_{5(solid)} + 5UCl_{4(melt)}, \quad (4.5.11)$$

$$K_{eq} = 10^{10\text{-}20} \text{ at 973 K.}$$

The permeation of zirconium and niobium in the UO_2 cathode deposit under its electrode position occurs due to exchange reactions (4.5.10) and (4.5.11).

Molybdenum, technetium, antimony. Molybdenum can be in several oxidation states in melt and it forms various oxychloride compounds. Its main oxidation state is (III) but Mo(II) can exist in equilibrium with metal.

The formal standard potentials of Mo can be described by the following equations [1]:

$$E^*_{Mo(II)/Mo} = -1.42 + 0.11/r^*_{Me^+} + (4.5.74 + 2.57/r^*_{Me^+})\cdot10^{-4}T, \quad (4.5.12)$$

$$E^*_{Mo(III)/Mo} = -1.98 + 0.52/r^*_{Me^+} + (4.72 + 0.20/r^*_{Me^+})\cdot10^{-4}T. \quad (4.5.13)$$

All of its higher chlorides and oxychlorides ($MoCl_4$, $MoCl_5$, $MoCl_6$, MoO_2Cl_2, $MoOCl_3$ and $MoOCl_4$) are volatile. Oxychlorides can be reduced on the cathode to oxides:

$$MoO_2Cl_2^{2-}{}_{(melt)} + 2e^- = MoO_{2(solid)} + 4Cl^-_{(melt)}. \quad (4.5.14)$$

In this case, the potential of molybdenum oxide deposition is closed to that UO_2 deposition.

The behavior of technetium in chloride melts was not studied and there is no information.

Antimony forms volatile chlorides such as $SbCl_3$ and $SbCl_5$, which are removed from melt by sublimation. The potential of antimony metal deposition is closed to that of UO_2 deposition (more positive than - 1V). Oxide of Sb_2O_3 dissolves in chloride melts.

Ruthenium, rhodium and palladium. Ru, Rh and Pd are most positive elements among FPs. The formal standard potentials of palladium were measured in NaCl-KCl melt:

$$E^*_{Pd(II)/Pd} = -0.374 \pm 0.008 \text{ ,V at 1000 K [45],} \quad (4.5.15)$$

or $$E^*_{Pd(II)/Pd} = -1.912 + 1.30/r^*_{Me}{}^{+} + (1.187\cdot10^{-4} - 8.5\cdot10^{-5}/r^*_{Me}{}^{+})\cdot T \pm 0.03 \text{ [46].} \quad (4.5.16)$$

For ruthenium and rhodium there are data for other mixtures too:

$$E^*_{Ru(III)/Ru} = -0.429 \pm 0.007, \text{ V at 723 in 3LiCl-2KCl [47],} \quad (4.5.17)$$

$$E^*_{Ru(III)/Ru} = -0.413 \pm 0.003, \text{ V at 785 in NaCl-2CsCl [48],} \quad (4.5.18)$$

$$E^*_{Rh(III)/Rh} = -0.518 \pm 0.004, \text{ V at 723 in 3LiCl-2KCl [47],} \quad (4.5.19)$$

$$E^*_{Rh(III)/Rh} = -0.696 + 0{,}00024\cdot T \pm 0.005, \text{ V in 3LiCl-2KCl [45],} \quad (4.5.20)$$

$$E^*_{Rh(III)/Rh} = -1.212 + 0{,}00090\cdot T \pm 0.003, \text{ V in NaCl-2CsCl [49].} \quad (4.5.21)$$

From these equations, the potentials of Ru and Rh deposition in melt are closed to zero too (vs. Cl^-/Cl_2).

Ru alone forms the relative volatile chlorides in this group. Its volatility at the melt chlorination can be caused by $RuCl_4$ compound and at the melt oxidation with the gaseous chlorine-oxygen mixture can be caused by the RuO_2Cl_2 type compounds. It was noted that in NaCl-KCl melt in the presence of plutonium at Ru/Pu = 1/100, over 70% of Ru is removed from melt into the sublimates at 1173 K for 6 hours.

The stability of $RuCl_3$, $RhCl_3$ and $PdCl_2$ is not high and it increases in the order of Ru – Rh - Pd [50,51]. Their chloride complexes are decomposed by decreasing the partial chlorine pressure in the system:

$$MeCl_m^{(n-m)-}{}_{(melt)} = Me_{(solid)} + n/2Cl_{2(gas)} + (m-n)Cl^-_{(melt)}. \quad (4.5.22)$$

The equilibrium pressure of chlorine over NaCl-2CsCl melt at 785 K and 0.16% mole fraction of their chlorides in melt is equal to 1.9 Pa, 32.6 Pa and 542 Pa for Pd, Rh and Ru, respectively. Similar effect could be expected but more pronounced due to the low complex-forming ability of NaCl-KCl mixture too. By introducing getter over melt to remove chlorine, these chlorides are decomposed up to metal. Introduction of U(III) ions into melt leads to formation of their metal slime too.

Ruthenium can form oxychlorides in melt containing the oxide ions. Treatment of KCl-$RuCl_3$ (1 mol.% Ru) melt by chlorine and oxygen gas mixture produces RuO_2 precipitates (while by argon produces ruthenium metal precipitates mainly). Formation of oxychloride compounds, which can be discharged on the cathode to form RuO_2, is verified in NaCl-CsCl-KCl melts [52]:

$$RuCl_{3(melt)} + O_{2(gas)} = RuO_2Cl_{2(melt)} + 1/2Cl_{2(gas)}, \quad (4.5.23)$$

$$RuO_2^{2+}{}_{(melt)} + 2e^- = RuO_{2(solid)}. \quad (4.5.24)$$

The potential of RuO_2 deposition is more negative (by 0.1-0.2V) then that of Ru metal deposition.

Precipitation of slime and change of melt spectrum were not observed in NaCl-2CsCl melt containing 0.015 mol.% of Rh under the treatment of air oxygen at 778-1078 K.

Silver, tellurium. Silver forms a stable AgCl, which is not decomposed by oxygen. In NaCl-KCl melt the formal standard potential of Ag(I)/Ag pair is equal to -0.845, -0.820 and -0.795V at 973, 1073 and 1173 K, respectively, or:

$$E^*_{Ag(I)/Ag} = -1.088 + 0.00025 \cdot T, \text{ V [53]}. \quad (4.5.25)$$

Electrodeposition of silver occurs at potential close to that of UO_2 that can result in contamination of the UO_2 deposit by silver.

In chloride melt, tellurium can form a strong volatile chloride $TeCl_2$ that will be removed into sublimates. Electrodeposition of Te metal on the cathode at low potentials (-(0.3-0.9)V [54]) is comparable to the potentials of UO_2 and PuO_2.

Rare-earth elements. All FP rare-earth elements (La, Ce, Pr, Nd, Pm, Sm and Eu) form stable and non-volatile chlorides. The deposition potentials of metallic REE are more negative than that of UO_2. At least, Sm and Eu metals can reduce Li from chloride melt. The process of overcharge of Eu(III)/Eu(II) occurs at the cathodic potential -(0.6-1.3)V that should effect on the current in UO_2 electrode position.

The following formal standard potentials were studied for various melts:

$$E^*_{La(III)/La} = -3.60 + 0.00069 \cdot T \text{ in 3LiCl-2KCl [1]}, \quad (4.5.26)$$

$$E^*_{Ce(III)/Ce} = -3.61 + 0.00074 \cdot T \text{ in 3LiCl-2KCl [1]}, \quad (4.5.27)$$

$$E^*_{Pr(III)/Pr} = -3.11 \pm 0.05, \text{ 723 K in 3LiCl-2KCl [47]}, \quad (4.5.28)$$

$$E^*_{Nd(II)/Nd} = -3.498 + 0.000634 \cdot T \text{ in 3LiCl-2KCl [55]}, \quad (4.5.29)$$

$$E^*_{Nd(III)/Nd} = -3.749 + 0.000943 \cdot T \text{ in 3LiCl-2KCl}, \quad (4.5.30)$$

$$E^*_{Sm(II)/Sm} = -4.573 + 0.00113 \cdot T \text{ in NaCl-KCl [56]}, \quad (4.5.31)$$

$$E^*_{Eu(II)/Eu} = -4.10 + 0.0008 \cdot T \text{ in NaCl-2CsCl [57]}, \quad (4.5.32)$$

$$E^*_{Eu(III)/Eu(II)} = -0.86 \pm 0.007 \text{ at 723 K in 3LiCl-2KCl [57]}, \quad (4.5.33)$$

$$E^*_{Eu(III)/Eu(II)} = -1.62, -1.56 \text{ V at 824 and 926 K respectively, in NaCl-2CsCl}. \quad (4.5.34)$$

Among REE, Sm and Eu have the most negative formal standard potentials.

Some REE form stable oxides and oxychlorides with free oxygen [58]:

$$LnCl_3 + 1/2O_2 = LnOCl + Cl_2, \quad (4.5.35)$$

$$4LnCl_3 + 3O_2 = 2Ln_2O_3 + 6Cl_2. \quad (4.5.36)$$

In NaCl-KCl melt with high content of REE (to 20 mass%), the extent of interaction with oxygen is decreased in order of $CeCl_3 > PrCl_3 > NdCl_3 > LaCl_3$ by forming CeO_2, Pr_2O_3, Nd_2O_3 and

La_2O_3. In NaCl-KCl melt containing 5-20 mol.% $CeCl_3$ the processes of oxide formation were studied and the diagram "Potential-oxygen index» was published [59]. Compared with the similar diagram for plutonium [15], the formation of CeO_2 takes place at higher content of oxide ions in melt than that of PuO_2.

Ce_2O_3 dissolution in NaCl-KCl-$CeCl_3$(0.3 mol/kg) melt at 1000K was determined as follows [60]:

$$\log_{10}S_{Ce_2O_3} = 5.0 + 1.5pO^{2-} + \log_{10}(1\cdot10^{-11}\cdot [O^{2-}]). \quad (4.5.37)$$

It was shown that Nd and Eu have not been precipitated by air in NaCl-2CsCl melt containing up to 1 mass% REE. No precipitation of Nd was observed with air exposure in melt in the presence of UO_2Cl_2. When the same melt containing $CeCl_3$, $LaCl_3$ or $SmCl_3$ is treated with air a suspension is formed. In the case of La and Sm, the portion of the precipitated REE does not exceed 45% at temperature 700-800°C and when the melt temperature lowed up to 510°C, the portion of the precipitated Sm decreases to 15%. Partial precipitation of Sm is observed too in melt containing UO_2Cl_2. Cerium chloride in interaction with air also forms a thin suspension in melt. Treatment of NaCl-KCl melt containing 0.5 mass% Ce, Ln and Sm chlorides with gas mixture of oxygen and argon containing 5 vol.% chlorine precipitates only CeO_2 that proves its strong affinity to oxygen.

Voltamperometric investigations of CeO_2 chlorination products in NaCl-KCl melt showed that oxychloride ions were formed during chlorination. They can discharge on the cathode at the potentials about -(1.7 ~ -1.9) V [36].

Alkali elements, alkali-earth elements, iodine. After dissolution of fuel, Cs and Rb become components of the salt-solvent as chlorides. Higher volatility of CsCl is due to its less complex formation in melt compared with other alkali metals. For example, about 1.2% cesium was removed from 1 kg of NaCl-KCl melt (0.2 mass% CsCl) treated by chlorine with the rate 0.08 l/hr during 1 hr at 700°C and that increases up to 12% cesium at 850°C.

Strontium and barium become also components of the melt as chlorides and do not take part in the processes.

With the fuel dissolution, stable iodides are formed but iodine is gradually removed with chlorine to gas phase during long chlorination.

Structural material impurities. Fe behavior was studied in the molten NaCl-KCl. It is known that $FeCl_2$ can exist in melt due to $FeCl_3$ decomposition.

$$Fe^{3+}_{(melt)} + Cl^-_{(melt)} = Fe^{2+}_{(melt)} + 1/2Cl_{2(gas)}. \quad (4.5.43)$$

The exchange reaction between $FeCl_2$ and UO_2 is impossible, i.e. under oxygen-free conditions UO_2 cannot be contaminated by iron. Similarity of discharge potentials of Fe^{2+} and UO_2 ions makes their joint presence in the melt. Gaseous oxygen introduced in the NaCl-KCl-

UO_2Cl_2-$FeCl_2$ melt results in oxidation of iron to Fe_2O_3 suspension to be included in the growing cathode deposit.

Iron is the extremely undesirable impurity in electrochemical process of uranium or MOX fuel. The formal redox potential of Fe^{3+}/Fe^{2+} pair, which can be calculated with help of equation [1]

$$E^*_{Fe^{3+}/Fe^{2+}} = - 0.20 +0.70/r^*_{Me^+} - (1,4 + 3.23/r^*_{Me^+})\cdot 10^{-4}T \pm 0.02 \text{ V}, \qquad (4.5.44)$$

has values, which are practically equal to redox potential of Cl_2/Cl^-. Oxidizing ability of the iron trichloride is very close to that of chlorine. Therefore, the iron impurity should promote the chlorination reactions in the chloride melt as if increasing the chlorine gas solubility in melt. The discharge of Fe^{3+}/Fe^{2+} pair decreases the efficiency of the cathode process during the electrolysis.

Behavior of Cr is almost similar to Fe. The melt with inert atmosphere involves $CrCl_3$ that does not enter into the exchange reaction with UO_2. Permanent stability of Cr^{3+} is confirmed in course of the UO_2^{2+} ions discharge at the cathode and their co-presence in the melt. Thus, Cr could not contaminate the UO_2 cathode deposit in inert gas. In the presence of oxygen, $CeCl_3$ can form Cr_2O_3 suspension that can contaminate the UO_2 deposit.

Nickel behavior was studied together with UO_2Cl_2. $NiCl_2$ does not enter into reaction with UO_2 or UO_2Cl_2. The potential of nickel reduction is more negative than that of uranium dioxide; therefore the co-deposition is only possible at high melt depletion of uranium (U mole-fraction concentration $<10^{-4}$). The melt treatment with air does not provide any essential changes and rule out the possibility of NiO formation when melt is affected by oxygen for a long time. So Ni will not contaminate the UO_2 deposit.

Formal standard potentials of Cr, Ni and Co in NaCl-KCl melt can be found from the following equations:

$$E_{Cr(II)/Cr} = -1.991 + 0{,}00040\cdot T \pm 0.001 \text{ [53]}, \qquad (4.5.45)$$

$$E_{Cr(III)/Cr} = -1.902 + 0{,}00065\cdot T \pm 0.001 \text{ [53]}, \qquad (4.5.46)$$

$$E_{Ni(II)/Ni} = -1.681 + 0{,}000711\cdot T \quad \text{при 973-1173 K [61]}, \qquad (4.5.47)$$

$$E_{Co(II)/Co} = -1.651 + 0{,}000495\cdot T \quad \text{при 973-1173 K [53]}. \qquad (4.5.48)$$

The main electrochemical characteristics of the basic impurity chlorides and their affinity for oxygen are summarized in Table 4.5.1 and 4.5.2

As shown in Table 4.5.1, PuO_2 and NpO_2 as well as Ru, Rh, Pd metals can be deposited at the cathode together with uranium dioxide in the electrochemical deposition of uranium dioxide at the cathodic potential from -0.60 to -1.10 V. The formal standard potentials of these elements (in magnitude) are less than those of UO_2. The rest of the elements have formal standard

potentials greater (in magnitude) than those of uranium dioxide, will not deposit together with uranium on the cathode, i.e. uranium will be decontaminated from these impurities.

Table 4.5.1. Formal standard potentials of elements
in molten chlorides (relative to chlorine reference electrode) [62]

Me(n)/Me(m)	$E^*_{Me(n)/Me(m)}$, V		
	3LiCl-2KCl T = 773 K	NaCl-KCl T = 1000 K	NaCl-2CsCl T = 873 K
Sm(II)/Sm	-3.58	-3.44 [56]	-3.58
Eu(II)/Eu	-	-	-3.39 [57]
Pr(III)/Pr	-3.11 (723 K) [47]	-	-
La(III)/La	-3.07 [1]	-	-
Am(II)/Am	-3.05 [38]	-	-
Ce(III)/Ce	-3.04 [1]	-	-3.08
Nd(III)/Nd	-3.02 [55]	-	-
Pu(III)/Pu	-2.82 [16]	-2.64 [16]	-2.83 [16]
Np(III)/Np	-2.315 [30]	-	-
U(III)/U	-2.31 [1]	-2.19 [1]	-2.39 [1]
Zr(IV)/Zr	-2.08 [1]	-1.98 [1]	-2.17 [1]
Sm(III)/Sm(II)	-2.04 (723 K)	-	-1.6 (906 K) [56]
Cm(III)/Cm	-	2.90 [29]	-
Cr(II)/Cr	-1.65 (723 K)	-1.59 [53]	-
Np(IV)/Np(III)	-1.51	-	-
U(IV)/U(III)	-1.40 [4]	-1.39 [4]	-1.45 [4]
Fe(II)/Fe	-1.38 [1]	-1.34 [1]	-1.48 [1]
Nb(III)/Nb	-1.35 [44]	-1.13 [40]	-
Ni(II)/Ni	-1.01	-0.97 [61]	-
Eu(III)/Eu(II)	-0.86 (723 K)	-	-1.56 (926 K)
Ag(I)/Ag	-1.06 (723 K)	-0.838 [53]	-0.932
Mo(III)/Mo	-0.90 [1]	-0.823 [1]	-0.97 [1]
UO_2(VI)/UO_2	**-0.50 [5]**	**-0.40 [5]**	**-0.65 [5]**
Pd(II)/Pd	-0.536 (723 K) [46]	-0.37 [45]	-0.48 [46]
Rh(III)/Rh	-0.51 [47]	-	-0.44 [49]
Ru(III)/Ru	-0.43 (723 K) [48]	-	-0.413 (783 K)
NpO_2(V)/NpO_2	-0.32 (723 K) [26]	-	-
Pu(IV)/Pu(III)	+0.01 [17]	+0.09 [17]	-0.05 [17,18]
PuO_2(VI)/PuO_2	+0.28 [15]	+0.34 [15]	+0.12 [15]

Various elements have different affinity to oxygen. In Table 4.5.2 the elements are arranged in the decreasing order of this parameter from top to bottom. U and Pu are arranged in the center of Table 4.5.2. It means that during electrolysis or some other process uranium and plutonium dioxides will be contaminated by the elements having more affinity for oxygen. The most

important elements for the technology are Zr and Nb, which should be removed from the melt before obtaining of UO_2, PuO_2 or their mixture.

Table 4.5.2. Oxide and oxychloride formation energy by the reactions*:
$MeCl_n + n/4O_2 \rightarrow MeO_{n/2} + n/2Cl_2$,
$MeCl_n + m/2O_2 \rightarrow MeO_mCl_{(n-2m)} + mCl_2$.

Reactions	- ΔG*,kJ/g-atom		
	3LiCl-2KCl 723 K	NaCl-KCl 1000 K	NaCl-2CsCl 785 K
$NbCl_3 \rightarrow NbO_2$	1077	-	-
$NbCl_3 \rightarrow NbO_{2.5}$	656	767	-
$NbCl_4 \rightarrow NbO_{2.5}$	-	756	-
$NbCl_4 \rightarrow NbO_2$	-	636	-
$ZrCl_4 \rightarrow ZrO_2$	493	628	465
$MoCl_3 \rightarrow MoO_2$	496	527	423
$NpCl_4 \rightarrow NpO_2$	457	-	-
$SmCl_2 \rightarrow SmOCl$	378	445	376
$CrCl_3 \rightarrow CrO_{1.5}$	366	470	-
$CeCl_3 \rightarrow CeO_2$	339	-	-
$RuCl_3 \rightarrow RuO_2$	315	-	332
$SmCl_2 \rightarrow SmO_{1.5}$	315	392	315
$EuCl_2 \rightarrow EuOCl$	-	-	315
$EuCl_2 \rightarrow EuO_{1.5}$	-	-	275
$PuCl_4 \rightarrow PuO_2$	318	388	264
$FeCl_3 \rightarrow FeO_{1.5}$	293	374	328
$UCl_4 \rightarrow UO_2$	**283**	**372**	**-**
$FeCl_3 \rightarrow FeO_{1.33}$	270	357	272
$PrCl_3 \rightarrow PrOCl$	266	-	-
$CrCl_3 \rightarrow CrOCl$	264	396	-
$FeCl_2 \rightarrow FeO_{1.5}$	256	264	206
$NdCl_3 \rightarrow NdOCl$	242	-	-
$LaCl_3 \rightarrow LaOCl$	240	-	-
$PrCl_3 \rightarrow PrO_{1.833}$	216	-	-
$RhCl_3 \rightarrow RhO_{1.5}$	196	-	214
$LaCl_3 \rightarrow LaO_{1.5}$	182	-	-
$NdCl_3 \rightarrow NdO_{1.5}$	157	-	-
$CoCl_2 \rightarrow CoO_{1.33}$	153	198	-
$NiCl_2 \rightarrow NiO$	150	211	-
$PdCl_2 \rightarrow PdO$	127	203	137
$AgCl \rightarrow AgO_{0.5}$	36	116	-

*It is calculated according to Table 4.5.1 and [63].

Additional opportunities of an estimation of formal standard potentials of elements in chlorides melt

Universal Equation for the formal standard potential estimation For an estimation of the formal standard potential value in the molten chlorides of alkali metals with the predetermined composition it is possible to apply the universal equation proposed by V.A. Lebedev [2,64]:

$$E^*Me^{n+}/Me = a + b/r^*_{Me}{}^{+} + (c + d/r^*_{Me}{}^{+})\cdot 10^{-4}\cdot T, \quad (4.5.49)$$

where

$$b = 0.91 - 0.10\cdot n/r_{Me}{}^{n+} \pm 0.01, \quad (r_{Me}{}^{n+} \text{ dimension is Angstroem unit}) \quad (4.5.50)$$

$$b = 0.091 - 0.0010\cdot n/r_{Me}{}^{n+} \pm 0.01, \quad (r_{Me}{}^{n+} \text{ dimension is nm}) \quad (4.5.50')$$

$$d = - 4.70 + 0.78\cdot n/r_{Me}{}^{n+} \pm 0.01. \quad (r_{Me}{}^{n+} \text{ dimension is Angstroem unit}) \quad (4.5.51)$$

$$d = - 0.470 + 0.0078\cdot n/r_{Me}{}^{n+} \pm 0.01. \quad (r_{Me}{}^{n+} \text{ dimension is nm}) \quad (4.5.51')$$

In the equations (4.5.49) – (4.5.51) the $r^*_{Me}{}^{+}$ parameter is the effective cation radius of the salt-solvent, the $r_{Me}{}^{n+}$ parameter is the effective cation radius of solute element, for which the potential will be calculated, and **n** is the cation electric charge of this element.

In order to employ the equation (4.5.49) for the potential calculation of any element in the required solvent (salt melt), it is necessary to have or obtain the temperature dependence of the potential of this element in other solvent (salt melt).

Let's consider example.

It is known from literature that

$$E^*_{Mg}{}^{2+}/Mg = - 3.142 + 5.0\cdot 10^{-4}T \quad (4.5.52)$$

for diluted solutions of $MgCl_2$ in the NaCl melt. Using the value of the Mg^{2+} ion moment (2/0.74 = 2.70) and relationships (4.5.50) and (4.5.51) the values of b and d parameters can be calculated: b = 0.64 and d = - 2.59. Taking in to account that the first component in equation (4.5.52) is $(a + b/r_R^+)$ and the second one is $(c + d/r_R^+)$, where $r^*_{Me}{}^{+} = r_{Na}{}^{+} = 0.98$Å, it is possible to find the values of a and c parameters: a = - 3.80 and c = 7.65. So more general equation for the E^*Mg^{2+}/Mg had been obtained:

$$E^*_{Mg}{}^{2+}/Mg = - 3.80 + 0.64/r^*_{Me}{}^{+} + (7.65 - 2.60/r^*_{Me}{}^{+})\cdot 10^{-4}\ T, V. \quad (4.5.53)$$

If the dimension for cation radiuses is nm, the following general equation for $E^*_{Mg}{}^{2+}/Mg$ will be obtained:

$$E^*_{Mg}{}^{2+}/Mg = - 3.80 + 0.064/r^*_{Me}{}^{+} + (7.65 - 0.26/r^*_{Me}{}^{+})\cdot 10^{-4}\ T, V. \quad (4.5.54)$$

For the KCl-NaCl melt ($r^*_{Me}{}^{+}$ = 1.155Å or 0.1155 nm) the E^*Mg^{2+}/Mg can be described by the calculated equation:

$$E^*_{Mg}{}^{2+}/Mg = - 3.25 + 5.40\cdot 10^{-4}T, \quad (4.5.55)$$

which coincides practically with the experimental equation

$$E^*_{Mg}{}^{2+}/Mg = - 3.26 + 5.63\cdot 10^{-4}T. \quad (4.5.56)$$

Equation for the lanthanides formal standard potentials calculation When the change of Gibbs' standard energy at formation from elements is known (accordingly the conventional standard potential can be calculated) for the lanthanide chlorides, there is an additional opportunity of an estimation of formal standard potential in any melt of alkali metals chlorides.

By analyzing the result of experimental data it was established that the difference between the standard potential (E^o) and the formal standard potential in the molten chlorides (E*) could be described by expression:

$$\Delta E^{*}_{Me^{n+}/Me} = E^{o}_{Me^{n+}/Me} - E^{*}_{Me^{n+}/Me} = a + b\cdot L_{Ln^{n+}}/l_{Me^{+}} + (c - d\cdot L_{Ln^{n+}}/l_{Me^{+}})\cdot 10^{-3}T, \quad (4.5.57)$$

$$(a = -0.096\pm0.015;\ b = 0.0897\pm0.0045;\ c = 0.029\pm0.011;\ d = 0.044\pm0.013)$$

where L_L and l_S are cation moments of the lanthanide chlorides and salt solvent.

This equation is exact enough (the correlation factor is 0.96) and convenient for the analysis. It allows solving inverse problems.

Let's consider an example of the equation (4.5.57) practical application for calculation of standard and formal standard potentials for rare earth elements.

If the standard potential ($E^{o}_{Me^{n+}/Me}$) is known, it is possible calculating the formal standard potentials ($E^{*}_{Me^{n+}/Me}$) with using the $\Delta E^{*}Me^{n+}/Me$ value:

$$E^{*}_{Me^{n+}/Me} = E^{o}_{Me^{n+}/Me} - \Delta E^{*}_{Me^{n+}/Me}. \quad (4.5.58)$$

And on the contrary, if the formal standard potential ($E^{*}_{Me^{n+}/Me}$) is known, it is possible calculating the standard potentials ($E^{o}_{Me^{n+}/Me}$) with using the $\Delta E^{*}_{Me^{n+}/Me}$ value:

$$E^{o}_{Me^{n+}/Me} = E^{*}_{Me^{n+}/Me} + \Delta E^{*}_{Me^{n+}/Me}. \quad (4.5.59)$$

The cation moments of the lanthanides and salt-solvent can be defined by the following equations:

$L_{Ln^{n+}} = n/r_{Ln^{n+}}$. (for lanthanides),

$l_{Me^{+}} = n_{Me^{+}}/r^{*}_{Me^{+}}$. (for salt-solvents, $n_{Me^{+}} = 1$),

where $L_{Ln^{n+}}$, $r_{Ln^{n+}}$, and $n_{Ln^{n+}}$ are the ion moment, radius and electric charge of lanthanide cations; $l_{Me^{+}}$, $r^{*}_{Me^{+}}$ and $n_{Me^{+}}$ are the ion moment, radius and electric charge of salt-solvent cations.

The relation of the cations moment of the lanthanide and salt-solvent, used in (4.5.57), is the dimensionless value, so it is not depend on the unit of the cation radius. It is important the same unit is used: Angstrom unites, or nanometers, because both units are very often used for atomic and ion radius.

For the mixed melts, it is necessary to use the effective cation moments:

$$L_{Me^{+eff}} = n_k/r_{Me^{+eff}},$$

and the effective cation radiuses of salt-solvent:

$$r^{*}_{Me^{+}} = \sum_{i=1}^{n} N_i r^{i}_{Me^{+}},$$

where N_i is the molar fraction of i–kind of cation.

For the concrete lanthanide in specific salt-solvent (L_i/l_k = constant) the equation for ΔE^{*} can be simplified:

$$\Delta E^{*}_{Me^{n+}/Me} = E^{o}_{Me^{n+}/Me} - E^{*}_{Me^{n+}/Me} = A + B\cdot 10^{-3}\cdot T, \quad (4.5.60)$$

where $A = a + b\cdot L_{Ln^{n+}}/l_{Me^{+eff}}$ and $B = c - d\cdot L_{Ln^{n+}}/l_{Me^{+eff}}$.

Check of the applicability of equation (4.5.57) for calculation of standard and formal standard potentials is carried out with using data from the Lebedev article [64].

Table 4.5.3 shows that the some data, presented in references, are differ each other. For example: for Eb, Ho, Nd, Pr, Ce, La the divergences of results exceed 0.1 V, for Tb, Dy, and Yb the divergences of results exceed 0.2 – 0.4 V, and for Sm and Eu the divergences of results exceed 0.5 V. In this connection, author [64] believes that it is difficult to use the E^{o} value for the correct thermodynamic calculations. While the formal standard potential E^{*} can be measured more accurately for the majority of the REE, consequently, it will be more reliable value for thermodynamic calculations.

The calculated results of the E^{o}, using E^{*}, and, on the contrary, calculated results of the E^{*}, using E^{o}, for some salt-solvents are presented in Table 4.5.4.

Table 4.5.3. Temperature dependencies and decomposition voltage E^o of the liquid individual chlorides of lanthanides [64]

Salt	Reference	Eo = a+ bT,V		Eo, V at T,K	
		-a	1000b	1000	800
$ScCl_3$	[65]	2.934	0.540	-2.394	-2.502
	[66]	2.980	0.580	-2.400	-2.516
Ycl_3	[65]	3.153	0.475	-2.678	-2.773
	[66]	3.233	0.578	-2.655	-2.771
	[67]	3.343	0.700	-2.643	-2.783
$LaCl_3$	[65]	3.561	0.538	-3.023	-3.131
	[66]	3.482	0.578	-2.904	-3.020
	[67]	3.477	0.620	-2.857	-2.981
$CeCl_3$	[65]	3.536	0.562	-2.974	-3.086
	[66]	3.438	0.564	-2.874	-2.987
	[67]	3.469	0.700	-2.769	-2.909
$PrCl_3$	[65]	3.533	0.580	-2.953	-3.069
	[66]	3.427	0.550	-2.877	-2.987
	[67]	3.455	0.660	-2.795	-2.927
$NdCl_3$	[65]	3.500	0.600	-2.900	-3.020
	[66]	3.334	0.550	-2.784	-2.894
	[67]	3.400	0.640	-2.760	-2.888
$PmCl_3$	[65]	3.421	0.500	-2.921	-3.021
	[66]	3.066	0.536	-2.530	-2.637

Salt	Reference	Eo = a+ bT,V		Eo, V at T,K	
		-a	1000b	1000	800
$SmCl_3$	[65]	3.386	0.490	-2.896	-2.994
$SmCl_3$	[66]	3.945	0.476	-3.469	-3.564
$EuCl_3$	[65]	3.345	0.481	-2.864	-2.960
$EuCl_2$	[66]	3.968	0.542	-3.426	-3.534
$GdCl_3$	[65]	3.333	0.490	-2.843	-2.941
	[66]	3.240	0.522	-2.718	-2.822
	[67]	3.312	0.640	-2.672	-2.800
$TbCl_3$	[65]	3.297	0.502	-2.795	-2.895
	[66]	2.948	0.534	-2.414	-2.521
$DyCl_3$	[65]	3.178	0.455	-2.723	-2.814
	[66]	2.875	0.548	-2.327	-2.437
$HoCl_3$	[66]	3.150	0.534	-2.616	-2.723
	[65]	3.141	0.495	-2.646	-2.745
$ErCl_3$	[65]	3.131	0.505	-2.626	-2.727
	[66]	3.094	0.535	-2.559	-2.666
$TmCl_3$	[65]	3.026	0.454	-2.572	-2.663
	[66]	3.094	0.550	-2.544	-2.654
$YbCl_3$	[65]	3.007	0.450	-2.557	-2.647
$LuCl_3$	[65]	3.017	0.519	-2.498	-2.602
	[66]	3.079	0.564	-2.515	-2.628

Table 4.5.4. Calculation results with equation (4.5.60) the value E^o with using E^* and on the contrary (**) for different salt-solvents [64]

System	Salt-solvent	$\frac{L_{Ln}^{n+}}{l_{Me}^{+eff}}$	Ref.	E* = a'+ b'T,V		E^o = a+ bT,V		-E^o, V at T.K	
				-a'	1000b'	-a	1000b	1000	800
1	2	3	4	5	6	7	8	9	10
Sc^{3+}/Sc	LiCl-KCl	3.40	[68]	3.240	0.607	3.031	0.486	-2.545	-2.642
	NaCl-KCl	4.17	[69]	3.437	0.754	3.159	0.600	-2.559	-2.679
	LiCl	2.46	**	3.215	0.619	3.090	0.540	-2.550	-2.658
Y^{3+}/Y	LiCl-KCl	2.91	[70]	3.680	0.790	3.515	0.691	-2.824	-2.962
	-"-	2.91	*	3.545	0.620	3.380	0.521	-2.859	-2.963
	-"-	2.91	[67]	3.360	0.380	3.195	0.281	-2.914	-2.970
	NaCl-KCl	3.57	[71]	4.050	1.110	3.826	0.982	-2.844	-3.040
	LiCl	2.10	**	3.472	0.626	3.380	0.563	-2.817	-2.930
La^{3+}/La	LiCl-KCl	2.71	[70]	3.620	0.700	3.473	0.610	-2.863	-2.985
	-"-	2.71	[1]	3.600	0.690	3.453	0.600	-2.853	-2.973
	-"-	2.71	[67]	3.530	0.540	3.383	0.450	-2.933	-3.023
	NaCl-KCl	3.33	**	3.656	0.718	3.453	0.600	-2.853	-2.973
	LiCl	1.96	**	3.533	0.657				
Ce^{3+}/Ce	LiCl-KCl	2.76	[1]	3.610	0.740	3.458	0.648	-2.811	-2.940
	LiCl-KCl	2.76	[67]	3.300	0.280	3.148	0.188	-2.961	-2.998
	NaCl-CsCl	4.18	[72]	3.730	0.750	3.451	0.595	-2.856	-2.975
	NaCl-KCl	3.40	**	3.667	0.769	3.460	0.650	-2.810	-2.940
	LiCl	2.00	**	3.541	0.707				
Pr^{3+}/Pr	LiCl-KCl	2.82	[67]	3.460	0.500	3.303	0.405	-2.898	-2.979
	NaCl-KCl	3.46	**	3.517	0.528	3.303	0.405	-2.898	-2.979
	LiCl	2.04	**	3.390	0.466				
Nd^{3+}/Nd	LiCl-KCl	2.88	[70]	3.540	0.650	3.378	0.552	-2.825	-2.936
	-"-	2.88	*	3.520	0.710	3.358	0.612	-2.745	-2.868
	-"-	2.88	[67]	3.525	0.700	3.363	0.602	-2.760	-2.881
	NaCl-KCl	3.54	**	3.580	0.739	3.358	0.612	-2.746	-2.868
	LiCl	2.08	**	3.449	0.675				
Pm^{3+}/Pm	LiCl-KCl	2.88	-	3.228	0.634	3.066	0.536	-2.530	-2.637
	NaCl-KCl	3.48	-	3.282	0.660				
	LiCl	2.06	-	3.155	0.598				
Sm^{3+}/Sm	LiCl-KCl	2.94	-	3.554	0.590	3.386	0.490	-2.896	-2.994
	NaCl-KCl	3.56	-	3.609	0.618				
	LiCl	2.10	-	3.478	0.553				
Sm^{2+}/Sm	LiCl-KCl	1.76	*	4.200	0.830	4.138	0.782	-3.357	-3.513
	-"-	1.76	[73]	4.280	0.910	4.218	0.862	-3.357	-3.529
	NaCl-KCl	2.16	[74]	4.570	1.130	4.472	1.064	-3.408	-3.621
	LiCl	1.27	**	4.236	0.889	4.218	0.862	-3.356	-3.528
Eu^{3+}/Eu	LiCl-KCl	2.94	-	3.513	0.581	3.345	0.481	-2.864	-2.960
	NaCl-KCl	3.56	-	3.568	0.609				
	LiCl	2.10	-	3.437	0.544				
Eu^{2+}/Eu	NaCl-CsCl	2.66	[75]	4.100	0.810	3.957	0.722	-3.235	-3.380
	LiCl-KCl	1.76	**	3.999	0.770	3.957	0.722	-3.215	-3.359
	NaCl-KCl	2.16	**	4.035	0.788				
	LiCl	1.27	**	3.955	0.749				

Continuation of Table 4.5.6.

1	2	3	4	5	6	7	8	9	10
Cd^{3+}/Cd	LiCl-KCl	3.00	[70]	3.520	0.670	3.347	0.567	-2.780	-2.893
	NaCl-KCl	3.68	**	3.581	0.700				
	LiCl	2.17	**	3.446	0.633				
Tb^{3+}/Tb	LiCl-KCl	3.20	-	3.139	0.646	2.948	0.534	-2.414	-2.521
	NaCl-KCl	3.88	-	3.200	0.676				
	LiCl	2.29	-	3.057	0.606				
Dy^{3+}/Dy	LiCl-KCl	3.20	*	3.45	0.65	3.259	0.538	-2.721	-2.828
	NaCl-KCl	3.94	**	3.516	0.682				
	LiCl	2.32	**	3.371	0.611				
Ho^{3+}/Ho	LiCl-KCl	3.31	-	3.351	0.651	3.150	0.534	-2.616	-2.723
	NaCl-KCl	4.01	-	3.414	0.681				
	LiCl	2.37	-	3.267	0.609				
Er^{3+}/Er	LiCl-KCl	3.32	*	3.51	0.8	3.308	0.683	-2.625	-2.762
	NaCl-KCl	4.08	**	3.578	0.834				
	LiCl	2.40	**	3.427	0.760				
Tm^{3+}/Tm	LiCl-KCl	3.35	-	3.298	0.668	3.094	0.550	-2.544	-2.654
	NaCl-KCl	4.06	-	3.362	0.700				
	LiCl	2.40	-	3.213	0.627				
Yb^{3+}/Yb	LiCl-KCl	3.52	-	3.227	0.576	3.007	0.450	-2.557	-2.647
	NaCl-KCl	4.26	-	3.293	0.608				
	LiCl	2.52	-	3.147	0.601				
Lu^{3+}/Lu	LiCl-KCl	3.56	-	3.302	0.692	3.079	0.564	-2.515	-2.628
	NaCl-KCl	4.31	-	3.370	0.725				
	LiCl	2.55	-	3.212	0.647				

"[68]" and so on - E^o calculated according to the direct experimental measuring of E^*;
"*"- E^* calculated according to data for the REE alloys with zinc [V.A. Lebedev, V.I. Kober, L.F. Yamtshikov. Allows thermochemistry of rare earth and actinide elements. In Russian. Chelyabinsk: Metallurgy, 1989, 335 p.;
"**"- Back calculation of E^* for other molten salts;
"–" - Calculation of E^* with data use of Table 4.5.3.

4.6. Pyrolytic graphite behaviour in NaCl-2CsCl melt

Pyrographite is widely used at RIAR as structural material in pyroelectrochemical technological procedures for the fast reactor MOX-fuel production and reprocessing. The procedures include stages, on which the pyrographite equipment is exposed to influence of gas oxygen and of the salt melt containing dissolved chlorine, oxygen, uranium and plutonium oxychlorides. The pyrographite behaviour in these media is of great practical interest from the point of view of the equipment service life. This section presents some results on the investigation of kinetics and mechanism of pyrographite corrosion under conditions, which are representative for the MOX fuel production procedure in NaCl-2CsCl.

The method to determine the carbon dioxide removal rate from an interaction zone was used to study the behaviour of pyrographite in oxygen-containing media (gas, salt melt) [76]. The

rate of pyrographite interaction with oxygen-containing media (R_0, mole/(hr*m^2) was calculated by expression,

$$R_0 = k\frac{w}{S}P_{CO_2}, \qquad (4.6.1)$$

where, w - flow of gas reagent in tight cell, m^3/hr; S - surface of sample, m^2; Pco_2 - CO_2 partial pressure in spent gas, Pa; k - constant, mole/(m^3*Pa).

Molecular oxygen. Character of Pco_2 change in gas leaving of the interaction zone of pyrographite sample with oxygen both in atmosphere and NaCl-2CsCl melt is shown on Fig. 4.6.1. It may be noted that Pco_2 becomes stable soon after temperature change. It provides an evidence for the following: a) stabilization of sample corrosion process and b) opportunity for calculating R_0 by expression (4.6.1). Experimental temperature dependencies of

$$O_2 + C = CO_2 \qquad (4.6.2)$$

reaction rate in gas and NaCl-2CsCl melt are satisfactorily described by equations:

$$R_0 = 15{,}2\cdot P_{O_2}\cdot e^{-110000/RT} \quad \text{(gas medium)} \qquad (4.6.3)$$

$$R_0 = 2.75\cdot 10^{-5}\cdot P_{O_2}^{1,25}\cdot e^{-51490/RT} \quad \text{(NaCl –2CsCl melt)} \qquad (4.6.4)$$

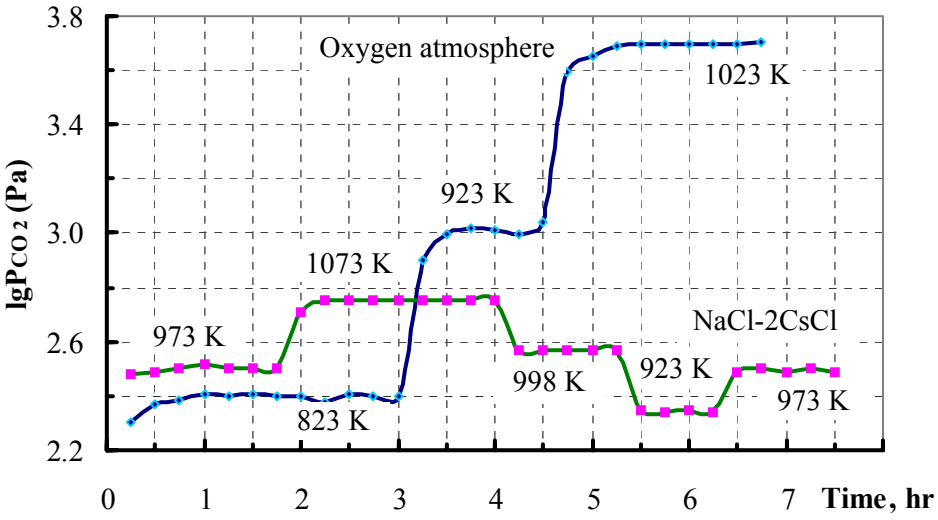

Fig. 4.6.1. Temperature depending $\log_{10}Pco_2$ change during the "pyrographite - O_2" interaction in atmosphere and NaCl-2CsCl melt at P_{O_2} = 101 kPa and w = $1.2\cdot10^{-3}$ m^3/hr [76]. Oxygen atmosphere: S = $9.0\cdot10^{-4}$ m^2. NaCl-2CsCl (V = $(29\pm1)\cdot10^{-6}$ m^3): S = $19.6\cdot10^{-4}$ m^2.

NaCl-2CsCl + UO_2Cl_2 Melt. Fig. 4.6.2, 4.6.3 and 4.6.4 show the influence of uranium concentration in the melt, as well as partial pressure of oxygen and chlorine in gas reagent on the pyrographite corrosion rate in uranyl-containing melt [77].

Two parallel processes can describe the mechanism of pyrographite corrosion in uranyl-containing melt, when treated with oxygen and chlorine mixture. Their rates are limited by chemical stages:

1) $UO_2Cl_2 + C + Cl_2 = UCl_4 + CO_2$, (slowly) (4.6.5)

2) $O_2 + 2UO_2Cl_2 = (UO_2)_2O_2Cl_2 + Cl_2$, (4.6.6)

$(UO_2)_2O_2Cl_2 + C + Cl_2 = 2UO_2Cl_2 + CO_2$. (slowly) (4.6.7)

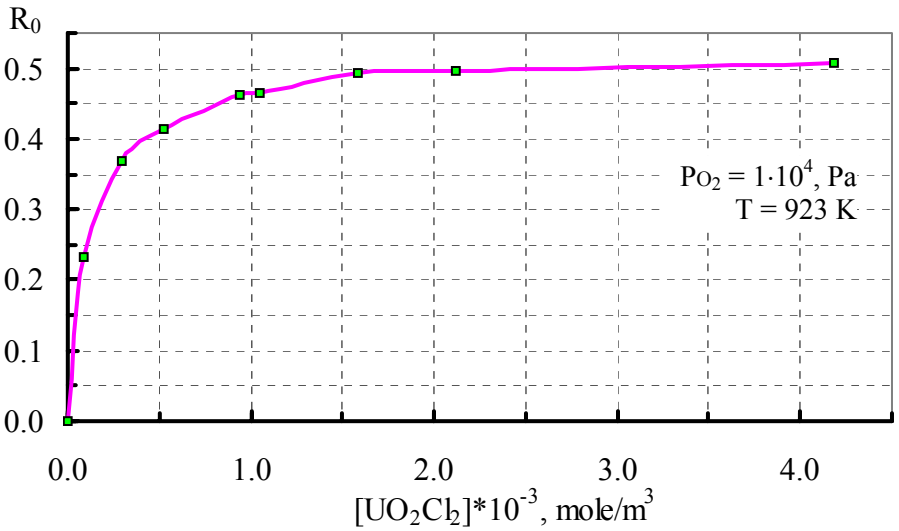

Fig. 4.6.2. Dependency of the pyrographite corrosion rate in NaCl-2CsCl + UO_2Cl_2 melt from the uranylchloride contents [77].

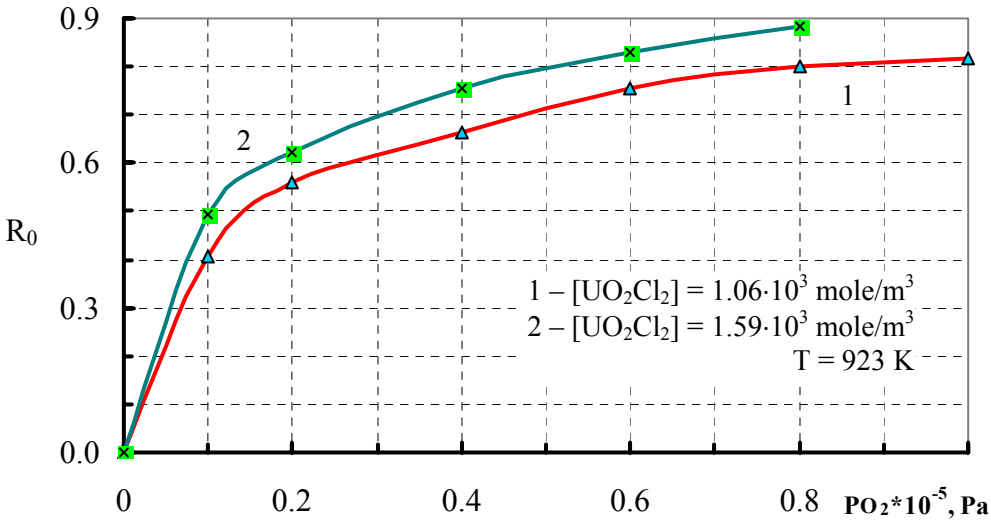

Fig. 4.6.3. Dependency of the pyrographite corrosion rate in NaCl-2CsCl + UO_2Cl_2 melt from Po_2 in the gas reagent [77].

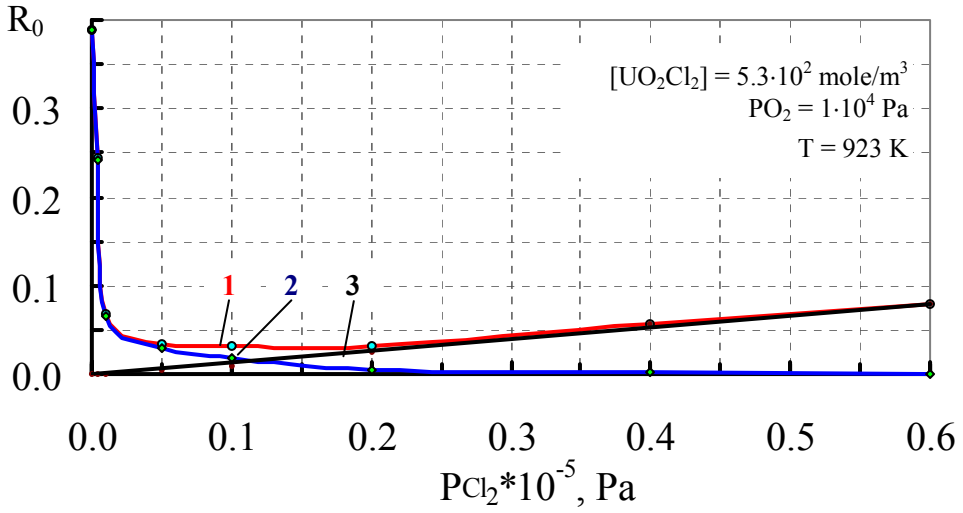

Fig. 4.6.4. Dependency of the pyrographite corrosion rate in NaCl-2CsCl + UO_2Cl_2 melt from P_{Cl_2} in gas reagent [77].

At 923 K the rate of pyrographite corrosion according to reaction (4.6.5) is described by expression

$$R_0 = 2{,}6\cdot10^{-9}\cdot PCl_2\cdot[UO_2Cl_2], \qquad (4.6.8)$$

and according to reactions (4.6.6 and 4.6.7) by following ratio

$$R_0 = \frac{P_{O_2}\cdot[UO_2Cl_2]^2}{8.2\cdot10^3\cdot[UO_2Cl_2]^2 + 3.4\cdot10^7\cdot P^*_{Cl_2}} \qquad (4.6.9)$$

where $P^*_{Cl_2} = P_{Cl_2}+3.3*10^{-8}*P_{O_2}*[UO_2Cl_2]^{2+}+7.0*10^{-2}*[UO_2Cl_2]$, i.e. chlorine, entered into a cell as a part of gas reagent, chlorine, formed as result of reaction of oxygen with chlorine anions, and chlorine, being in equilibrium with a uranylchloride melt solution (1-st, 2-nd and 3-rd items, accordingly), is taken into account.

The effect of electrochemical titration of ions $(UO_2)_2O_2^{2+}$ on the pyrographite anode is found out (see Fig. 4.6.5). It can be presented by the following electrode reaction

$$(UO_2)_2O_2^{2+}{}_{(melt)} + C_{(anode)} + 2e^- = 2UO_2^{2+}{}_{(melt)} + CO_{2(gas)}, \qquad (5.6.10)$$

the rate of which is ten times faster than the rate of interaction without current.

The area in the mole expression under curves in Fig. 4.6.5 corresponds to the allocated CO_2 quantity, which, according to reaction (5.6.10), is equal to the quantity of the compound $(UO_2)_2O_2Cl_2$ titrated.

The content determination of the ions $(UO_2)_2O_2^{2+}$ in melt has allowed to estimate the equilibrium constant and the change of Gibbs's energy at reaction (See Table 4.6.1)

$$O_{2(gas)} + 2UO_2Cl_{2(melt)} = (UO_2)_2O_2Cl_{2(melt)} + Cl_{2(gas)}. \qquad (4.6.11)$$

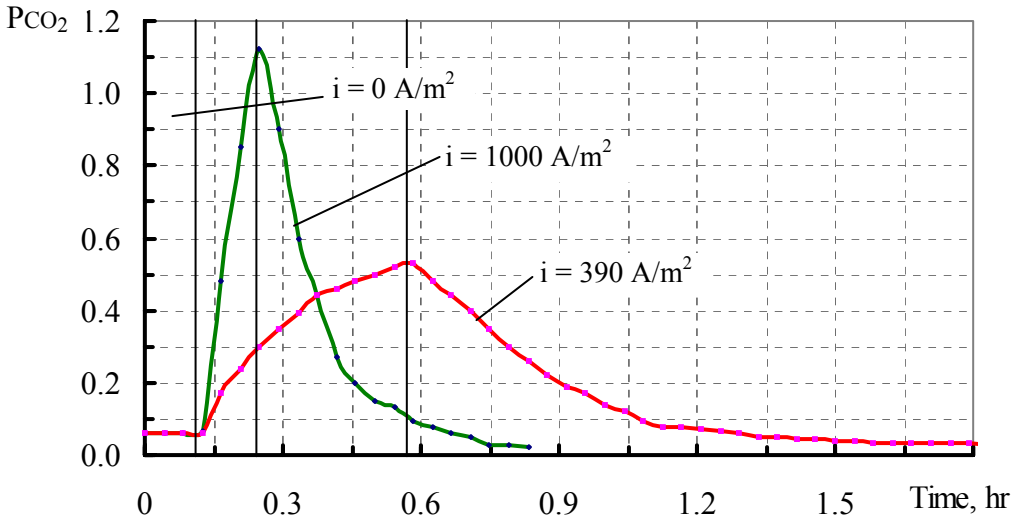

Fig. 4.6.5. Pco_2 change in interacting pyrographite with NaCl-2CsCl + UO_2Cl_2 melt on imposing an anodic current on a sample [78].

Table 4.6.1. Equilibrium parameters and equilibrium constant calculated for reaction (4.6.11) in NaCl-2CsCl melt at 923 K [78]

№	$[UO_2Cl_2]$	$[(UO_2)_2O_2Cl_2]$	P_{Cl_2}	P_{O_2}	$K^*_{4.6.11}$
	mole portion		Pa		
1	$3.01\cdot10^{-3}$	$6.44\cdot10^{-4}$	$1.11\cdot10^{1}$	$9.39\cdot10^{3}$	$8.40\cdot10^{-2}$
2	$1.33\cdot10^{-2}$	$1.77\cdot10^{-3}$	$3.56\cdot10^{1}$	$8.34\cdot10^{3}$	$6.67\cdot10^{-2}$
3	$1.79\cdot10^{-2}$	$1.97\cdot10^{-3}$	$1.30\cdot10^{2}$	$8.16\cdot10^{3}$	$9.80\cdot10^{-2}$
4	$1.95\cdot10^{-2}$	$1.18\cdot10^{-3}$	$3.80\cdot10^{2}$	$8.89\cdot10^{3}$	$1.33\cdot10^{-1}$
5	$2.11\cdot10^{-2}$	$3.76\cdot10^{-4}$	$1.13\cdot10^{3}$	$9.66\cdot10^{3}$	$9.88\cdot10^{-2}$
6	$3.67\cdot10^{-2}$	$2.33\cdot10^{-3}$	$3.67\cdot10^{2}$	$7.94\cdot10^{3}$	$8.00\cdot10^{-2}$
7	$4.16\cdot10^{-2}$	$2.36\cdot10^{-3}$	$4.45\cdot10^{2}$	$7.93\cdot10^{3}$	$7.65\cdot10^{-2}$
8	$4.01\cdot10^{-2}$	$3.13\cdot10^{-3}$	$8.16\cdot10^{2}$	$1.72\cdot10^{4}$	$9.23\cdot10^{-2}$
9	$3.88\cdot10^{-2}$	$3.68\cdot10^{-3}$	$1.56\cdot10^{3}$	$3.67\cdot10^{4}$	$1.07\cdot10^{-1}$
10	$3.75\cdot10^{-2}$	$4.41\cdot10^{-3}$	$3.78\cdot10^{3}$	$9.61\cdot10^{4}$	$1.23\cdot10^{-1}$
11	$6.76\cdot10^{-2}$	$2.59\cdot10^{-3}$	$9.46\cdot10^{2}$	$7.80\cdot10^{3}$	$6.87\cdot10^{-2}$
12	$6.53\cdot10^{-2}$	$3.68\cdot10^{-3}$	$1.78\cdot10^{3}$	$1.65\cdot10^{4}$	$9.31\cdot10^{-2}$
13	$7.13\cdot10^{-2}$	$6.35\cdot10^{-4}$	$3.26\cdot10^{4}$	$2.95\cdot10^{4}$	$1.38\cdot10^{-1}$
14	$6.48\cdot10^{-2}$	$3.81\cdot10^{-3}$	$3.45\cdot10^{3}$	$3.52\cdot10^{4}$	$8.89\cdot10^{-2}$
15	$6.40\cdot10^{-2}$	$4.38\cdot10^{-3}$	$5.12\cdot10^{3}$	$5.31\cdot10^{4}$	$1.03\cdot10^{-1}$
16	$6.35\cdot10^{-2}$	$4.61\cdot10^{-3}$	$6.79\cdot10^{3}$	$7.05\cdot10^{4}$	$1.10\cdot10^{-1}$
17	$9.09\cdot10^{-2}$	$4.57\cdot10^{-3}$	$1.63\cdot10^{3}$	$7.57\cdot10^{3}$	$1.19\cdot10^{-1}$
18	$1.83\cdot10^{-1}$	$3.74\cdot10^{-3}$	$6.03\cdot10^{3}$	$7.26\cdot10^{3}$	$9.28\cdot10^{-2}$
Average of equilibrium constant $K^*_{4.6.11}$					$(9.85 \pm 0.48)\cdot10^{-2}$
The change of Gibbs energy at reaction (11), kJ/mole					17.8

NaCl-2CsCl + Pu melt. In the alkali metal melts, the plutonium compounds (PuO_2Cl and PuO_2Cl_2) are less stable than those of uranium, and they have always mixed with chlorides compounds $PuCl_3$ and $PuCl_4$. These plutonium compounds interact with carbon materials practically limited by the diffusion rate. In this case, the pyrographite corrosion in the NaCl-2CsCl + Pu (5 wt.%) melt is limited by the oxidation process of the plutonium chloride forms by oxygen according to reaction

$$PuCl_3(PuCl_4) + O_2 = PuO_2Cl(PuO_2Cl_2) + Cl_2. \qquad (4.6.12)$$

Influences of the oxygen and chlorine partial pressure on pyrographite specific rate of interaction in NaCl-2CsCl melt containing 5 wt.% of Pu at 650°C are shown on Fig 4.6.6. These experimental data can be described by the following equation

$$R_o = \frac{1.6\cdot10^{-6}\cdot P_{O_2}}{(3.5\cdot10^{-3}\cdot P_{Cl_2}{}^{1/2}+1)}, \text{ mole/(hr·m}^2\text{)}. \qquad (4.6.13)$$

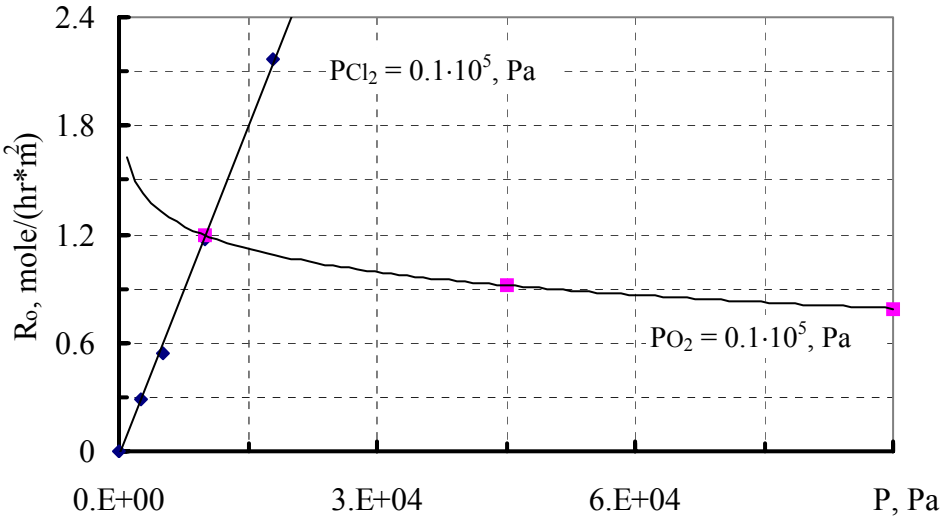

Fig. 4.6.6. Specific rate of pyrographite interaction with NaCl-2CsCl melt containing 5 wt.% of Pu at 650°C depending on oxygen and chlorine partial pressure

The results of these studies reveal the mechanism of pyrographite corrosion in the various oxygen-contented media. They are useful for estimating the life of pyrographite equipment depending on the operation conditions and can be used for constructing mathematical model of the pyroelectrochemical processes for the MOX-fuel deposition.

5. Production experience of uranium dioxide granular powder

In 1981, the experimental reactor BOR-60 (RIAR, Russia) was converted into the MOX fuel, which was granular powder of mechanical mixture of UO_2 and PuO_2 [79]. A facility has been built for the production of the UO_2 granulated. Theoretical base and experience of the realization

of the electrochemical process for the uranium dioxide crystallization are described in this section.

5.I. Chemical and electrochemical bases of the process

Theoretical base of the electrochemical process for the uranium dioxide crystallization is very simple. The process consists of two stages: dissolution of an initial oxide material in the molten salt, and electrolysis of the molten salts. Both stages were in one apparatus called "Chlorinator-Electrolyzer" (ChE).

Chlorination stage. Chlorination by any chlorinating reagent is the way for the uranium oxide material dissolution in the melt. Chlorine was chosen at RIAR as a chlorinating agent, because the uranyl form of uranium was required for the electrolysis step.

Interaction between chlorine and uranium oxides can be presented by the follow reactions

$$UO_{2(solid)} + Cl_{2(gas)} = UO_2Cl_{2(melt)} \quad (5.1.1)$$

and

$$U_3O_{8(solid)} + Cl_{2(gas)} + C_{(solid)} = 3UO_2Cl_{2(melt)} + CO_{2(gas)}. \quad (5.1.2)$$

Some amounts of uranium compounds with an excess of oxygen (such as $U_3O_8Cl_2$, $(UO_2)_2O_2Cl_2$ and others) can appear in melt when U_3O_8 is starting material. Their presence in the melt is undesirable to next stage, because the electrodeposition of the uranium dioxide with ratio O/U>2. But in this case, as graphite is being used as structural material for the electrolyzer bath, both the carbon and uranium tetrachloride decompose usually the uranium compounds with an excess of oxygen, because its high affinity to oxygen. Uranium tetrachloride is the product of the following reaction [80]

$$UO_2Cl_{2(melt)} + C_{(solid)} + Cl_{2(gas)} = UCl_{4(melt)} + CO_{2(gas)} \quad (5.1.3)$$

Besides, some amount of UCl_4 must be always in an electrolyte to provide the ratio of oxygen to uranium of 2 in the uranium dioxide cathode deposit during the electrolysis. But a large concentration of UCl_4 decreases the current efficiency, because of decreasing the UO_2Cl_2 concentration in the melt.

Efficiency of the chlorine at the chlorination stage depends on the process temperature, the salt composition, the properties of initial material, the mixing intensity of a solid phase in the melt, and the ways of the melt saturation with the chlorine.

Reasons are following:

- The temperature influences on rate of chemical reaction, chlorine solubility in melts;
- Salt composition influences on chlorine solubility in melts;
- Properties of initial material determine the crystal structure of chlorinated material and its specific surface;
- Mixing of solid phase in the melt leads to increasing of homogenization of both liquid and solid phases and to eliminating of dead zones of chlorination;

- Ways of the melt saturation with the chlorine determine the pseudo-equilibrium saturation coefficient of chlorine in the melt through the dissolution rate of chlorine in the melt.

Variation of these parameters allows finding the optimal conditions for the chlorination stage. The lab-scale experiments have shown the efficiency of the chlorine use at the chlorination stage can be increased up to 70 – 80 % and more.

Electrolysis stage. In case, the cathode space is not isolated from the anode space, the electrochemical process of the uranium dioxide preparation can be described by the following electrode reactions

$$UO_2^{2+}{}_{(melt)} + 2\ e^- = UO_{2(solid)}, \qquad \text{(cathode reaction)} \quad (5.1.4)$$

$$2\ Cl^-{}_{(melt)} - 2\ e^- = Cl_{2(gas)}. \qquad \text{(anode reaction)} \quad (5.1.5)$$

The cathode current efficiency is usually less than 100% because the interaction of dissolved chlorine with cathode product. But, because of the perfect crystal structure of the cathode product, the interaction between chorine and cathode uranium dioxide is not intensive. In this connection, the cathode current efficiency is usually between 92 and 95 %. These are real data from the actual facility.

An iron impurities have very strong influence on the cathode current efficiency because the low value of the Fe^{3+}/Fe^{2+} formal potential. When the dissolved iron is present in the melt, the following electrode reactions

$$Fe^{2+}{}_{(melt)} - e^- = Fe^{3+}{}_{(melt)} \qquad \text{(anode reaction)} \quad (5.1.6)$$

$$Fe^{3+}{}_{(melt)} + e^- = Fe^{2+}{}_{(melt)} \qquad \text{(cathode reaction)} \quad (5.1.7)$$

create a parasitic circulating current, which decreases the cathode current efficiency.

When the cathode space is isolated from the anode space, the uranium dioxide electrodeposition can be described by following cathode reactions

$$UO_2^{2+}{}_{(melt)} + 2e^- = UO_{2(solid)}, \qquad (5.1.4)$$

$$UO_2^{+}{}_{(melt)} + e^- = UO_{2(solid)}. \qquad (5.1.8)$$

In this case, the potential of the melt will be more negative. Because uranyl chloride will decompose partly up to UO_2Cl compound under the absent of dissolved chlorine, and ions UO_2^+ will stable in the melt. The electrochemical equivalent of the UO_2^+ ions is 10.04g/(A·h) that is twice more than that of ions UO_2^+ (5.02g/(A·h)).

In real experiments with a separated anode, the average electrochemical equivalent have achieved the value about 8.5 g/(A·h). It means that the part of the reaction (5.1.8) can be significant at the uranium dioxide electrodeposition in the electrolyzer with separated anode.

It should be to noted, that the influence of impurities (like a iron) on the cathode current efficiency can be eliminated if anode is separated in the electrolyzer as the ions Fe^{3+} are instable

in the melt without chlorine. (This possibility of the uranium dioxide electrodeposition improvement was not yet implemented.)

It is necessary to note the importance of recording the cathode polarization curves during the UO_2 electrodeposition. Figure 5.1.1 demonstrates an example of cathode polarization curves estimated at different situations of electrolysis: before electrolysis (curve 1), during electrolysis (curves 2, 3 and 4), and at the end of the electrolysis (curve 5). A value of residual currents (I_{res}), and the initial electrolysis current (I_o) were being estimated from the character of the initial polarization curves. Usually, the value of I_o had to provide the cathode potential of – 0.65 V in the NaCl-2CsCl melt at 630°C or – 0.60 V in the NaCl-KCl melt at 700°C.

Fig. 5.1.1. Cathode polarization before and during the uranium dioxide electrodeposition at the extracted uranium portion:
1 – 0%; 2 – 30%; 3 – 50%; 4 – 80%; 5 – 98%

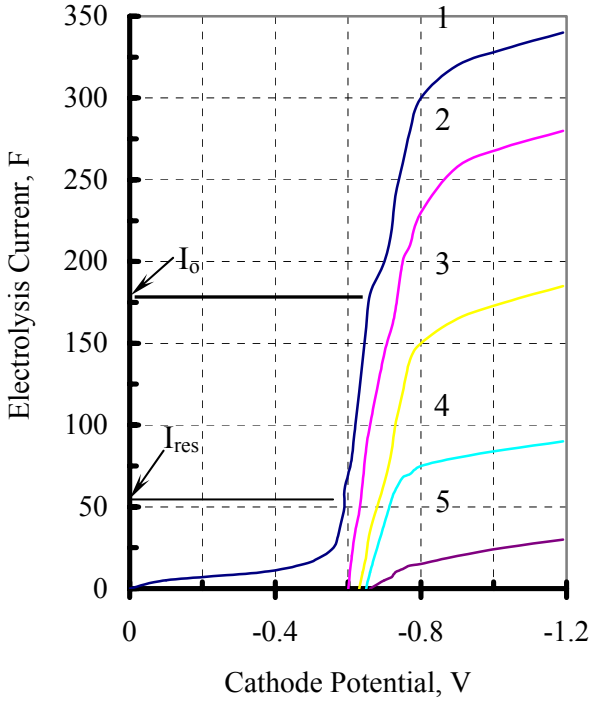

5.2. Laboratory scale realization

RIAR has begun the routine production of the uranium dioxide granular powder at the end of 70th. It was time of extended tests of vibropac uranium dioxide fuel in the BOR-60 reactor. Because these tests had demonstrated the high serviceability of the vibropac UO_2 fuel, it had been decided to convert the BOR-60 reactor core onto the vibropac MOX fuel. At the first step, the mechanical mixture of granular powders of uranium and plutonium dioxides was supposed

as a MOX fuel. Two facilities had been constructed for production of the granular plutonium dioxide (K-16 facility) and of the granular uranium dioxide (Bld. 120).

Description of facility for the UO_2 granular powder production

Equipment of the facility for production of uranium dioxide granular powders was placed in 10 gloves boxes with common atmosphere. Only one room of 72 m^2 was used for the facility. Productivity of the first facility was about 2 kg UO_2 granular powder per 1 day.

The following operations were being carried out in the glove boxes:

Box 1. Opening of containers with an initial material (UO_2 or U_3O_8); sampling; oxide batches preparation for the processing.

Box 2. Weighing of initial oxide materials, intermediates and end products.

Box 3. Production of UO_2 cathode deposits by the electrolysis. (The chlorator-electrolyzer and the column for the off gas chlorine neutralization were installed inside this box.).

Box 4. Crushing of cathode deposits up to a fragment size of 20 to 30 mm; Grinding of cathode deposit fragments up to a particle size of < 1 mm.

Box 5. Washing of UO_2 granulate (4 cycles of nitric acid lean solution with pH = 3, and 4 cycles of distilled water and 2 cycles of alcohol.).

Box 6. Drying of UO_2 granulate (200^oC); classification into 5 size classes; Sampling.

Box 7. Thermo-vacuum treatment of UO_2 granulates at temperature 900^oC, and at residual pressure of 0.1 Pa.

Box 8. Canning of end-products for storage.

Initial salt-electrolyte and auxiliary devices were being prepared in an Exhaust case.

Exhausted equipment and spent electrolyte ingots were being kept in special box 9.

There were two control panels in the facility. One was providing the electrolysis control, the control of resistor furnaces, and supplying the electricity to all electric equipment and devices. The gas control panel was providing the chlorine at the chlorination. It was also supplying the compressed air or nitrogen/argon to the equipment by for cooling or protection from corrosion.

The facility has included additional box 10 intended for studying of the effects founded during the chlorator-electrolyzer operation.

Boxes with numbers 10, 7, 9, 3 and the exhaust case are the capital equipment of the building. The chain of the island boxes with numbers 1, 2, 8, 6, 5 and 4 was created for the given work. All boxes were connected to the ventilation and decontamination systems of building.

During the fuel production program, the chlorator-electrolyzer was under 24-hours/day service. Other equipment was in two-shifts service (12 hours).

The analytical department was providing the routing control of process, the certification of the end-products, intermediates and wastes.

Description of the technological stages. Two stages, the chlorination of uranium oxides in the chloride melts of alkali metals and the melt electrolysis, were used for production of uranium dioxide granular powder. NaCl-KCl (melting point 660^{o}C) and NaCl-2CsCl (melting point 495^{o}C) melts were used as a salt-electrolyte.

Uranium oxides chlorination. UO_2 and U_3O_8 were the initial materials of the process. At first, the uranium oxides were chlorinated in NaCl-KCl melts at working temperature of 700^{o}C. In this case, the strong corrosion of the pyrographite crucible was observed. Later, the NaCl-2CsCl melt was chosen as electrolyte, and the temperature was decreased up to 630 – 650^{o}C. Individual alkali chlorides had usually qualifications of "Pure for Analysis" or "Chemically Pure".

Up to 6 kg of the uranium oxides were processed usually in one cycle. Initial uranium oxides mass was divided onto 6 portions, which was loaded in melt through 2 hours. Chlorine flow rate was up to 100 l/h. A mechanical device of an impeller type was used for the agitation of the bottom precipitate. At first, the melt samplings were taken every 2 hours, before loading of the next portion of uranium oxide. After loading of last portion, melt was chlorinated during 6 or 8 hours. When the uranium content in the melt became stable, chlorination was being stopped. Total time of the chlorination stage was about 16 –18 hours.

As the personnel gained experience, an amount of the melt analyses was gradually reduced. It was decreased to only 3 or 4 examinations, beginning from 2 hours after loading of last uranium oxide portion. Instead, the bottom of the crucible was investigated with a quartz probe before loading of the next portion of the uranium oxide. But basically, the full dissolution of uranium oxide was not required because of the constant isotopic composition of uranium. So, the last decision was only 1 melt examination at 2 hours after last portion. It was expected, and it was so that remainders of uranium oxides were dissolved in the melt during the electrolysis at the anode process. It allowed decreasing the total time of chlorination stage up to 12 – 14 hours.

A maximum concentration of U in both melts was usually 26 to 27 mass %. Sometimes concentration of U in NaC-2CsCl melt achieved 35 mass %, and in this case, high-grade granular powder of uranium dioxide was obtained.

A coefficient of chlorine use was the same both the NaCl-KCl and NaCl-2CsCl melts. A decreasing of the working temperature, when NaCl-2CsCl melt was used, was compensated by the solubility increasing of chlorine in comparison with NaCl-KCl melt. At first, the use efficiency of chlorine have averaged about 25 to 30 %, and then it achieved 40 % by decreasing the chlorination stage' total time described above.

A change of the mechanical device of impeller type, which was used for the agitation of the bottom precipitate, to a mixer of pulsating type was made to eliminate rotating components of the chlorator. It led to increasing the chlorination stage total time for 40 to 50 %, and, as a result, to decreasing the coefficient of chlorine use down to 20–25 %. However, the pulsating mixer was more stable in operation.

Electrolysis of the melt. Electrolysis of the melt follows for the uranium oxides chlorination. A cathode was being installed at the cover after a chlorination tube removal, and then a cathode polarization curve is being recorded relatively to the pyrographite crucible (which was a anode) through ~20 milliseconds after the current switching-off. Value of residual currents, and the initial electrolysis current were being estimated from the character of the initial polarization curves. The value of initial electrolysis current had to provide the cathode potential of – 0.65 V in the NaCl-2CsCl melt at 630^{o}C or of – 0.60 V in the NaCl-KCl melt at 700^{o}C.

During the uranium dioxide electrodeposition the cathode potential was measured relative to the pyrographite crucibles through every 15 minutes. The cathode potential increased in time of each constant current. It was connected with the decreasing of the uranium concentration in the melt during the uranium dioxide electrodeposition. To provide the quality of the cathode deposit and to prevent the alkali metal electrodeposition, the electrolysis current is being usually decreased with the decreasing of the uranium content in the melt. In the laboratory studies it has been found out, for providing the high quality of crystals in the cathode deposit at reasonable process productivity, it is necessary to keep the cathode potential in the middle of the uranyl reduction wave.

The electrolysis was being carried out on program, which made provision for the linear decreasing of the U content in the melt during the electrolysis. The melt was being analyzed through every 2 hours. Usually, the electrolysis was being stopped if the cathode potential reached –1.1 V, and the U concentration in the melt was about 1.0 ÷ 0.5 mass %.

In fresh electrolyte, the current efficiency was 92 –95% (4.62 – 4.77g/A·h). Gradually, it decreased up to 50 – 45 % (2.56 – 2.26 g/A·h). The above effect can be caused both by the iron impurities accumulation in the melt and by the crucible aging.

5.3. Preparation of uranium dioxide granular powder

After the electrolysis was stopped, the cathode with the uranium dioxide deposit was raised over the melt for the draining of molten salts and for cooling inside electrolyzer under argon/nitrogen atmosphere. In 15 or 20 minutes the cathode was moved from electrolyzer to a container for cooling up to room temperature. In the course of cooling, the cathode deposit cracks, and then it can be easy separated from cathode.

Usually the cathode deposit consists of columnar crystals of the uranium dioxide.

The process of the uranium dioxide granulate preparation includes the following steps:

- Crushing;
- Grinding;
- Water washing for extraction of captured salts;
- Thermo-vacuum treatment for removal of captured salts;
- Classification;
- Certification, and
- Containerization.

Jaw crusher was developed for crushing of the cathode deposit onto fragments with sizes of 20 to 30 mm.

The grinder of rotary type was created for the deposit fragments grinding into powder with the size of particles less than 1 mm.

The washing machine of rotary type was constructed for extraction of captured salts from the uranium dioxide granulates.

Thermo-vacuum treatment has been tasted for removal of captured salts from inside of the uranium dioxide granulates.

The granulometric composition of the final UO_2 granulates has to satisfy the requirements of the vibropac technology.

UO_2 granulates for BOR-60 reactor conversion into MOX fuel was produced at this facility.

5.4. Pyrographite crucible serviceability

The pyrographite crucible is the most important component of the “chlorator-electrolyzer”. It is the container for salt-electrolyte and it is the anode at the uranium dioxide electrodeposition. The pyrographite crucible serviceability is influencing directly onto the process productivity as a whole. Besides, the pyrographite is very expensive structural material.

In NaCl-KCl melt (the working temperature of 700^{o}C), the pyrographite crucible could stand of 240 hours. For this time, 30 to 42 kg of the uranium dioxide could be produced in one crucible during 5 to 7 “chlorination-electrolysis” cycles.

The pyrographite corrosion was observed on the interface of three phases: solid, liquid and gas. In NaCl-2CsCl melt (the working temperature of 650 - 630^{o}C), the pyrographite crucible could stand of 1000 hours. In this case, 120 to 150 kg of the UO_2 granulated fuel could be produced during 20 to 25 “chlorination-electrolysis” cycles.

This serviceability increase of pyrographite crucible had two reasons. The first was the working temperature decreasing. The second reason was caused by a structure perfection and thickness increasing of the pyrographite layer.

6. RIAR MOX Fuel Processing Experience

6.1. Choice of technology flow sheet

In RIAR, the wide experience of the UO_2, PuO_2 and MOX granular powders production had been gained, and the vibropac technology was established for the fuel elements manufacturing from the "pure" initial materials by 1984. Reactor tests and post irradiation investigations had confirmed the reliability of fuel produced by both pyroelectrochemistry and vibropac methods.

For this work a special group was organized with the following tasks:

- Generalization of the scientific information on behaviour of fuel components;
- Development of the technological process flow sheet;
- Preparation and execution of reprocessing with irradiated fuel.

It was solved that plutonium, as the most valuable component, will be returned in a fuel cycle, while the irradiated uranium will be used as a matrix for fission products and to be stored up to time when new operation methods will be available. Instead, the depleted uranium, which is stored in the hexafluoride form, will be used in a fuel cycle.

It was supposed, that new fuel would be fabricated of mechanical mixture of the reprocessed granular PuO_2 and the granular UO_2 produced through UF_6 conversion.

In such approach, the following advantages were expected.

1. Process of the fuel processing will consist of four simple stages:

- **Chlorination** of initial spent fuel in the chloride melts;
- **Electrolysis** of reduced melt for the partly uranium dioxide extraction with the some fission products;
- **Volume precipitation** for the granular plutonium dioxide producing;
- **Electrolysis** of oxidized melt for the primary melt purification with the purpose of salts recycle and some fission products concentrating.
- **Phosphate precipitation** for the melt fine cleaning with the purposes of salts to use repeatedly and the most fission products concentrating in the form, suitable for the further controllable storage and the subsequent burial storage.

All these stages were already checked in the "hot" cell conditions. Their realization does not need any complex equipment. The operation can be provided by remote methods only.

Granular PuO_2 is the processing product, which can be used for fuel elements manufactured by the vibropac method.

2. Conversion of the UF_6 into granular UO_2 can be carried out in "cold" conditions. Fluorine, which is the valuable raw material in the industry, is released at the same time.

3. Use of a mechanical mixture of the UO_2, PuO_2 (and, perhaps, burning out absorber) granular powders will allow to realize the high flexibility of the vibropac technology in manufacturing of fuel elements with the given configuration and structure, for example:

- Fuel elements with the different plutonium content for the different regions of the reactor core;
- Fuel elements with the plutonium profile distribution;
- Fuel elements with the profile distribution of both plutonium and burning out absorber content.

By analyzing the fuel materials and fission products properties, we have found that the fuel chlorination and first electrolysis can be repeated several times for the plutonium accumulation in melts. Calculations had shown that the productivity increases with number of repetition. The repetitions number can be restricted for three reasons:

- By nuclear safety;
- By accumulation of impurities, which influence negatively to the parameters of the technological stages and the products quality;
- Exhaustion of a service life of the equipment.

Since 1985 up to 1991, the technological study has been carried out on laboratory facility with total loading of UO_2 and PuO_2 up to 500 g. Fuel simulator corresponding to 10 % burnup was used. These researches have confirmed the practicability of chosen approach. With using of the laboratory researches results the technological flow sheet was developed for demonstration experiments with real fuel. This flow sheet has included all stages, which could be applied in future technology. The detailed flow sheet of demonstration experiments is presented on Fig. 6.1.1. The melt check chlorination was foreseen for the effectiveness analysis of each stage.

Four demonstration experiments on uranium oxide and MOX fuel reprocessing have been carried out with this flow sheet at the K-16 facility with fuel loading up to 6 kg [81-84].

In the 1991 experiment, the NaCl-KCl eutectic melt with working temperature about 690 - 700^{o}C was used as an electrolyte [81]. In the 1995 experiment, the melt of LiCl-4.5NaCl-4.9KCl-0.66CsCl alkali metal chlorides mixture was used to decrease the process working temperature up to 630 – 650^{o}C [82]. Such composition of electrolyte was chosen to provide the closeness of the thermodynamic properties of both melts. Experiments on uranium dioxide fuel reprocessing and MOX fuel reprocessing on scheme “MOX to MOX’ were conducted in NaCl-2CsCl melt [84].

The main task of second experiment (1995) [82] was the investigation of the technology’s ecological effect. And so, the fuel with high activity (burn up is 21,4 and 24,4 % h.a., cooling time is 3 and 2 years, accordingly.) was used in the experiment.

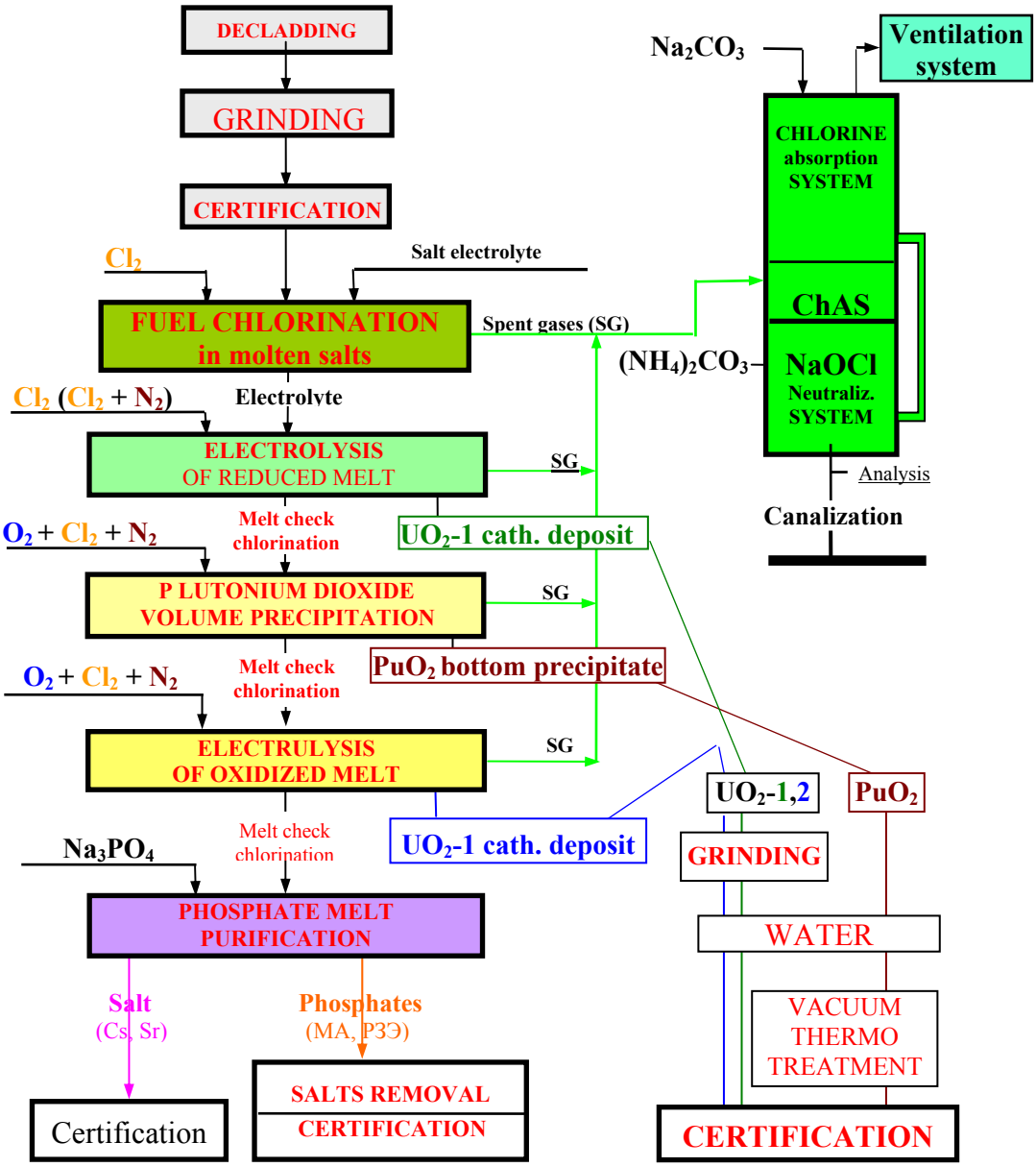

Fig. 6.1.1. Principal flow sheet of the demonstration experiments on the spent oxide fuel reprocessing

The uranium dioxide and MOX irradiated fuel (2000 – 2001) have been processed on this scheme too. The PuO_2 volume precipitation stage was changed to the electrolysis for UO_2 or MOX cathode deposition. The rest stages were not changed.

6.2. Experimental Facility

Large-scale laboratory facility for testing of the pyroelectrochemical process of the fast reactor irradiated fuel reprocessing is located in the hot cell K-16, operator rooms and repair corridor close to the shield cell. It was allowed to operate with 15 kg MOX fuel on this facility.

The hot cell involves the four compartments: upper compartment (K-16u), inter-cell room, lower compartment (K-16l) and under-cell room.

The K-16u and K-16l compartments present the heavy cells of about 8 cubic meters volume connected by the vertical transporter. They are provided for the observation systems, the copying manipulators and all other life-support systems i.e. systems of intracell lighting, power and compressed air supply, technological vacuum, drainage, stationary and portable decontamination system, etc. The K-16 is connected with other cells and laboratories of the building through the K-16u compartment by horizontal and vertical transporters.

The K-16u is equipped with couple of telescope lifters and bridge crane providing the maintenance of technological equipment and the connection of the upper and lower parts. The inter- and under-cell rooms are hermetically insulated from the cell working capacity and joined to the repair corridor of building through exits. These compartments are designed for location of unattended equipment. Retorts of chlorinator-electrolyzer (ChE) are deepened in the inter-cell room. Furnaces provide the heating of apparatuses with the sensor of electrolyzer neutron phone located between. The pits of monte-jus and oxidizer furnace vessel are deepened in the under-cell room.

All technological equipment for reprocessing of irradiated fuel and obtained product is located within the cell.

Two Chlorinator-Electrolyzer and block of joints for connecting to their utility systems are mounted in the K-16u. There are two pits in the cell for storage of the cathodic and agitating assemblies.

The following equipment is set in the K-16l: vibro-jaw grinder; device for water washing of deposits and precipitates; two Monte-jus for collection of washing solution; oxidizer providing a vacuum retort simultaneously; classifier; column for chlorine absorption from the off-gases leaving ChE; device for accumulation of ChE bottom deposits which is raised into the K-16u only at the moment of operation.

The main apparatus so called “Chlorator-Electrolyzer” is presented in Fig. 6.2.1 [82]. Up to 7 liters of molten salts and 6 kg of MOX fuel can be loaded in the “ChE” simultaneously. Apparatus is shown in two working positions. The fuel chlorination stage and the plutonium dioxide volume precipitation stage can be carried out in “a” position.

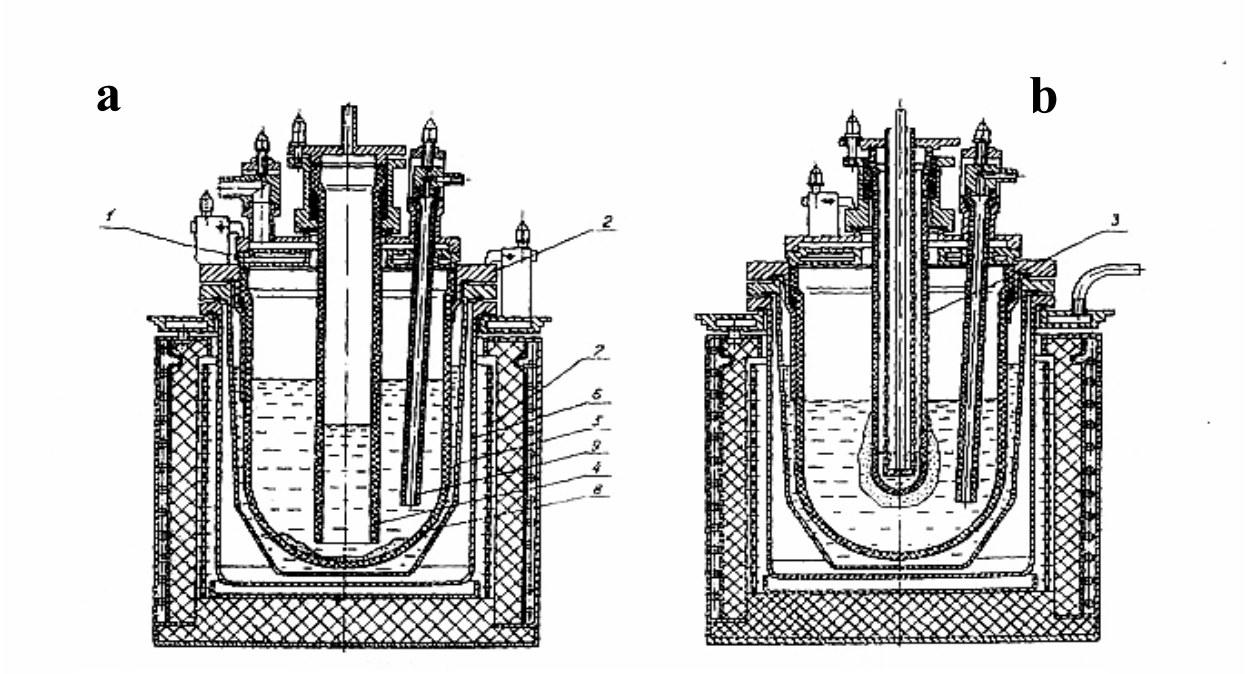

Fig. 6.2.1. Chlorinator-Electrolyzer [82]

a – chlorination and PuO_2 volume precipitation stages; b – electrolysis stages.
1 - cover, 2 – flange, 3 – cathode, 4 – agitating tube, 5 – vessel, 6 – defense vessel,
7 – furnace, 8 – pyrographite bath, 9 – gas-supply tubes.

The electrolysis of reduced or oxidized melt stages can be carried out in "b" position. The position without the agitation tube and cathode is used usually for the phosphate precipitation.

The apparatus is made of 12Cr18N1OTi steel. Assemblies and work pieces operating in high temperature regions and aggressive media are made of high-temperature steel and pyrolytic carbon or graphite.

The Chlorate-Electrolyzer involves:

- Electrical furnace 7 located under K-16u floor; - Safeguard vessel 6; - Working vessel 5;

Basket-flange 2; - Pyrographite bath (crucible) 8; - Apparatus cover 1; - Agitating assembly 4;

- Gas supply pipes 9; - Cathodic assembly 3.

Safeguard vessel 6 protects the furnace heater against working vessel. The working vessel 5 is intended for arrangement of pyrographite crucible. The basket-flange 4 is intended for mounting and sealing of the pyrographite bath in the working vessel. The pyrographite bath (crucible) 8 presents a spherical bottom cylinder of volume 16 liters.

The apparatus cover (Fig. 6.2.1, p.1) provides sealing of apparatus and mounting of assemblies on it (agitating and cathodic assemblies, bottom deposits collector and technological gases supply devices). It involves a sleeve for salt melt sampling; joints for cover cooling by compressed air; joints for lowing way off-gases; sleeve for connection of monometer to the blowing away cavity.

The agitating assembly (Fig. 6.2.1, p.4) presents pyrolytic carbon or graphite pipe of 100 mm diameter by 500 mm long provided for a sealing ring and a cap with a sleeve for argon supply.

The cathodic assembly (Fig. 6.2.1, p.3) presents a pyrolytic graphite cup of 70 mm diameter by 500 mm long with spherical bottom where the sealing ring and current-arraying cap are set up.

The device for technological gases supply to ChE (Fig. 6.2.1, p.9) presents 30 mm diameter by 450 mm long pipe made of pyrolytic carbon or graphite fitted in a special joint on the apparatus cover. There are two joints on the cover.

Slide screw clamps mounted on the working vessel and on the cover seal the basic ChE assemblies. The safeguard and working vessels, basket-flange and cover are fixed.

6.3. Some results of the demonstration experiments

In experiment of 1991 – 1992, the MOX fuel of BN-350 reactor with burning up to 4.7 % and cooling time about 6 years was taken in process. In experiment of 1995 – 1996, two FAs of BOR-60 reactor with MOX fuel were processed. One of them was irradiated up to 21.4 % and it had the cooling time about 3 years. Other FA was irradiated up to 24.4 % and it had the cooling time about 2 years. In experiment of 2000 two FAs of BOR-60 reactor with uranium dioxide fuel reprocessed. Both FA were irradiated up to 12 %, but one FA was removed from reactor 23 years ago, and other 12 years ago.

It should be noticed that the during the 1995 experiment the salts was loaded into chlorator in two steps. It was made to provide the indirect melt check weighting by dilution method after the fuel dissolution.

Table 6.3.1. Parameters of demonstration experiments [81-83]

Parameters		Type of fuel, Reactor		
		MOX Fuel, BN-350	MOX Fuel, BOR-60	UO_2 Fuel, BOR-60
Salt electrolyte		NaCl-KCl	(Li-Na-K-Cs)Cl	NaCl-2CsCl
Salt loading, g		8000	6000 + 3000*	15000
Initial fuel loading, g		4100	3258	5435.7
Temperature, ^{o}C	Chlorination	700	650	650
	Electrolysis of reduced melt	680	650	650
	PuO_2 volume precipitation	680	630	-
	Electrolysis of oxidized melt	700	630	650
	Phosphate melt purification	700	630	650

* Salts was loaded in two stages: fuel was dissolved in 6000 g of electrolyte and then 3000 g of salts were added for calculation possibility of the total salt mass.

The main characteristics of the products obtained during the MOX fuel reprocessing experiment of 1995 year are presented on Table 6.3.2. These data were used in the material balance calculation.

Table 6.3.2. Main characteristics of the products of the MOX fuel reprocessing (Experiment of 1995 [82,83])

Characteristics	Initial fuel	UO_2-1	PuO_2	UO_2-1	Phosphates	Spent electrolyte
Mass, g	3258	489	504	1510	442	8114
Contents, mass %:						
U	54.6	84.7	1.7	86.6	<0.001	<0.001
Pu	12.6	0.3	77.4	0.3	<0.001	<0.001
Np	0.54*	2.0	0.077	0.33	0.057	0
Am	0.47	0.0026	0.54	0.035	2.5	0.0015
Cm	$1.8\cdot10^{-3}$	$1.5\cdot10^{-5}$	0	$1.5\cdot10^{-4}$	$1.1\cdot10^{-2}$	$5.7\cdot10^{-7}$
Activity of fission products, Ci/g:						
Ru(Rh_-106	$1.4\cdot10^{-1}$	$1.1\cdot10^{0}$	$1.3\cdot10^{-1}$	$2.2\cdot10^{-2}$	$9.5\cdot10^{-4}$	$5.5\cdot10^{-5}$
Sb-125	$1.3\cdot10^{-2}$	$9.8\cdot10^{-3}$	$2.1\cdot10^{-3}$	$9.5\cdot10^{-4}$	$1.3\cdot10^{-1}$	$3.0\cdot10^{-5}$
Cs-137	$1.0\cdot10^{-1}$	$1.1\cdot10^{-4}$	$2.0\cdot10^{-4}$	$8.0\cdot10^{-5}$	$4.6\cdot10^{-4}$	$5.6\cdot10^{-2}$
Ce(Pr)-144	$2.1\cdot10^{-1}$	$5.3\cdot10^{-3}$	$5.3\cdot10^{-2}$	$1.9\cdot10^{-3}$	$2.6\cdot10^{0}$	$6.6\cdot10^{-3}$
Eu-154	$3.0\cdot10^{-3}$	$7.9\cdot10^{-5}$	$5.8\cdot10^{-4}$	$1.4\cdot10^{-3}$	$2.4\cdot10^{-2}$	$1.7\cdot10^{-4}$

* Np was added specially to initial spent fuel.

For the experiment mass balance calculation, besides above products (See Table 6.3.2), the following materials were taken into consideration:

- Salts obtained after concentration by evaporation of water solutions that were used for salt washing from uranium dioxide deposits or plutonium dioxide and phosphate precipitates. All salts were integrated, melted down, and certificated (Evs);

- Sublimates, which were collected and certificated (Sbl);

- Salt samples, which were used for the process monitoring. Nuclear materials and impurities content were calculated using the analysis results (Smp).

Uranium and plutonium distribution among the products of the experiments is shown on Fig. 6.3.1 [82,83]. The main amount of these elements is concentrated in the products, which are obtained on the stages having a special purpose. Evaporated salts (ES) are recycle materials, which must be returned into the next pyroelectrochemical cycle. It needs the modifying the electrolysis and volume precipitation stages to decrease the uranium and plutonium content in the phosphate precipitate. A considerable amount of the nuclear materials is in the salt samples. It is connected with this work's experimental character, which demands gathering of information as much as possible.

MA and FP distribution among the experiment products is presented on Fig. 6.3.2. Distribution of elements corresponds their electrochemical properties. At the reduced melt electrolysis neptunium and NM can be co-deposited with the uranium dioxide. At the oxidized

melt electrolysis many of elements have ability to co-deposition with the uranium dioxide, especially at hard conditions of the melt oxidation. The americium and curium behaved like the rare earth elements one.

Fig. 6.3.1. Uranium and plutonium distribution
among the experiment products [82, 83]

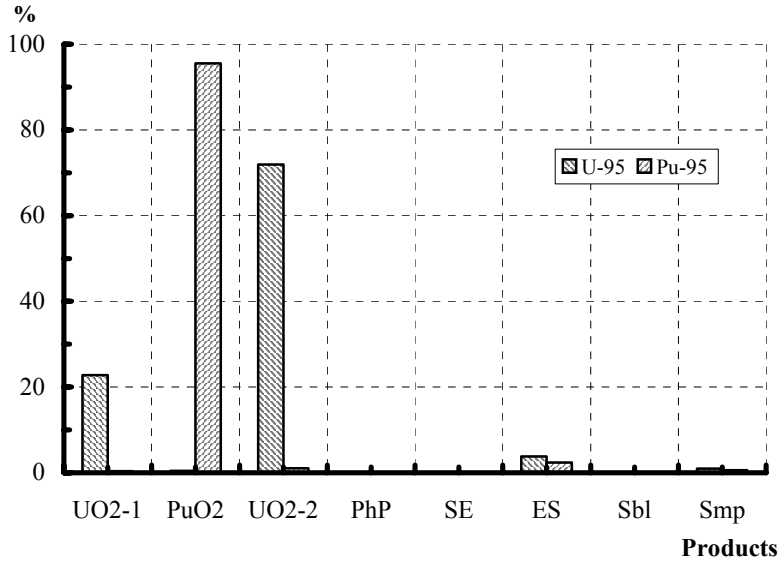

Distribution indicator (DI) of impurities between the melt and the products at the main stages of the spent fuel pyroelectrochemical processing is presented in the final Table 6.3.3 [82,83]. DI is not a decontamination factor, which must be higher. DI shows the stage effectiveness, only. So, when this parameter is less than unit, it means, that an element has the big propensity to the co-deposition (or co-precipitation) with the main product. Good example is the neptunium and ruthenium behaviour at the reduced melt electrolysis. In principle, all stages satisfy to physics demands of the fast reactors.

7. Conclusion

In fact, experiments presented here are the first experience of the MOX fuel reprocessing in such scale. Nevertheless, the results of these experiments are very promising.

Also, it is possible to read in additional literature [85 – 99] about further development of the pyrochemical technology and application of its processes for conversion of military origin metallic plutonium into MOX fuel and for the minor actinides recovering and preparing for burning in nuclear reactors.

Fig. 6.3.2. Distribution of MA and FPs among experiment products [82, 83]

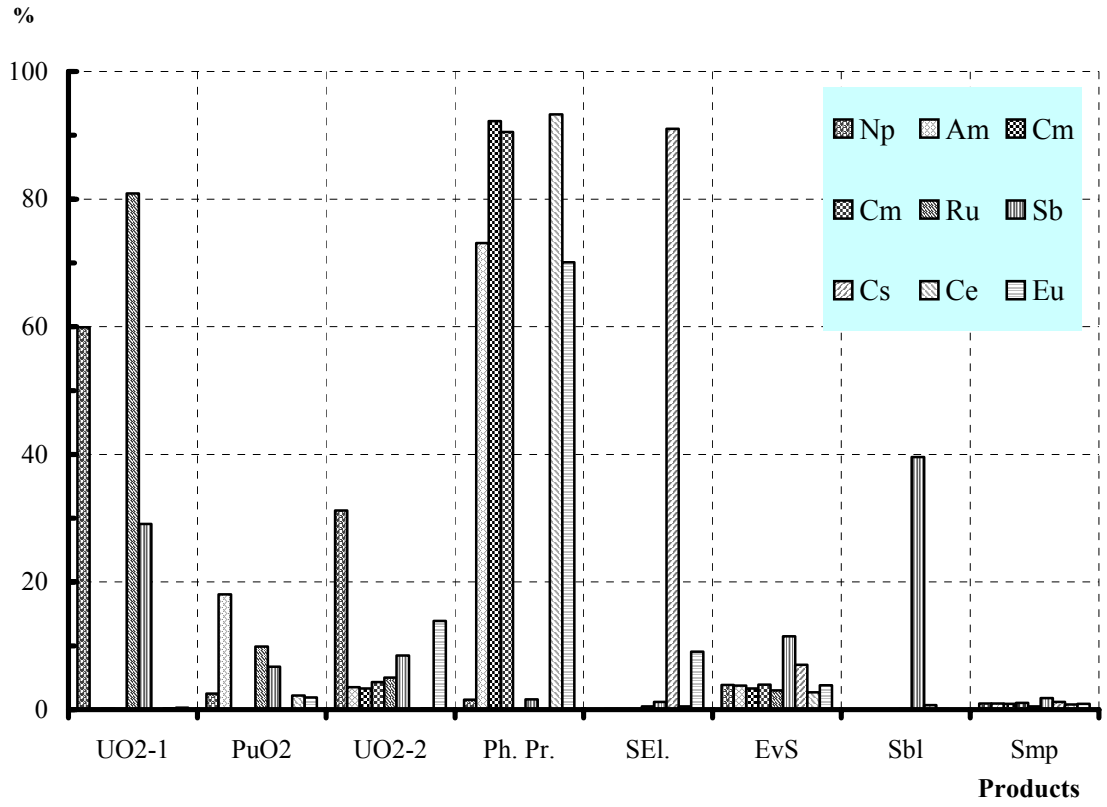

Table 6.3.3. Distribution Indicator of impurities between the melt and the products at the main stages of the irradiated fuel reprocessing process
(Data of the 1995 experiment [82,83])

Element	Electrolysis of reduced melt	Volume precipitation of plutonium dioxide	Electrolysis of oxidized melt
U	1	160	1
Pu	67	1	1.8
Np	0.37	16	1.1
Am-241	260	5.3	20
Cm-242	140	900	24
Cm-244	200	940	21
Ru-106	0.28	3.9	96
Rh-106	0.28	3.9	96
Cs-134	2200	4800	220000
Cs-137	2100	4700	230000
Ce-144	110	44	20300
Pr-144	110	44	20000
Eu-154	86	50	400

References

1. M.V. Smirnov. ：The electrode potentials in fused salts. In Russian. Publish House "Nauka", Moscow, (1973).
2. V.A. Lebedev. ：Selectivity of the liquid-metal electrodes in molten halides. In Russian. Chelyabinsk, "Metallurgy" , (1993).
3. Yu.V. Baybakov, M.M. Vetyukov. ：Electrolysis of molten salts. In Russian. Publish House "Metallurgy", Moscow, (1966) .
4. A.V. Bychkov, O.V. Skiba, S.K. Vavilov et al. ："Current situation and future development work for the pyrochemical production of mixed actinides oxides for nuclear fuels", Proc. Int. Conf. On Actinides. Actinide'97. Sept. 11-14, pp. 912-917, (1995).
5. M.V. Smirnov, V.Ya. Kudyakov, V.E. Komarov et al. ："Equilibrium electrode U(IV)-U and redox U(IV)-U(III) potentials in molten chlorides of alkali metals." In Russian, Electrochemistry, vol. 15, No.2, pp. 269 – 272, (1979).
6. N.P. Nekrasova, V.E. Komarov. ："Thermodynamic of the formation of uranyl monochloride and dichloride in molten alkali metal chlorides", Radiochemistry, vol. 25, No. 2, pp. 219-223. (1983). (Translated from Radiokhimiya, Vol. 25, No. 2, pp. 233-237, March-April, (1983).
7. V.E. Komarov, N.P. Nekrasova. ："Equilibrium electrode potentials of uranium dioxide in fused potassium chloride, In yearbook Physical chemistry and electrochemistry of molten and solid electrolytes", In Russian. Sverdlovsk, USSR Science Academy, Ural Science Center, Electrochemistry Institute, pp. 24 – 27, (1981).
8. S.K. Vavilov, G.N. Kasantsev, T.I. Sabanova. ：Reaction kinetics of uranium (IV) oxidation with oxygen in NaCl-2CsCl melt. In Russian. Preprint, RIAR-35(394), Dimitrovgrad. p.26 , (1979).
9. V.V. Gutshin, O.V. Skiba, V.M. Barinov. ： "Use of SF-4A and IKS-14 spectrophotometers for absorption spectra measuring of molten salts.", In Russian, Apparatus and Technique of Experiment. USSR Science Academy, No. 3. pp. 276 – 277, (1972).
10. P.V. Danckwerst. ： Gas-Liquid reactions. (In Russian, translated from English.) Moscow, Chemistry, p.256 , (1973).
11. N.M. Emanuel, D.G. Knorre. ：Course of The Chemical Kinetics. Moscow, High School, p.400., (1974).

12. A.N. Baraboshkin. ：Electro-crystallization of metals from the molten salts. In Russian. Moscow: "NAUKA", p.279 , (1976).

13. O.V. Skiba, M.V. Smirnov, T.F. Hazemova. ："Diffusion coefficients of U^{3+}, U^{4+}, UO_2^{2+} ions in the NaCl-KCl melt", In Russian, Works of the Electrochemistry Institute of the Ural division of the USSR Science Academy. Sverdlovsk, Issue 4, pp. 11– 15, (1963).

14. M.V. Smirnov, V.E. Komarov, N.P. Borodina. ："Diffusion coefficients of trivalent uranium in the molten chlorides of alkali metals. In Russian", Works of the Electrochemistry Institute of the Ural division of the USSR Science Academy. Sverdlovsk, Issue 19, pp. 29 – 32. , (1972).

15. M.V. Smirnov, N.P. Borodina, I.A. Pahmutov. ：Correlation relationships for estimation of diffusion coefficients of ions in the molten chlorides of alkali metals. In Russian, Electrochemistry, vol. 22, No. 4, pp. 478 - 482, (1986).

16. Yu.P. Savotchkin. ："Interaction of plutonium with oxygen in chloride melts", In Russian Preprint, RIAR-5(788), Dimitrovgrad, p.35 , (1990).

17. V.I. Silin, O.V. Skiba. ："Influence of salt-solvent on the reaction formation thermodynamics of plutonium trichloride in diluted solutions of alkali metal chlorides", In Russian Preprint RIAR. P-118, Dimitrovgrad, (1971).

18. Y.P. Savochkin, T.I. Sabanova, O.V. Skiba. ："Thermodynamics of tetravalent plutonium in alkali metal chloride melts", In Russian Preprint RIAR-37 (396), Dimitrovgrad. p.22, (1979)

19. S.K. Vavilov, G.N. Kazantsev, V.V. Gutshin. ：Spectro-photometric study of equilibrium of $Pu^{4+} + Cl^- = Pu^{3+} + 1/2Cl_2$ reaction in NaCl-2CsCl melt In Russian", Atomic Energy, vol. 49, No. 2, pp. 94 – 98. , (1980).

20. G. Landresse and G. Duyckaerts. ："Stude par spectrophotometrie d'absorption de l'quilibre $Pu^{4+}+Cl^-=Pu^{3+}+1/2Cl_2$ dans le melange LiCl-CsCl (55045 mol.%) fondu", Ibid., vol. 10, No. 11, p. 1051, (1974).

21. G. Landresse and G. Duyckaerts. ："Stude par spectrophotometrie d'absorption de l'quilibre $Pu^{4+}+Cl^-=Pu^{3+}+1/2Cl_2$ dans l'eutectique LiCl-KCl fondu.", Inorg. Nucl. Chem. Letters, vol. 10, No. 8, p. 675, (1974).

22. G. Landresse and G. Duyckaerts. ："Stude par spectrophotometrie d'absorption de l'quilibre $Pu^{4+}+Cl^-=Pu^{3+}+1/2Cl_2$ dans le melange LiCl-KCl (70-30 mol.%) fondu", J. Radioanal. Chem., vol. 35, p. 63, (1974).

23. S.K. Vavilov, G.N. Kazantsev, O.V. Shishalov. ："Spectro-photometric study of equilibrium of PuO_2^{2+} + Cl^- = PuO_2^{2+} + 1/2Cl_2 reaction in NaCl-2CsCl melt", In Russian, Atomic Energy, vol. 56, No. 2, pp. 88 – 91, (1984).

24. G. Landresse and G. Duyckaerts. ： "Stude par spectrophotometrie d'absorption de l'equilibre PuO_2^{2+}+Cl^-=PuO_2^++1/2Cl_2 dans le melange LiCl-CsCl (55-45 mol.%) fondu", Inorg. Nucl. Chem. Letters, vol. 10, No. 11, p. 1059, (1974).

25. S.K. Vavilov, P.T. Porodnov, Yu.P. Savotchkin et al. ："Thermodynamics and kinetics of plutonium redox and electrode reactions in melt of NaCl-CsCl eutectic mixture", Radiochemistry, vol. 27, No 1, pp. 116 – 121, (1985).

26. R. Lysy, G. Landresse, G. Duyckaerts. ："Reactions chimiques de composes de neptunium dans l'eutectique LiCl-KCl fondu", Bull. Soc. Chim. Belg, vol. 83, No. 7-8, pp.227-233, (1974).

27. L. Martinot, G. Duyckaerts. ："Diagrammes potential/pO^{2-} du neptunium et du plutonium dans l'eutectique LiCl-KCl", Anal. Chim. acta, vol. 66, No. 3, pp. 474-476, (1973).

28. L. Martinot, J. Fuger. ："Determination of Solubility Products of Various Actinide Oxides in The (Na-K)Cl and (Li-K)Cl eutectics and calculation of new potential- pO^{2-} diagrams", J. Less-Common Metals, vol. 120, No. 1-2, pp. 255-266, (1986).

29. Lysy R., Duyckaerts G. ："Diagramme potential - pO^{2-} du neptunium dans l'eutectique LiCl-KCl 660^0C", Anal. Chim. acta, vol.96, No. 1, pp. 125-132, (1926).

30. L. Martinot, F. Caligara. ："Electrochemistry of Actinides in Molten Salts", Atomic Energy Review, vol. 11, No. 1, pp.3-61, (1973).

31. C.L. Krueger, T.S. Storvick, J.J. Roy et al. ："Measurement of the Standard Potential of the Np(III)/Np(0) Couple in LiCl-KCl Eutectic", J. Electochem. Soc., vol. 138, No. 4, pp. 1186 - 1187, (1991).

32. R. Lysy, G. Duyckaerts. ："Etude des reactions d'oxigo reduction du neptunium dans le melange RbCl-CsCl (25-75 % mol)", Anal. Chim. acta, vol. 94, No. 2, pp.385-394, (1977).

33. Lysy R., Landresse G., Duyckaerts G., Etude ："Quantitative D'equilibres chimiques en solution dans les Sels fondus par Spectrophotometrie d'absorption", Anal. Chim. acta, vol. 72, No. 2, pp. 205-215, (1974).

34. Lysy R., Duyckaerts G. ："Etude quantitative D'equilibres chimiques en Solution dans le melange LiCl-KCl (70-30% mol). Application a neptunium", Inorg. and Nucl. Chem. Lett, vol. 12, No. 2, pp. 205-215, (1976).

35. R. Lysy, G. Duyckaerts. ："Etude quantitative du systeme NpO_2^{2+}-NpO_2^{+} dans le melange LiCl-CsCl (55-45 % mol) fondu", Inorg. and Nucl. Chem. Lett., 1975, vol. 11, No. 2, pp.79-88.

36. L.F. Grantham, J.J. Roy, D.L. Grimmaett(a) et al. ："The Standard Potential of Am/$AmCl_3$. ", Electrochemical Society Meeting in Honolulu, pp. 1985 - 1986, (1993).

37. M.N. Astaf'ev, G.N. Kazantsev, V.P. Kolesnikov. ："Volt-ampere metric study of chlorination products of uranium, plutonium, americium and cerium oxides with carbon tetrachloride in NaCl-KCl melt. In Russian", "VIth All-Union Conference on Physical Chemistry of Ionic Melts and Solid Electrolytes". Report's Theses. Kiev, "Naukova Dumka", Part 2, p. 19, (1976).

38. A.V. Bychkov, O.V. Skiba, P.T. Porodnov et al. ："Development of the pyroelectrochemical process for demonstration fuel cycle of an actinide burner reactor", Proc. Int. Conf. On Evaluation of Emerging Nuclear Fuel Cycle Systems. GLOBAL'95. Sept. 11-14, 1995, Versailles, France, v.1, pp. 516-523, (1995).

39. L. Martinot, J.C. Spirlet, G. Duyckaerts et al. ："Measure des Potentials Standards du ouple Am(III)/Am(0) dans L'Eutectique LiCl-KCl entre 400 et 600 C.", Bull. Soc. Chim. Belg., vol. 81, No..11-12, pp. 449 - 455, (1974).

40. L. Martinot, J. Reul, G. Duyckaerts et al. ："Standard free energy of formation of $CmCl_3$ in (Li-K)Cl eutectic", Bull. Soc. Chim. Belg, 1975, vol. 84, No. 6, pp.657-662.

41. V.F. Pimenov. ："Nb equilibrium potential in NaCl-KCl melt. In Russian", Proceedings of the Colleges. Series "Non-ferrous metallurgy", No.3, pp. 72-74, (1967).

42. V.E. Komarov, V.E. Krotov. ："Solubility of zirconium dioxide in equimolar mixture of sodium and potassium chlorides", In Russian. Works of the Electrochemistry Institute of the Ural division of the USSR Science Academy. Sverdlovsk, Issue 27, pp. 61– 64, (1978).

43. L.E. Ivanovsky, I.G. Rozanov, M.T. Krasil'nikov et al. ："Electrolysis of molten chlorides with NbO and NbO_2 anodes. In Russian", Works of the Electrochemistry Institute of the Ural division of the USSR Science Academy. Sverdlovsk, Issue 5, pp. 111– 117, (1964).

44. T.F. Babikova, Yu. S. Sokolovsky, M.M. Sroelova. ："About interaction of uranyl chloride with zirconium tetrachloride in chloride melts of sodium and potassium", In Russian. Atomic Energy, vol. 40, Issue 5, p. 412. (Dep. 842/8111) , (1976).

45. V.E. Komarov, N.P. Borodina, Z.S. Martem'yanova. ："Influence of zirconium and niobium on cathodic deposition of uranium dioxide from alkali chloride melts", Radiochemistry , vol. 37, No. 4, pp. 300-303. (Translated from Radiokhimiya, vol. 37, No. 4, pp. 326-330, (1995).

46. R. Combes, J. Vedel, B. Tremillon. ："Standard Potential Determinations in Molten NaCl-KCl", J. Electroanal. Chem., vol..27, No. 1, pp.170-174, (1970).

47. B.D. Vasin, A.S. Kazakov, M.V. Popov et al. ： "Equilibrium potential of palladium in molten alkali metal chlorides", In Russian. Electrochemistry, vol. 19, No. 3, pp. 400-402, (1983).

48. J.A. Plambeck. ："Encyclopedia of Electrochemistry of the Elements", Vol.10, Fused Salt Systems. N.Y, p.440 , (1976).

49. B.D. Vasin, A.S. Kazakov, I.F. Nichkov et al. ："Reduction of ruthenium (III) in chloride melts. In Russian", Proceedings of the Colleges. Series “Non-ferrous metallurgy”, No.1, pp. 62-64, (1984).

50. B.D. Vasin, V.A. Ivanov, V.B. Musaev et al. ："Potentiometric study of chloride melts containing rhodium (III)", In Russian. Proceedings of the Colleges. Series “Non-ferrous metallurgy”, No.2, pp. 77-79, (1984) .

51. V.V. Burtsev, B.D. Vasin, A.S. Kazakov et al. ："Spectroscopic study of molten chlorides containing ruthenium ions", In Russian, Ural Polytechnic institute, Sverdlovsk, p.6. (Manuscript is deposited in ONIITEChim, Cherkassy town, 24.06.80, No. 527xp-D80) , (1980).

52. N.A. Saltykova, S.N. Kotovsky, A.N. Baraboshkin. ："Cathode processes at the ruthenium electrodeposition from chloride melts", In Russian, Electrochemistry, vol. 21, pp. 674 – 679, (1985).

53. A.A. Burnaeva, A.I. Kryukova, G.N. Kazantsev. ："Study of the ruthenium behavior in chloride melts. II. About ruthenium interaction with chlorine-oxygen mixtures and about the ruthenium oxichlorides formation", In Russian, Radiochemistry, vol. 27, Issue 4, pp. 408 – 412, (1985).

54. S.N. Flengas, T.R. Ingraham. ："Electromotive Force Series of Metals in Fused Salts Activities of Metal Chlorides in 1:1 Molar KCl-NaCl Solution", J.Electrochem.Soc., v.106, No. 8. pp.714-721, (1959).

55. S.M. Zahar’yash, V.P. Han, V.I. Amosov. ："Electrochemical behavior of fused LiCl-KCl eutectics containing the TeO_2 and $CdCl_2$", In Russian, Melts, Issue 5, pp. 29 - 34, (1989).

56. P.M. Usov, V.M. Butorin. ："Equilibrium of the metallic neodymium with its ions in fused mixture of lithium and potassium chlorides", In Russian, Electrochemistry, vol. 7, No. 8, pp. 1161 – 1163, (1971).

57. B.D. Vasin, V.A. Ivanov, A.V. Prokof’ev, et al. ："Potentiometric study of the samarium-containing chloride melts", In Transactions: Fifth Kola workshop on the electrochemistry of rare and non-ferrous metals. The report thesis. Apatity, p.33, (1986).

58. B.D. Vasin, A.V. Vasil'ev, V.A. Ivanov, S.P. ："Raspopin. Europium electrochemical properties in molten chlorides of alkali metals", In Russian, Melts, vol. 2, No. 3, pp. 84 – 88, (1988).

59. I.S. Morozov, Fam Ngok T'en. ："Mechanism of the oxygen interaction with the fused mixture of rare earth elements", In Russian J. of Inorg. Chem., vol. 14, No. 9, pp. 2556 – 2560, (1969).

60. R. Combes, M.-N. Levelut, B. Tremillon. ："Oxo-acidity and its influence on the electrochemical properties in molten mixtures of $CeCl_3$ and equimolar NaCl-KCl at 1000 K", Electrochim.Acta, v.23, n.10, pp.1291-1295, (1978).

61. R. Combes, M.-N. Levelut, B. Tremillon. ："Conditional solubility versus pO^{2-} of cerium(III) oxide in molten equimolar NaCl-KCl at 727°C", J.Electroanal.Chem, v.91, n.1, pp.125-131, (1978).

62. K.A. Simpson. ："Workshop on chemical reactivity of oxide fuel and fission product release", Nucl. Energy, 27, N 1, p.13, (1988).

63. O.V. Skiba, A.A. Mayorshin, V.A .Makarov et al. ："Development and operation experience of the pilot plant for fuel pin and assembly production based on vibropac uranium-plutonium fuel", Proc. Int. Conf. on Fast Reactors and Related Fuel Cycles, Oct.28 - Nov.1, Kyoto, Japan, V.2, Report 15-4, (1991).

64. Edited by V.P. Glushko："Thermal constants of substances", In Russian, Moscow, VINIPI, issue 6, part 1, 1972, p.369.; issue 7, part 1, 1974, p.34.; issue 8, part 1, p.535, (1978).

65. V.A. Lebedev. ："Standard and conventional standard potentials of lanthanides and theirs alloys in molten chlorides", In Russian, Electrochemistry, v. 31, No. 1, pp. 41 – 50, (1995).

66. W.J. Hamer, M.S. Malberg, B . Rubin., ： Electrochem. Soc. , V. 103. p.8, (1956).

67. K. E. Weeks, F.E. Blok. ：Thermodynamic properties of 65 elements, their oxides, halides, carbides, nitrites. In Russian. Moscow: "Metallurgy", p240, (1965).

68. J.J. Roy, L.F. Granthem, L.R. McCoy et al. ：Molten salt chemistry and technology , Ed. Chelma M. and Devilliers D.. Mater. Science Forum, Switzerland: Copyright Trans Tech Publications, V. 73 – 76. p. 547, (1991).

69. A.B. Shubin, L.F. Yamtchikov, S.P. Raspopin et al. ： In Russian, Melts, No. 6, p. 102. (Шубин А.Б., Ямщиков Л.Ф., Распопин С.П., Бретцер-Портнов И.В. // Расплавы. 1991. Вып. 6. С. 102.) , (1991).

70. A.B. Shubin, L.F. Yamtchikov, S.P. Raspopin. ： "X Conference on the physical chemistry and electrochemistry of ionic melts and solid electrolytes", In Russian, Report

thesis. Ekaterinburg, Ural Scientific Center of the Russia's Science Academy, p. 142, (1992).

71. Yang L., Hudson R.G. ： Trans. Met. Soc. AIME. ,V. 215. p. 589, (1959).
72. V.P. Butorov, I.F. Nichkov, E.A. Novikov et al., In Russian. ：Proceedings of the All-Union Conference on the physical chemistry and electrochemistry of ionic melts and slags. Part 1. Thermodynamics and composition of ionic melts. In Russian. Kiev: Naukova Dumka, p. 142, (1969).
73. B.D. Vasin, V.A. Ivanov, S.P. Raspopin, S.V. Savtchenko. ： In Russian. Melts, No. 3, p. 100, (1989).
74. V.A. Lebedev, A.V. Kovalevskii, I.F. Nichkov et al. ： In Russian. Electrochemistry, vol. 10, p. 1342, (1974).
75. B.D. Vasin, V.A. Ivanov, A.V. Prokof'ev et al. ： In Russian. Proceedings of Institutes of Higher Education. Non-ferrous Metallurgy, No.1, p. 122, (1987).
76. B.D. Vasin, V.A. Ivanov, A.V. Vasil'ev, S.P. Raspopin. ： In Russian. Melts, No. 3, p. 84, (1988).
77. S.K. Vavilov, Yu.P. Savotchkin, L.G. Babikov et al. ："Investigation method of carbon-graphite materials interaction with oxygen-containing melts", In Russian, Melts.. No 5. pp. 96 – 102, (1991).
78. S.K. Vavilov, Yu.P. Savotchkin, L.G. Babikovet al. ："Kinetics and mechanism of carbon-graphite materials interaction with uranyl containing melt of sodium and caesium chlorides", In Russian, Melts. , No 2. pp. 27 – 33, (1994).
79. S.K. Vavilov, P.T. Porodnov, O.V. Skiba. ："Equilibrium of the $O_2 + 2UO_2Cl_2 = (UO_2)_2O_2Cl_2 + Cl_2$ reaction in NaCl-CsCl melt", In Russian, Melts, No 5. pp. 45 – 53, (1996).
80. R. Bunk, U. Leske, R. Krompasset al. ："Operation of an experimental facility for fabrication of fuel elements and fuel assemblies of the BOR-60 containing vibrocompacted fuel", Atomic Energy, Vol. 67. No. 5, pp. 802-806. (Translated from Atomnaya Energiya, Vol. 67, No. 5, pp.320-323, November, 1989), (1989).
81. V.E. Komarov, N.P. Nekrasova. ："Absorption spectra of uranyl ions in fused halides of alkali metals", In Russian, Radiokchimiya, No. 2, pp. 260 – 264, (1980).
82. A.V. Bychkov, S.K. Vavilov, O.V. Skiba et al. ："Pyroelectrochemical reprocessing of irradiated FBR MOX fuel. Experiment on irradiated fuel of the BN-350 reactor", Proc. Int. Conf. On Evaluation of Emerging Nuclear Fuel Cycle Systems. GLOBAL'95. Sept. 11-14, 1995, Versailles, France, v. 2, p. 988, (1995).

83. A.V. Bychkov, S.K. Vavilov, O.V. Skiba et al. ："Pyroelectrochemical reprocessing of irradiated FBR MOX fuel. III. Experiment on high burn-up fuel of the BOR-60 Reactor", Proc. Int. Conf. On Future Nuclear Systems. GLOBAL'97. Oct. 5-10, 1995, Yokohama, Japan, v.2, pp. 912-917, (1995).

84. A.V. Bychkov, S.K. Vavilov, P.T. Porodnov et al. ： "Pyrochemical reprocessing of irradiated mixed oxide fuel in molten salts", Molten Salt Forum Vols. 5-6 , Dresden Germany, August , pp. 525-528, (1998).

85. A.V. Bychkov, M.V. Kormilitsyn, S.K. Vavilov et al. ："Pyroelectrochemical reprocessing of the spent FBR fuel. V. Testing and demonstration of the "$UO_2 \rightarrow UO_2$" and "MOX→MOX" flow-sheets on the real spent fuel of the BOR-60 reactor", Proc. Int. Conf. "Back-end of the fuel cycle: from research to solutions". GLOBAL 2001. 9-13 September, Paris, France, Topic 1.3.6. (№ 284), (2001).

Additional literature.

86. V.B. Ivanov. ："New technologies in nuclear power", Atomic Energy, Vol. 81. No. 2, pp. 566-568. (Translated from Atomnaya Energiya, Vol. 89, No. 2, pp.109-112, August, 1996), (1996).

87. V.A. Tsikanov, G.I. Gadzhiev, E.V. Kirillov et al. ："Factors in the preliminary assessment of the economic effectiveness of an atomic fuel and power complex based on atomic plants with fast reactors", Atomic Energy, Vol. 67. No. 3, pp. 625-628. ,(Translated from Atomnaya Energiya, Vol. 67, No. 3, pp. 163-166, September, 1989), (1989).

88. V.B. Ivanov, O.V. Skiba, A.A. Mayershinet et al.. ："Experimental, economical and ecological substantiation of fuel cycle based on pyroelectrochemical reprocessing and vibropac technology", Proc. Int. Conf. On Future Nuclear Systems. GLOBAL'97. Oct. 5-10, 1995, Yokohama, Japan, v.2, pp. 906-911, (1995).

89. O.V. Skiba, A.A. Mayorshin, P.T. Porodnov et al. ："Nuclear fuel cycle based on pyroelectrochemical method of MOX fuel reprocessing and technology of vibropac fuel elements and assemblies production", Proc. Int. Conf. On Evaluation of Emerging Nuclear Fuel Cycle Systems. GLOBAL'95. Sept. 11-14, 1995, Versailles, France, v.1, p. 336, (1995).

90. O.V. Skiba, A.A. Mayorshin, A.V. Bychkovet et al, ：" Nuclear fuel and power complex, included the modul-type fast reactor with low capacity and the plant for dry reprocessing of

fuel and vibropacked fuel pins assemblies productions", Proc. Int. Conf. On Future Nuclear Systems. GLOBAL'97. Oct. 5-10, 1995, Yokohama, Japan, v.1, pp. 143-147, (1995).

91. V.M Poplavskii, A.N. Chebeskov, A.G. Kalashnikovet et al. ："Use of plutonium in reactor fuel", Atomic Energy, Vol. 89. No. 4, pp. 834-842. (Translated from Atomnaya Energiya, Vol. 89, No. 4, pp. 314-325, October, 2000), (2000).
92. P.T. Porodnov, A.G. Osipenko, O.V. Skiba et al ："A pyrochemical procedure for the conversion of military origin metallic plutonium into MOX fuel", Proc. Int. Conf. On Evaluation of Emerging Nuclear Fuel Cycle Systems. GLOBAL'95. Sept. 11-14, 1995, Versailles, France, v. 2, p. 1346, (1995).
93. A.V. Bychkov, O.V. Skiba, Mayershinet et al. ："Fuel cycle of actinide burner-reactor. Review of investigations by "DIVITA" program", Proc. Int. Conf. On Future Nuclear Systems. GLOBAL'97. Oct. 5-10, 1995, Yokohama, Japan, v.1, pp. 657-661, (1995).
94. A.P. Kirillovich, A.V. Babikov, O.V. Skibaet et al. ："Safety analysis of fuel cycle processes based on "Dry" pyrochemical fuel reprocessing and vibropac technology", Proc. Int. Conf. On Future Nuclear Systems. GLOBAL'97. Oct. 5-10, 1995, Yokohama, Japan, v.1, pp. 900-905, (1995).
95. A.F. Grachev, A.V. Bychkov, O.V. Skiba et al. ："Main aspects of fuel cycle for reactors with inherent safety without extraction pure uranium and plutonium", Proc. Int. Conf. "Back-end of the fuel cycle: from research to solutions". GLOBAL'2001. 9-13 September, Paris, France, Topic 1.3.2. (№ 279) , (2001).
96. A.A. Mayorshin, V.A. Kisly, O.V. Shishalov et al. ："Recycling of the BOR-60 and BN-350 vibropac fuel after pyrochemical reprocessing", Proc. Int. Conf. "Back-end of the fuel cycle: from research to solutions". GLOBAL'2001. 9-13 September, Paris, France, Topic 1.3.2. (№ 280), (2001).
97. Yu.F. Volkov, A.N. Lukinykh, S.V. Tomilin, et al. ："Effect of alpha-irradiation on the properties of titanate ceramic designed for plutonium immobilization", Proc. Int. Conf. "Back-end of the fuel cycle: from research to solutions". GLOBAL'2001. 9-13 September, Paris, France, Topic 1.3.2. (№ 280), (2001).
98. A.F. Grachev, O.V. Skiba, A.V. Bychkov et al. ："Experience on Russian origin plutonium conversion into fast reactor nuclear fuel", Proc. Int. Conf. "Back-end of the fuel cycle: from research to solutions". GLOBAL'2001. 9-13 September, Paris, France, Topic 1.3.2. (№ 283), (2001).
99. M.V. Kormilitsyn, A.V. Bychkov, V.S. Ishunin et al. ："Experiment on reduction of LWR spent fuel by lithium for developing of advanced spent fuel storage method", Proc. Int. Conf. "Back-end of the fuel cycle: from research to solutions". GLOBAL'2001. 9-13 September, Paris, France, Topic 1.3.2. (№ 285), (2001).

100. M.I. Mel’nik, A.V. Bychkov, M.V. Kormilitsyn et al. ："Nuclear fuel reprocessing for cascade subcritical molten-salt reactor", Proc. Int. Conf. “Back-end of the fuel cycle: from research to solutions”. GLOBAL’2001. 9-13 September, Paris, France, Topic 1.3.2. (№ F288), (2001).